Response to Reviewer 1

Summary and Evaluation: This is a potentially interesting and potentially useful study for the scientific community devoted to improving our understanding and numerical weather forecasts of damaging tropical cyclones threatening populated coastal communities throughout the world. However, the current manuscript suffers from limitations involving a lack of clarity, poor scholarship in some places and multiple instances of muddled scientific writing. I was very disappointed to discover this state of affairs, given the large number of co-authors (7), including several senior (& expert) co-authors.

We very much appreciate Dr. Montgomery for his thoughtful and constructive comments. The manuscript has been revised accordingly based on his comments. We hope that the revised manuscript is satisfactory for publication. Below is the point-to-point response to reviewer's comments.

The authors begin their presentation by trying to argue that improvements in the forecast of rapidly intensifying storms will follow: a) once eddy momentum and eddy heat flux processes are properly accounted for in the eyewall and rainband regions; and b) once in-cloud turbulent mixing parameterizations are developed for the eyewall and rainband regions. These are certainly plausible points of view (but see point 2 below for an opposing view). The authors then propose a simple revision of the sub-grid-scale (SGS) turbulence closure scheme for the Hurricane Weather Research Forecast (HWRF) model. The proposed scheme recognizes the prevalence of turbulence in deep (presumably) rotating convection in tropical cyclone vortices. The revised closure is elementary and consists of redefining the height of the boundary layer in deep convective regions, such as the developing eyewall or rainband region, to a height of approximately 5 km altitude based on a model-derived reflectivity threshold of 28 dBZ (Figs. 4e, 4f). This revised boundary layer height definition is called the 'turbulence layer' (TL) and is an extension of the current HWRF scheme (based on pioneering work of Larry Marht and colleagues, and subsequent work in 1996 by Hong and Pan, etc.).

Two things we want to clarify here. First, we are not saying that the improvements in the numerical forecast of TC intensification solely depend on a correct accounting for eddy momentum/heat fluxes and appropriate parameterization of in-cloud turbulent mixing in the eyewall and rainbands. It is a required but not sufficient condition in 3D full-physics simulations. There are important environmental factors, such as SST and large-scale wind shear, and other internal dynamics that can affect TC intensification. In this study, we show that for certain environmental conditions, the numerical simulations of TC intensification, in particular rapid intensification (RI), are sensitive to the parameterization of eyewall/rainband in-cloud turbulent mixing above the boundary layer. Such a sensitivity results from the fact that the TC inner-core structure, model-resolved eddy forcing, and secondary overturning circulation depend strongly on the parameterized in-cloud turbulent mixing processes.

Second, as we admitted in the manuscript (Page 13, lines 21-13; page 19, lines 19-20), the method that we used to treat the effects of in-cloud turbulent mixing in HWRF is crude and does not consider the specific mechanisms in generating in-cloud turbulence, and thus, the scheme in its current form may not be directly used in operational forecasts. Nonetheless, this simple modification clearly demonstrates the sensitivity of TC intensification to in-cloud turbulent mixing parameterization. It allows us to look into and examine the role of eyewall/rainband eddy forcing above the PBL in TC intensification.

HWRF model simulation experiments invoking the new turbulence parameterization appear to be significantly improved over the standard Hong and Pan (1996) scheme that uses a gradient Richardson-number to define the boundary layer height (typically 1 km). Although the *eddy momentum and heat flux divergent tendencies* diagnosed from the new simulations are shown to be approximately *five times greater than the corresponding SGS tendencies (pg. 13, bottom paragraph, Figs. 10, 11), the authors argue that the revised SGS tendencies are ultimately responsible for the improved forecasts.* The authors appear to base their assertion on some mysterious coupling between the turbulence closure scheme and the cloud microphysical processes, and its corresponding coupling to the latent heating rate field associated with the aggregate of deep (presumably) rotating clouds in the inner-core region of the developing vortex.

Indeed, our diagnoses show that the model-resolved eddy forcing is about five times larger than the SGS eddy forcing above the boundary layer, but the former shows a strong dependence on the parameterization of in-cloud SGS turbulent mixing processes. Such a dependence likely stems from the fact that large energy-containing turbulent eddies are not resolved but parameterized in HWRF. It may also result from the microphysical-dynamical interaction since in-cloud turbulent mixing is intimately involved with cloud microphysics. However, the coupling between the parameterized microphysical and turbulent mixing processes is complicated and remains poorly understood. To clarify issues associated with the microphysical-dynamical interaction in 3D full-physics simulations will be one of the focuses of our future research.

I am certainly willing to entertain the scientific possibility of a subtle nonlinear feedback involving the SGS tendencies and the microphysics, but the proffered feedback mechanism should be clearly articulated in this manuscript to help support the empirical evidence of the HWRF experiments in real cases. It is unclear, for example, which is most important: the revised turbulence closure scheme for momentum, heat, or moisture?

We have done two additional experiments. In the first experiment, we only modified the eddy exchange coefficient for momentum k_m while keeping the eddy exchange coefficient for heat and moisture $k_{t,q}$ the same as the default. We reversed such a change in the second experiment. Figure R1 below compares the simulated intensity and track of Hurricane Jimena (2015) from different numerical experiments. Both the modified turbulence closures for momentum alone and for heat/moisture alone show non-negligible impacts on TC

intensification. This result is not unexpected. While the tangential eddy forcing for momentum directly involves in the acceleration or deceleration of the primary circulation of a TC, the thermodynamic eddy forcing is sufficiently strong to modulate the secondary overturning circulation that interacts with the primary circulation during TC evolution. Note that in numerical models including HWRF, the eddy exchange coefficients for heat and moisture are usually treated as the same, thus, we did not further separate them in our experiments.

These two addition experiments have been included in the revised manuscript. Please see Page 14, lines 17 – 26, and the updated Figure 7 in the revised manuscript.

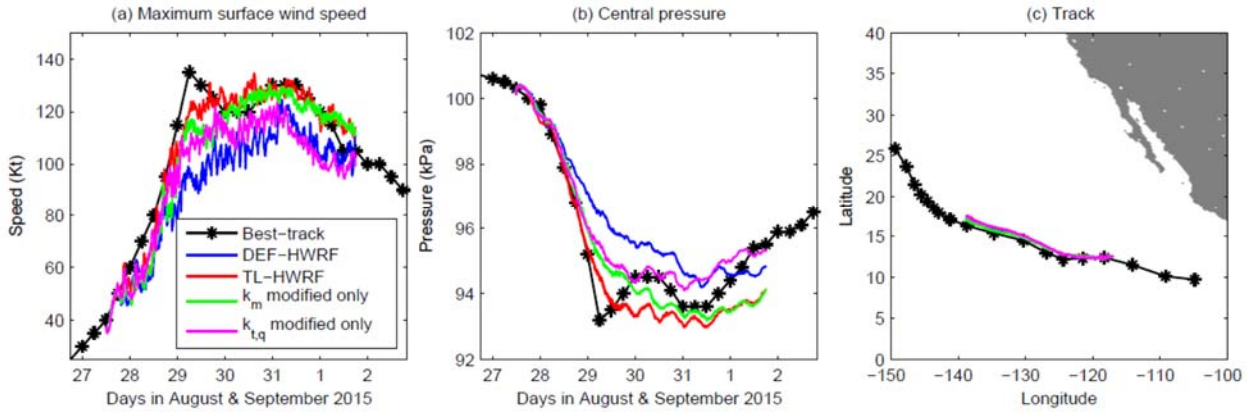

Figure R1: Comparison of HWRF simulated maximum surface wind speed, storm central pressure, and track of Jimena (2015) with the best track data (Black). Blue curve indicates the simulation by the default HWRF (DEF-HWRF). Red curve indicates the simulation by the HWRF with inclusion of in-cloud turbulent mixing parameterization (TL-HWRF). Green curve represents the simulation in which only the eddy exchange coefficient for momentum is modified while keeping the eddy exchange coefficient for heat and moisture the same as the default. Magenta curve is opposite to the green curve in which only the eddy exchange coefficient for heat and moisture is modified.

An alternative (and simpler) hypothesis might be that the structure of the resolved eddy forcing between the control and updated experiments might be more important in accounting for the improved forecasts. This alternate hypothesis originates from a cursory examination of Fig. 11 wherein the resolved eddy forcing of the mean tangential velocity tendency equation in the TL-HWRF experiment is more spatially concentrated and of higher intensity than the DEF-HWRF experiment. (Of course, the different eddy forcings are in part the result from the different SGS formulations, but the larger magnitude of the resolved eddy forcing seems to be a more plausible agent for influencing the spin up process.)

We agree with the comments. Indeed, the TC inner-core structure shows a substantial sensitivity to the in-cloud turbulent mixing parameterization in the eyewall and rainbands. The larger magnitude of the resolved eddy forcing appears to be a more plausible agent for the spin-up process. We will further explore this sensitivity in our future research.

Finally, throughout the manuscript, I was disappointed to find that the authors never asked the basic question of whether a *down-gradient turbulence closure for all predicted quantities* is indeed appropriate in the rotating, convective turbulence region that pervades a rapidly intensifying tropical cyclone vortex? (see, e.g., Persing et al. 2013, their section 6.)

An appropriate parameterization of SGS turbulence is critical for simulating all atmospheric phenomena including TCs. But depending on the problems, the focuses of turbulent mixing parameterization could be different. For example, for shallow stratocumulus clouds, the above boundary layer turbulence is negligible since the clouds are normally capped by a strong inversion. Because of that, representing turbulent mixing associated with the strong cloud-top entrainment becomes important to successfully simulate the evolution of stratocumulus-topped boundary layer. In this case, an appropriate treatment of cloud-top radiave cooling and evaporative cooling is a key since they are intimately involved in the buoyancy production of turbulence in clouds. Drizzling is also an important factor to consider since it can cause the decoupling of the cloudy boundary layer. In a TC environment, however, the boundary layer top entrainment is a minor since no inversion can be found in convective regimes except for the TC eye or moat regions where weak inversion may exist. In this case, the above-boundary-layer turbulent mixing generated by the cloud processes in the eyewall and rainbands becomes important since the in-cloud buoyancy-driven turbulent eddies can generate efficient vertical transport and can directly interact with cloud microphysics in the eyewall and rainbands. The main issue that we are addressing in this paper is what needs to be included in the vertical turbulent mixing scheme for a successful numerical prediction of TCs. We believe that the in-cloud turbulent mixing above the boundary layer in the eyewall and rainbands is one of the key components of SGS turbulent processes that must be considered in TC simulations. But it has not been included or well represented in the current models used for TC prediction.

The down-gradient turbulence closure is a commonly used approach for representing turbulent transport by mimicking molecular diffusion. The difference is that the conductivity for down-gradient molecular diffusion is determined by material, but the eddy exchange coefficient for down-gradient turbulent transport is the function of motion (or turbulence). However, the down-gradient transport is basically a local transport mechanism, it does not hold for convective cells or large eddies because their transport mechanism is fundamentally nonlocal. This problem has been recognized for a long time. Nowadays, many turbulent mixing schemes do include nonlocal mixing component in the schemes when parameterizing vertical turbulent transport. For example, the YSU scheme, the NCEP Global Forecast System scheme, the ACM2 scheme, the UW PBL scheme, the TEMF scheme, the Shin-Hong Scale-aware scheme, the Grenier-Bretherton-McCaa scheme, and the MRF scheme all include non-local mixing effect. The PBL scheme used in the latest version of HWRF also considers non-local mixing based on the method of GFS PBL scheme. This is different from the horizontal mixing schemes used in models. To our knowledge, non-local mixing has not been considered in any horizontal turbulent mixing schemes. Most of models use Smagorinsky type (local) schemes to treat SGS horizontal turbulent mixing. As we stated in the manuscript, the main focus of this paper is not to discuss the advantage or disadvantage of down-gradient (local)

and non-local mixing approaches, but to address if in-cloud turbulent mixing generated by cloud processes above the boundary layer in the eyewall and rainbands needs to be included in the vertical turbulent mixing scheme for TC simulations.

There are other substantive issues that need to be addressed by the authors and these issues are noted below.

Recommendation: Major Revision. The paper requires substantial improvement in several areas (listed above and below) before I can consider recommending the paper for acceptance in this journal.

The manuscript has been substantially revised based on the comments.

Major comments:

First and foremost, the entire manuscript needs to be read carefully by the native English speaking co-authors. I have come across multiple instances of ambiguous or inaccurate statements that need attention. I highlight some of these instances below. I have not provided an exhaustive list however.

1. The first sentence of the Abstract typifies the lack of clarity that occurs in the manuscript:

"The fundamental mechanism underlying tropical cyclone (TC) intensification may be understood from the conservation of absolute angular momentum, where the primary circulation of a TC is driven by the torque acting on air parcels resulting from asymmetric eddy processes, including turbulence."
If the fundamental mechanism underlying TC intensification can be understood from the material conservation of absolute angular momentum (AAM), why, then, are *eddy torques* being invoked in the SAME sentence to explain *how the primary circulation is driven by the torque* acting on air parcels resulting from *asymmetric eddy processes, including turbulence*? While I might be called out for singling out one sentence of the paper, it is the first sentence of the Abstract. Sentences like this abound in the manuscript and portray an alarming state of confusion concerning the mechanisms of tropical cyclone intensification.

The sentence was meant to describe the budget equation of azimuthal-mean absolute angular momentum (AAM) , $\frac{D\widetilde{\bar{M}}}{Dt} = r(F_\lambda + F_{sgs\_\lambda})$, where F_λ and F_{sgs_λ} are the azimuthal-mean tangential eddy correlation terms resulting from the model-resolved and parameterized sub-grid scale (SGS) asymmetric eddy processes. It is clear that for certain external conditions, such as large-scale wind shear and SST, the spin-up and spin-down of the mean vortex of a TC is driven by the eddy forcing represented by the terms on the right-hand side of the equation. In real TCs, the eddy forcing possesses a continuous spectrum from eyewall/rainband mesoscale convective features down to small-scale turbulence. In numerical simulations, however, the continuous eddy forcing is artificially split into two

parts: the model-resolved and parameterized SGS eddy forcing due to discrete model grids. The two split components of eddy forcing not only are sensitive to model grid resolution but also depend strongly on each other. For SGS eddy forcing, the research to date mainly focuses on the boundary layer turbulence. However, the boundary layer classically viewed as a shallow layer adjacent to Earth's surface becomes ill-defined as the radial inflow ascends swiftly along the eyewall. In this case, there is no physical interface that separates the turbulence generated by the shear and buoyancy production associated with the surface processes and by the cloud processes aloft. While the importance of boundary layer turbulent transport to TC intensification is well recognized, little attention has been paid to the turbulent mixing aloft in the eyewall/rainband clouds. The main motivation of this study is to examine the role of eddy forcing resulting from eyewall/rainband clouds above the boundary layer in TC intensification. We showed that the simulated TC inner-core structure and the model-resolved eddy forcing (and thus, the TC intensification) depend strongly on the parameterization of in-cloud turbulent mixing.

To avoid confusion, this sentence has been removed from the revised manuscript. The abstract has been rewritten.

2. How come the CHIPS model (Emanuel et al. 2004) is never mentioned in this paper? How come the latest Emanuel (2012) theory for tropical cyclone intensification is never mentioned in this manuscript?

The reason I am asking these questions is that some have suggested that the CHIPS model currently beats *all* deterministic forecast models (see Jonathan Vigh's talk from the recent AMS conference on Hurricanes and Tropical Meteorology in Ponte Verde, Florida, April 2018). In that context, some have advocated that the turbulence closure problem examined here is a red herring. How will the authors address these questions in the revised manuscript?

We are aware of D r. Jonathan Vigh et al.'s recent work on exploring the upper bound of TC intensification by comparing the rapid intensifications (RIs) simulated by the CHIPS model with those by the state-of-the-art 3D full-physics numerical models (presented at the AMS 33rd Conference on Hurricanes & Tropical Meteorology). The CHIPS model refers to a simple axisymmetric 2D radius-height dynamic model developed by Emanuel et al. (2004). They showed that CHP6 (an ensemble member of the CHIPS simulations) outperforms all 3D numerical models in terms of guidance for estimating the upper bound of TC intensification. Based on this result, they concluded (their presentation PPT file is available at AMS website) that (1) the dynamics of very RI (VRI ~30 kt in 12 h) and extreme RI (ERI ~ 40 kt in 12 h) are primarily axisymmetric and do not require a 3D full-physics framework; and (2) the general pathway to VRI/ERI can be captured by an axisymmetric numerical model. It should be noted here that CHP6 was initialized with an intensity enhanced by 3 ms^{-1} of the previous 24-hr forecast with vertical wind shear set to ZERO at all times, so, the setting is basically assumed to be ideal for TC intensification. Here we want to clarify a few things as follows.

First, we agree with Vigh et al.'s argument that the dynamics governing VRI/ERI are primarily axisymmetric. This result is supported by previous studies. For example, Nolan and

Grasso (2003) and Nolan et al. (2007) showed that it is the vortex axisymmetric response to the azimuthally-averaged diabatic heating (rather than the heating associated with individual asymmetries) that is responsible for the resultant intensity change. In fact, our HWRF simulations are consistent with these results. This is clearly seen in Figs. 9b & 9d and Figs. 14e & 14f, the HWRF with the inclusion of an in-cloud turbulent mixing parameterization successfully simulated the nearly axisymmetric ring of convection around the storm center consistent with satellite observations (Fig. 8 and Figs. 14a & 14b). The closed convective ring feature is an evidence to support that the RI of Hurricanes Jimena (2015) and Harvey (2017) indeed can be explained by the axisymmetric dynamics. So, there is no conflict between our simulations and Vigh et al.'s conclusion.

Second, we do not think that the turbulent closure problem investigated in this paper is a red herring to the RI driven by axisymmetric dynamics. The fact that the default HWRF fails to simulate the observed TC inner-core structure including the quais-closed ring feature suggests that the realization of axisymmetric dynamics underlying TC intensification in 3D full-physics models is not scientifically trivial. It is a difficult problem since it involves a complicated interplay between model dynamic core and various physics modules in 3D models. As we showed in the paper, although the direct eddy forcing from the parameterized SGS eyewall/rainband in-cloud turbulent processes is only minor compared with the model-resolved eddy forcing, the simulated TC inner-core structure, the secondary circulations, and model-resolved eddy processes all show substantial sensitivity to the in-cloud turbulent mixing parameterization. Therefore, the impact of SGS processes on TC intensification should not be considered as an isolated effect since it can induce changes in TC internal dynamics. Such a sensitivity of TC evolution to in-cloud turbulent mixing parameterization may stem from the fact that current model grid spacing (~1 – 2 km) used for TC prediction cannot resolve large energy-containing turbulent eddies. Our result also suggests that the SGS physics involving with the in-cloud turbulent mixing above the PBL facilitates the realization of the axisymmetric dynamics underlying the RI of TCs in 3D full-physics simulations.

Third, there is no doubt that some observed RIs can be well explained by the axisymmetric dynamics, but that does not mean that 3D full-physics models can be replaced by axisymmetric models such as CHIPS for real-time TC prediction. According to Dr. Vigh's presentation, only one ensemble number of CHIPS, CHP6, is able to capture the observed RIs. Figure R2 below shows an example of CHIPS ensemble simulations of Hurricane Patricia (2015). Except for CHP6, all the other member simulations fail to reproduce the observed RI and peak intensity. This is the same for Typhoon Meranti (2016) and Hurricane Maria (2017, not shown here but is available in Dr. Vigh's presentation). Recall that CHP6 was configured ideal for TC intensification with vertical wind shear set to ZERO at all times for all tested TCs. But this is not a realistic ambient condition for some RI TCs. As shown in Fig. R2, when the ambient conditions were set to those used by deterministic forecast modes, the control run of CHIPS ensemble simulations (member CHIP) completely missed the Patricia's RI. So, it is not an accurate statement that CHIPS model "*beats all deterministic forecast models",* it's just one member of CHIPS with ZERO wind shear that generates the intensification rate close to observations in some cases. CHIPS provides a great framework to examine the sensitivity of

TC intensification to ambient conditions, but it would be inappropriate to use the ZERO-wind-shear setting for real-time forecasts as the real condition may be far away from it. Moreover, Vigh et al. (2018)'s results are unable to explain why RI, VRI, or ERI can happen for some real TCs when environmental shear is not exactly zero.

Finally, we agree with the argument that the upper limit on intensification is determined by the conversion of latent heating to kinetic energy. The reason that this conversion is often less efficient in a 3D intensification process than that in a 2D axisymmetric model is likely due to the fact that the convection in a 3D model has not yet organized into an annular ring, and thus, the azimuthally averaged heating rate is smaller than that in a 2D axisymmetric model. This probably is the case in Vigh et al.'s simulations. However, there are examples in literature that showed the energy conversion in 3D model simulations can be as efficient as that in an axisymmetric model. For instance, Persing et al. (2013) reported that "there is a short period of time when the rate of spin-up in the 3-D model exceeds that of the maximum spin-up rate in the axisymmetric model, and during this period the convection is locally more intense than in the axisymmetric model and the convection is organized in a quasi ring-like structure resembling a developing eyewall" (see Page 12336 of their paper). This is a situation similar to our simulations with the inclusion of eyewall/rainband in-cloud turbulent mixing parameterization.

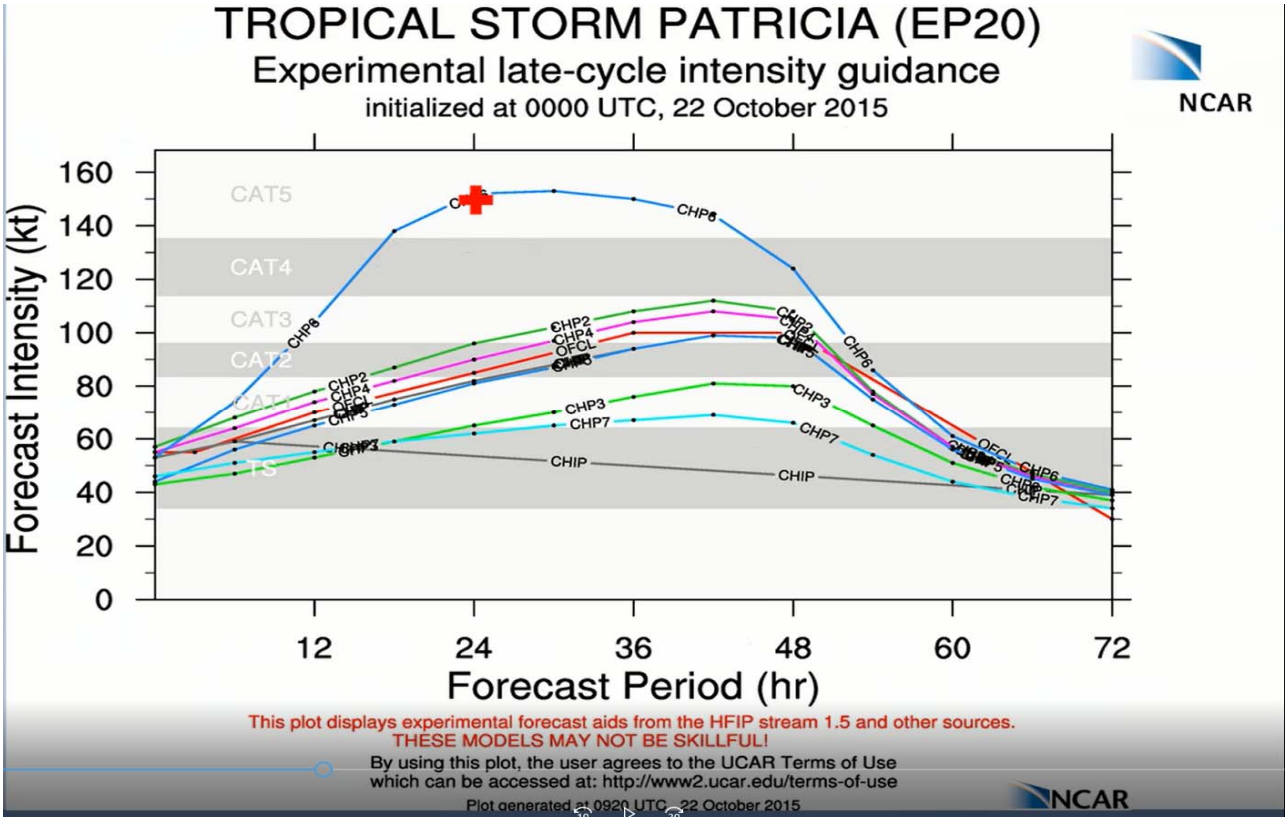

Figure R2: CHIPS ensemble simulations of Hurricane Patricia (2015) adopted from Vigh et al.'s presentation at the AMS 33rd Conference on Hurricanes & Tropical Meteorology.

In 3D numerical simulations, the conversion from latent heating to kinetic energy depends on many factors, such as, model resolution, initial vortex structure, and interaction between

resolved and parameterized processes. The representation of SGS physics is apparently a source of uncertainty in modeling TC intensification. In this paper, we mainly focused on one particular problem of SGS physics --- the parameterization of turbulent mixing above the PBL generated by cloud processes. We have been trying to understand the impact of eyewall/rainband eddy processes (both resolved and SGS) on TC intensification and improve in-cloud turbulent mixing parameterization in operational models.

As for Emanuel (2012) paper, his "self-stratification" intensification hypothesis argued that the turbulence in the outflow is important because it acts to set the thermal stratification of the outflow. The resultant gradients of outflow temperature provide a control of an intensifying vortex. In our study, the defined "Turbulent Layer (TL)" does not include the turbulence generated by the anvil clouds in the upper troposphere where the eyewall up-flow turns outward, becoming outflow. Outside a convection regime, the anvil clouds are detached from the PBL in vertical model columns, thus, "TL" concept does not apply. In their analyses (Emanuel and Rotunno 2011; Emanuel 2012), the instability for generating small-scale mixing was estimated by the gradient Richardson number. However, since numerical models use stretching grids in the vertical, it is very difficult to parameterize the SGS turbulent mixing in the outflow regions using the bulk Richardson number at a very low vertical resolution. Moreover, since the main focus of this study is on the turbulent mixing generated by cloud processes above the PBL within the convective eyewall and rainbands, we want to isolate this problem from the complication of outflow turbulence. For these reasons, the outflow turbulence above the PBL is not discussed in this study.

These issues have been clarified in the revised manuscript. Please see Page 6, lines 13– 24; Page 13 lines 1 - 12; and Page 15, lines 18 – 25 in the revised manuscript.

3. Pg. 2, Line 11: What is the mechanism underlying TC intensification? Surely, the material conservation of M above the BL (the ice skater model, i.e.) is an essential element of the spin up process above the frictional boundary layer. But what is the mechanism that supports the continued spin up of the vortex? You have not articulated the mechanism(S), other than a passing reference to CISK or cooperative intensification. I believe this is an inadequate state of affairs that needs to be corrected.

For an axisymmetric vortex free of forcing in an inviscid flow, the conservation of absolute angular momentum is an essential element of the spin up process of the vortex. But in reality, there are asymmetric eddies with a spectrum of scales from mesoscale convective elements down to small-scale turbulence superimposed on the mean axisymmetric vortex. On a radius-height plane of the mean vortex, the aggregate effects of the asymmetric eddies are represented by the forcing terms appearing in the azimuthal-mean governing equations. For example, the budget equations for azimuthal-mean tangential, raidial, and vertical velocities may be written as,

$$\frac{\partial \overline{v}}{\partial t} + \overline{u}\frac{\partial \overline{v}}{\partial r} + \overline{w}\frac{\partial \overline{v}}{\partial z} + \overline{u}\left(f + \frac{\overline{v}}{r}\right) = F_{\lambda} + F_{sgs\_\lambda},$$

$$\frac{\partial \bar{u}}{\partial t} + \bar{u}\frac{\partial \bar{u}}{\partial r} + \bar{w}\frac{\partial \bar{u}}{\partial z} - \left(\frac{\bar{v}^2}{r} + f\bar{v}\right) + \frac{1}{\bar{\rho}}\frac{\partial \bar{p}}{\partial r} = F_r + F_{sgs\_r},$$
$$\frac{\partial \bar{w}}{\partial t} + \bar{u}\frac{\partial \bar{w}}{\partial r} + \bar{w}\frac{\partial \bar{w}}{\partial z} + \left(\frac{1}{\bar{\rho}}\frac{\partial \bar{p}}{\partial z} + g\right) = F_w + F_{sgs\_w}.$$

To date, a great effort has been devoted to elucidating how eddy forcing drives the primary and secondary circulations of a TC vortex. The importance of SGS eddy processes and the associated vertical transport in the PBL to TC evolution has long been recognized. The early theories of TCs (e.g., Charney and Eliassen 1964, Ooyama 1982, Emanuel 1986, Emanuel 2003) all recognized the role of turbulence in transporting latent heating obtained from ocean surface and converging moisture in the PBL to sustain eyewall/rainaband deep convection. From eddy forcing perspective, all these studies basically focused on the SGS eddy forcing within the PBL. The advanced 3D rotating convective updraft paradigm (Montgomery and Smith 2014) recognized the importance of asymmetries, such as hot towers, to TC intensification. Persing et al. (2013) compared the TC intensification rate in a 3D full-physics model with that in an axisymmetric model.

What has received little attention and has yet be explored is the SGS eddy forcing above the boundary layer. As we stated in the paper, the classic definition of boundary layer does not apply to the eyewall and rainbands because there is no physical interface separating the turbulence generated by the buoyancy and shear production related to the surface processes and cloud processes aloft. The turbulent processes associated with the eyewall/rainband convective clouds also acquire nearly annulus-like or spiral feature depending on the detailed structures of eyewall and rainbands. The in-cloud turbulent mixing is thus important not only because it forms a component of eddy forcing directly involving in the evolution of the primary and secondary circulations of a TC, but also because it interacts with cloud microphysics to affect diabatic heating. This may explain why the simulated TC inner-core structure, secondary circulation, and model-resolved eddy forcing are all sensitive to in-cloud turbulent mixing parameterization. Moreover, since numerical models usually have a coarse vertical resolution above the boundary layer, it makes difficult to appropriately parameterize in-cloud turbulent mixing in models.

We have redrafted the related paragraphs and sentences in the revised manuscript based on the comments. Please see Page 2, line 23 – Page 3, line 19; Page 4, lines 13 – 28; and Page 5, lines 5 – 13 in the revised manuscript.

4. Pg. 2, lines 19-20: Re eddy forcing in BL:

"In the PBL, eddy forcing $F\lambda + Fsgs\_\lambda$ is negative definite, meaning that it always slows down the motion; thus, it physically represents the frictional force in the tangential direction. "

"… is negative definite … always slows down the motion" seems to be an assertion without proof of substantiation. Is this a property of the three-dimensional Navier-Stokes equations? (Ans: No.) Is it based in observations? Please give references.

This statement was written following Montgomery and Smith (2014) paper (*Paradigms for Tropical Cyclone Intensification*). On Page 41-42 in their paper, they wrote: "The key element of vortex spin-up in an axisymmetric setting can be illustrated from the equation for absolute angular momentum per unit mass, $\frac{\partial M}{\partial t} + u\frac{\partial M}{\partial r} + w\frac{\partial M}{\partial z} = F$. … In regions where frictional forces are appreciable, F is negative definite (provided that the tangential flow is cyclonic relative to the earth's local angular rotation, $v/r > -f$), and M decreases following air parcels.". We interpreted that "the regions where frictional forces are appreciable" refer to the boundary layer. Negative F in the friction layer is consistent with what Charney and Eliassen (1964) stated that friction acts to dissipate kinetic energy, and is also supported by Fig. 11 and Fig. 12 in our paper where we showed the eddy forcing is negative in the inflow layer.

The reference has been added in the revised manuscript, and the related sentence has been rewritten. Please see Page 2, lines 14 – 15 in the revised manuscript.

5. Pg. 2, line 29: "In other words, the evolution of the primary circulation of a TC vortex *must be* (emphasis mine) accompanied by a secondary overturning circulation."

This sentence is insufficiently precise. Purely asymmetric motions can cause an evolution of the mean vortex without mean secondary (overturning) circulation (e.g. a barotropic nondivergent vortex Rossby wave packet and its accompanying wave, mean flow and wave-wave interaction).

Agree. Indeed, as shown by Montgomery and Kallenbach (1997), the propagation of vortex Rossby wave packets and the associated wave-mean-flow interaction can lead to the evolution of vorticity monopoles without the mean secondary circulation in a barotropic nondivergent framework.

The sentence has been removed from the revised manuscript. The paragraph has been rewritten.

Pg. 6, line 1: "Physically, this overturning circulation *is induced by* (emphasis mine) *friction* within the PBL and *diabatic heating* of convection."
Again, this statement should be sharpened. A moving, inviscid, baroclinic vortex on a beta plane will cause asymmetries, which will generally induce an overturning circulation and mean vortex evolution even without friction and diabatic heating (see, e.g., Flatau et al. 1994, JAS).

Agree. For a baroclinic vortex, the horizontal advection of the relative vorticity caused by the β effect is much greater in the lower troposphere (where the vortex is strongest) than it is in the upper troposphere (where the vortex is weakest). This causes the lower tropospheric portion of the vortex to be advected to the northwest more rapidly than it is in the upper troposphere. It also results in a slightly upwind-tilted structure of the vortex. The quasi-geostrophic omega equation enables us to diagnose vertical motions as a function of the

differential advection of cyclonic relative vorticity. In this scenario, forcing for descent is found to the northwest and forcing for ascent is found to the southeast. However, we note that the resulting secondary (overturning) circulation by the β effect is much weaker than that induced by friction in the boundary layer and diabatic heating.

The sentence has been removed from the revised manuscript. The paragraph has been rewritten.

7. Pg. 3, line 10. Re WISHE and Emanuel 1986. This is a misleading and inaccurate description of scientific history. Emanuel 1986 is a steady-state hurricane theory (!) and not an intensification theory. The WISHE acronym was not introduced until 5 years later by Yanno and Emanuel 1991. The WISHE *feedback mechanism* of intensification was articulated by e.g. Emanuel (2003). Following the credible scientific challenges of Montgomery et al. (2009, 2015), WISHE has now been redefined (Zhang and Emanuel 2016) to mean just the formula for the wind dependent moist enthalpy flux at the air-sea interface.

Agree. The sentence has been removed from the revised manuscript. The paragraph has been rewritten.

Continued:

Line 14. Potentially misleading. Smith and Montgomery were well aware of the limitations of the boundary layer definition used in the hurricane community and noted as such in Smith and Montgomery (2010).

Smith and Montgomery (2010) has been referenced in the manuscript. This is one of papers that motivated our study.

Line 16: Inaccurate. Smith and Montgomery did not assume that the vertical velocity was zero in the boundary layer! (If a slab boundary layer model was being used, then there would be no vertical advection of AAM *out of the boundary layer* assuming the boundary layer was well mixed in AAM. This is hardly the same as assuming that the vertical velocity is zero *within* the boundary layer!)

We agree on the comments that Smith and Montgomery did not assume the vertical velocity was zero in the boundary layer. However, there is something we want clarify here. It is important to distinguish the mean vertical velocity $\overline{w}$ and vertical velocity fluctuations w' in the boundary layer. While $\overline{w}$ is important in mass conservation and in the advection of material, it is less important in terms of vertical transport since fluxes are determined by the covariance of the perturbation of a scalar and w'. In the boundary layer, $\overline{w}$ is considerably small compared to w'. When calculating vertical turbulent fluxes, $\overline{w}$ is often neglected (Stull 1988). This is what we meant when we say "the mean vertical velocity in the PBL is negligible". This has been clarified in the revised manuscript. Please see Page 3, lines 23 – 24 in the revised manuscript.

8. Pg. 4, Lines 14-15. Inaccurate. Montgomery and Kallenbach 1997 and Persing et al. 2013 did not root their interpretation of eddy spin up on upscale energy cascade. These authors used a momentum-based approach, which hinges on the eddy vorticity flux (in the barotropic nondivergent case) and the eddy vorticity flux and eddy vertical advection of eddy tangential momentum in the 3D cloud-representing configuration (see Persing et al. 2013, their section 6). The difference is subtle because the eddies can act *locally* to spin up the maximum mean tangential wind and radial inflow/outflow *even while consuming energy from the system-scale mean vortex.*

Agree. The sentence has been removed from the revised manuscript. The paragraph has been rewritten.

Continued:

Line 26: "multiplication by density first" is missing.

Agree. The paragraph has been rewritten in the revised manuscript.

9. Pg. 5, Lines 4-5: "In numerical simulations, Eq. (6) is the equation that governs the azimuthal-mean overturning circulation of a TC vortex."

This statement is physically misleading. The azimuthal mean overturning circulation in a legitimate 3D forecast model such as HWRF is governed in part by the radial and vertical momentum equations. Equation (6) is merely a constraint that must apply at all times and does not "govern" the overturning circulation.

Agree. In 3D models, the azimuthal-mean overturning circulation is governed in part by the radial and vertical momentum equations.

However, one may derive a secondary overturning circulation from Eq. (6) with certain assumptions. For example, neglecting eddy forcing terms in Eq. (6) and assuming that a vortex is in a steady state, i.e., a vortex satisfying hydrostatic balance and gradient wind balance, Eq. (6) simplifies to the thermal wind relationship, $g\frac{\partial \overline{x}}{\partial r}+\frac{\partial(\overline{x}C)}{\partial z}=0$, where $\overline{\chi}=\frac{1}{\overline{\theta}}$. Smith et al. (2005) and Bui et al. (2009) showed that by taking the time derivative of this equation, eliminating the time derivatives of $\overline{\chi}$ and $\overline{v}$ using the azimuthal-mean heat budget equation and tangential wind budget equation, and representing the azimuthal-mean radial and vertical velocity in terms of a streamfunction ($\overline{u}=-\frac{1}{r\overline{\rho}}\frac{\partial\overline{\psi}}{\partial z}$, $\overline{w}=\frac{1}{r\overline{\rho}}\frac{\partial\overline{\psi}}{\partial r}$), an analytical expression of the overturning circulation known as Sawyer-Eliassen equation (SEE) can be derived,

$$\frac{\partial}{\partial r}\left[-\frac{1}{r\overline{\rho}}\frac{\partial\overline{\psi}}{\partial z}\frac{\partial(C\overline{\chi})}{\partial z}-g\frac{1}{r\overline{\rho}}\frac{\partial\overline{\psi}}{\partial r}\frac{\partial\overline{\chi}}{\partial z}\right]+\frac{\partial}{\partial z}\left[\left(\overline{\chi}\xi(f+\zeta)+C\frac{\partial\overline{\chi}}{\partial r}\right)\frac{1}{r\overline{\rho}}\frac{\partial\overline{\psi}}{\partial z}-\frac{1}{r\overline{\rho}}\frac{\partial\overline{\psi}}{\partial r}\frac{\partial(C\overline{\chi})}{\partial z}\right]=g\frac{\partial}{\partial r}(\overline{\chi}^2Q)+\frac{\partial}{\partial z}(C\overline{\chi}^2Q)-\frac{\partial}{\partial z}\left[\overline{\chi}\xi\left(F_\lambda+F_{sgs_\lambda}\right)\right],$$

where $\xi = f + \frac{2\overline{v}}{r}$, $\zeta = \frac{\overline{v}}{r} + \frac{\partial \overline{v}}{\partial r}$, $C = \frac{\overline{v}^2}{r} + f\overline{v}$, and $Q = \dot{\theta} + F_\theta + F_{sgs\_\theta}$ representing diabatic heating and eddy forcing for heat. Since the hydrostatic balance and gradient wind balance are used, SEE can only diagnose the overturning circulation in response to diabatic heating and tangential eddy forcing. It does not provide any information on how radial and vertical eddy forcing affects the overturning circulation, in other words, SEE cannot be applied in an unbalanced framework when radial eddy forcing is important. Smith et al. (2009) showed that one of the spin-up mechanisms of the mean tangential circulation involves the convergence of AAM within the boundary layer associated with the development of supergradient wind speeds in the boundary layer.

With Eq. (6), one may derive a SEE-like equation to diagnose the mean overturning circulation in response to those factors that were omitted by SEE. For example, we may include the radial eddy forcing in the simplified Eq. (6), then, the thermal wind relationship is replaced by $g\frac{\partial \overline{\chi}}{\partial r} + \frac{\partial [\overline{\chi}(C+F_R)]}{\partial z} = 0$, where $F_R = F_r + F_{sgs\_r}$ is the radial eddy forcing. Following the same procedure, one may derive a SEE-like equation,

$$\frac{\partial}{\partial r}\left[-\frac{1}{r\overline{\rho}}\frac{\partial \overline{\psi}}{\partial z}\frac{\partial (C\overline{\chi})}{\partial z} - g\frac{1}{r\overline{\rho}}\frac{\partial \overline{\psi}}{\partial r}\frac{\partial \overline{\chi}}{\partial z}\right] + \frac{\partial}{\partial z}\left[\left(\overline{\chi}\xi(f+\zeta) + C\frac{\partial \overline{\chi}}{\partial r}\right)\frac{1}{r\overline{\rho}}\frac{\partial \overline{\psi}}{\partial z} - \frac{1}{r\overline{\rho}}\frac{\partial \overline{\psi}}{\partial r}\frac{\partial (C\overline{\chi})}{\partial z}\right] = g\frac{\partial}{\partial r}(\overline{\chi}^2 Q) + \frac{\partial}{\partial z}(C\overline{\chi}^2 Q) - \frac{\partial}{\partial z}\left[\overline{\chi}\xi\left(F_\lambda + F_{sgs_\lambda}\right)\right] + \left\{\frac{\partial}{\partial r}\left[\frac{1}{r\overline{\rho}}\frac{\partial \overline{\psi}}{\partial z}\frac{\partial (F_R\overline{\chi})}{\partial z}\right] + \frac{\partial}{\partial z}\left[F_R\left(-\frac{1}{r\overline{\rho}}\frac{\partial \overline{\psi}}{\partial z}\frac{\partial \overline{\chi}}{\partial r} + \frac{1}{r\overline{\rho}}\frac{\partial \overline{\psi}}{\partial r}\frac{\partial \overline{\chi}}{\partial z} + \overline{\chi}^2 Q\right) - \overline{\chi}\frac{\partial F_R}{\partial t}\right]\right\}.$$

Similar to SEE, this is an elliptical partial differential equation but includes additional radial eddy forcing terms. It can be solved using the same method of solving SEE. Likewise, we can include different terms in Eq. (6) to derive SEE-like equations with different complexities, and use these diagnostic equations to evaluate how different factors regulate the overturning circulation in an unbalanced framework. We have been using this method to diagnose HWRF model output. The results will be reported in a separate paper.

We understand the reviewer's concern. Since Eq. (6) is not so critical for this study, we have removed it from the revised manuscript. The related sentences have been rewritten in the revised manuscript. Please see Page 5, lines 5– 13 in the revised manuscript.

Continued:

Line 6: "In classic TC theories". Citations please.

Citations have been provided in the revised manuscript. The related sentences have been rewritten. Please see Page 5, line 5 in the revised manuscript.

Lines 7-8: This statement is incorrect. The eddy forcing terms can be zero, but acceleration terms may still be nonzero.

Lines 7-8? We couldn't find the sentence in the manuscript, but we agree on the comment that the eddy forcing can be zero, but acceleration may still be nonzero. This is easy to see from the azimuthal-mean tangential wind budget equation.

Line 10: Why is Equation (8) to be time differentiated? Please explain.

As we explained previously, the purpose to differentiate Eq. (8) with respect to time is to derive a diagnostic equation for the mean secondary overturning circulation. Eq. (8) has been removed from the revised manuscript and the related paragraph has been rewritten.

10. Pg. 7, the text pertaining to Equations (9) and (10). My reading of this text is as follows: the HWRF model uses this two-component formulation for Km (i.e. the Hong and Pan closure in the BL/TL (Eq. 9) and the Smagorinsky closure with stability modification by Lilly above the BL/TL (Eq. 11), respectively) in the vertical and horizontal mixing terms for momentum, heat and moisture. Is this summary correct? Please clarify.

To answer this question and the question below, let's first review the main characteristics of turbulence. On the turbulent energy spectrum, large turbulent eddies are directly generated by the instabilities of the mean flow and obtain energy directly from the mean flow. These large energy-containing eddies, such as convective thermal plumes or boundary layer roll vortices generated by the inflection-point instability, are anisotropic. Large eddies then transport their energy through the energy cascade process to smaller-scale eddies. Smaller eddies contain less energy and are less flow-dependent and more isotropic than larger eddies. Eventually the eddy energy is dissipated into heat via molecular viscosity. On the energy spectrum, there is an intermediate range of scales known as inertial sub-range where the net incoming energy from larger-scale eddies is in equilibrium with the net energy cascading to smaller-scale eddies. The turbulent kinetic energy is neither generated nor dissipated in the inertial sub-range, just transferring from larger to smaller eddies. Eddies with scales smaller than inertial sub-range are commonly considered to be isotropic.

For numerical simulations with horizontal grid spacing smaller than inertial sub-range, such as large eddy simulations (LESs), large anisotropic energy-containing eddies are explicitly resolved by models, thus, only small eddies need to be parameterized.
Since eddies with scales smaller than inertial sub-range are isotropic, LES models treat the isotropic SGS horizontal and vertical turbulent mixing using 3D SGS turbulent mixing scheme, which is directly coded within the model dynamic core, rather than placing it a physics module outside the dynamic core. Smagorinsky SGS turbulent model (Smagorinsky 1963) is a 3D SGS mixing scheme widely used in LESs in which the eddy exchange coefficient is calculated by $\boldsymbol{K(x,y,z,t)} = (\boldsymbol{c}\Delta)^2 \left[\frac{\partial \bar{u}_i}{\partial x_j}\left(\frac{\partial \bar{u}_i}{\partial x_j} + \frac{\partial \bar{u}_j}{\partial x_i}\right)\right]^{\frac{1}{2}}$, where $\Delta = (\Delta \boldsymbol{x}\Delta \boldsymbol{y}\Delta \boldsymbol{z})^{\frac{1}{3}}$ and $\boldsymbol{c}$ is an empirical coefficient. Note that the original Smagorinsky scheme does not consider the stability effect. In the later practice, many LES models use the Smagorinsky scheme along with stability correction, e.g. MacVean and Mason (1990) stability correction. Deardroff 3D TKE SGS scheme is another 3D SGS mixing scheme is widely used in LESs.

In contrast, for numerical models with large horizontal grid spacing (e.g., greater than 1 km), large energy-containing eddies are not resolved, but are part of the SGS processes. In this case, it is not appropriate to use 3D SGS scheme to parameterize these large eddies since they

are anisotropic. Therefore, the vertical and horizontal SGS mixing must be treated differently in these numerical models. The current method is to retain the SGS mixing (or diffusion) model built within the dynamic core to treat the SGS horizontal mixing, but to have a separate physics module often called PBL scheme (or more precisely the vertical turbulent mixing scheme) outside the dynamic core to handle SGS vertical mixing. The PBL scheme for treating vertical SGS mixing is a one-dimensional (1D) scheme.

Now for the reviewer's question, Eq. (9) and Eq. (10) in the original manuscript only describe the vertical eddy exchange coefficients within and above the diagnosed PBL height used in the 1D PBL scheme module outside the dynamic core. The above-PBL eddy change coefficient, Eq. (10), is determined based on the resolved vertical shear and gradient Richardson number ($K_m = l^2 f_m(Ri_g)\sqrt{\left|\frac{\partial \tilde{u}}{\partial z}\right|^2 + \left|\frac{\partial \tilde{v}}{\partial z}\right|^2}$). This method has been adopted by many PBL schemes, such as YSU scheme. So, it is not the Smagorinsky diffusion model. As we stated previously, in numerical models, the Smagorinsky diffusion model is not a separate physics module but is built within the model dynamic core. In HWRF, the SGS diffusion model built within the dynamic core is a revised 2D Smagorinsky scheme, which is used to treat SGS horizontal mixing. The horizontal eddy exchange coefficient is determined by $K_h = L_h^2 D_h$, where L_h is a tunable mixing length and $D_h = (\frac{\partial \tilde{v}}{\partial x} + \frac{\partial \tilde{u}}{\partial y})^2 + (\frac{\partial \tilde{u}}{\partial x} - \frac{\partial \tilde{v}}{\partial y})^2$ is the deformation (Zhang et al. 2018).

Bryan and Rotunno (2009) and Bryan (2012) use a much higher value of Km for horizontal diffusion than employed here. How do the authors explain this difference in model formulation compared to Bryan and Rotunno?

As explained previously, in mesoscale models, the SGS horizontal mixing and vertical mixing are treated separately because of the unresolved anisotropic large eddies. SGS horizontal mixing is handled within the model dynamic core by a built-in diffusion model, whereas SGS vertical mixing is treated by a separate physics module known as PBL scheme outside the dynamic core. Bryan and Rotunno (2009) and Bryan (2012) focused on the horizontal diffusion problem and investigated the sensitivity of TC evolution to horizontal eddy exchange coefficients by adjusting the tunable mixing length. In our study, we did not touch anything related to the SGS horizontal mixing. We only focused on the SGS vertical mixing, particularly, the vertical turbulent mixing above the PBL generated by the cloud processes associated with the eyewall and rainband convection. This has been clarified in the revised manuscript. Please see Page 7, lines 9 – 18.

Within the 1D PBL scheme framework, there are two ways that we may use to include in-cloud turbulent mixing parameterization in the scheme. The first method is what we did in this study to extend the diagnosed boundary layer so that the layer includes turbulence generated by both surface processes and cloud processes aloft. The disadvantage is that this method has problems to include the turbulence in the anvil clouds in the upper troposphere associated with outflow because the anvil clouds are detached from the PBL turbulence in a vertical model column. The second method is to keep the current 1D turbulent mixing parameterization framework unchanged but improve the stability calculation above the

boundary layer by including cloud effects. Currently, most of the schemes used today calculate the Brunt-Vaisala frequency as $N^2 = \frac{g}{\theta_0}\frac{\partial \overline{\theta_v}}{\partial z}$. But this formula is not sufficient to account for the buoyancy generated by clouds. Emanuel and Rotunno (2011) and Emanuel (2012) also suffered this problem when they calculated the Brunt-Vaisala frequency in the outflow.

Using a parcel theory, Durran & Klemp (1982) showed that an accurate Brunt-Vaisala frequency in the saturated atmosphere can be expressed as $N_m^2 = g\left\{\frac{1+B}{1+A}\left[\frac{d\ln\theta}{dz} + \frac{1}{C_pT}\left(1+\frac{q_s}{\varepsilon}\right)\left(AC_p\frac{dT}{dz} - Bg\right)\right] - \frac{dq_t}{dz}\right\}$, where $A = \frac{L^2 q_s}{C_p R_v T^2}$, $B = \frac{Lq_s}{RT}$, q_s and q_t are the saturated and total mixing ratio including condensate and precipitation. We have been testing this method in HWRF simulations (see our presentation at 2018 HFIP Annual Review Meeting). We will report the second method and the results in a separate paper.

Another advantage of the second method by calculating accurate Brunt-Vaisala frequency in clouds is that it may be used to improve horizontal SGS mixing parameterization. Current studies (e.g. Bryan and Rotunno 2009, Bryan 2012, Zhang et al. 2018) simply adjusted the mixing length, which does not have much physics behind it. In-cloud stability changes resulting from the accurate calculation of Brunt-Vaisala frequency in clouds can also affect horizontal SGS mixing. We shall investigate this issue in our future research.

11. Pg. 14, Lines 1-2. " . . . since the large energy-containing turbulent eddies are not resolved at the current model resolution of 2 km." What are these large energy-containing eddies in these simulations and in real-life tropical cyclones?

The unresolved large eddies at the model resolution of 2 km may include buoyancy-driven kilometer and sub-kilometer convective cells or elements in the eyewall and rainbands and roll vortices generated by the inflection-point instability in the boundary layer. These large eddies can induce effective non-local vertical mixing. However, the above-PBL convective elements are difficult to parameterize since the stretching vertical grid used by models causes low vertical resolutions above the boundary layer. Even with the relative high vertical resolution within the boundary layer, Zhu (2008) showed that PBL schemes used in WRF cannot appropriately account for the vertical transport induced by roll vortices explicitly simulated by WRF-LES. This has been clarified in the revised manuscript.

12. Figures 10 and 11. The resolved eddy-forcing tendency for the azimuthally averaged tangential velocity tendency equation is plotted in cross section and on several horizontal height surfaces. In these panels the units are displayed as inverse seconds. Shouldn't the units be that of acceleration (if instantaneous tendencies averaged over some finite time interval) or meters per second (if integrated over some time finite interval)? Please clarify here and elsewhere.

We are very sorry for this mistake. The unit should be ms^{-2}. This has been corrected.

Response to Reviewer 2

This study introduces an in-cloud turbulent mixing parameterization for the HWRF model. The rationale for this parameterization is that the classic HWRF PBL parameterization scheme does not account for intense mixing in eyewall/rainband clouds. The authors admit their scheme is a rather crude approximation of mixing, but it seems to help with producing better hurricane intensity predictions.

This is a promising study. Under the premise that the results are not cherry-picked, the improvements are quite astonishing. However, there are a number of issues that should be addressed to improve the manuscript. One of them is some amount of carelessness when describing the results and the figures. This and other issues are detailed below.

We very much appreciate the reviewer for his thoughtful and constructive comments. The manuscript has been revised accordingly based on the comments. We hope that the revised manuscript is satisfactory for publication. Below is the point-to-point response to reviewer's comments.

General Comments:

1. One of the weaknesses of this study is that the authors do not discuss why the eddy forcing would be responsible for TC spin-up. There are some hand-wavy arguments about interactions between the turbulence and microphysics but the reader is left in the dark with what's actually going on.

To date TC rapid intensification (RI) is still not fully understood. One of the arguments is that the processes governing RI are primarily axisymmetric. Vigh et al. (2018) showed that the observed RI of several major hurricanes can be well reproduced by the CHIPs model, a simple axisymmetric 2D radius-height dynamic model developed by Emanuel et al. (2004). Their results are consistent with previous studies by Nolan and Grasso (2003) and Nolan et al. (2007) who showed that it is the vortex axisymmetric response to the azimuthally-averaged diabatic heating (rather than the heating associated with individual asymmetries) that is responsible for the resultant intensity change in their simulations. These theoretical studies are supported by observations. From a large amount of 37 GHz microwave products, Kieper and Jiang (2012) showed that the appearance of a cyan color ring around the storm center is highly correlated to subsequent RI, provided that environmental conditions are favorable. This result is supported by the TRMM Precipitation Radar (PR) data (Jiang and Ramirez 2013; and Tao and Jiang 2015), which showed that nearly 90% of RI storms in different ocean basins formed a precipitation ring around the storm center prior to RI.

Back to the question of how eddy forcing contributes to the RI. The answer lies in the fact of how eddy forcing facilitates the realization of axisymmetric dynamics responsible for RI. A key difference between a 3D full physics simulation and a 2D axisymmetric simulation is that a TC vortex is prescribed to be axisymmetric in the latter, whereas in the former a simulated TC vortex is often not axisymmetric enough to efficiently convert latent heating to kinetic energy. Thus, whether a 3D full physics simulation can well capture RI depends on if TC internal dynamics including eddy forcing can organize the eyewall convection into a convective annulus. This may explain why the azimuthally averaged heating rate in a 3D full

physics simulation is often smaller than that in a 2D axisymmetric simulation. However, there are examples in literature that showed the energy conversion in 3D full physics model simulations can be as efficient as that in an axisymmetric model simulation. For instance, Persing et al. (2013) reported that "there is a short period of time when the rate of spin-up in the 3D model exceeds that of the maximum spin-up rate in the axisymmetric model, and during this period the convection is locally more intense than in the axisymmetric model and the convection is organized in a quasi ring-like structure resembling a developing eyewall".

In our simulations, the modified HWRF is able to produce a well-defined quasi-closed ring around the storm center and the size of the ring is similar to the observed one, implying that the RI of simulated hurricanes is likely governed by the axisymmetric dynamics articulated by Vigh et al. (2018) and Nolan et al. (2007). In contrast, the default HWRF is unable to simulate the observed TC inner-core structure, suggesting that it fails to generate the TC axisymmetric dynamics needed for the RI. Our results also indicate that the SGS physics involving with the eyewall in-cloud turbulent mixing above the PBL and the resultant change in storm structure and resolved eddy forcing facilitate the realization of the axisymmetric dynamics responsible for RI in 3D full-physics simulations. Our simulations are consistent with Persing et al. (2013) who showed that the 3D eddy processes can assist the intensification process by contributing to the azimuthally averaged heating rate, to the radial contraction of the maximum tangential velocity, and to the vertical extension of tangential winds through the depth of the troposphere. The discussions/comparisons between our simulations and Persing et al. (2013) simulations have been included in the revised manuscript. Please see Page 2, line 23 – Page 3, line 7; Page 6, lines 13 – 25; Page 15, lines 18 - 25; Page 16, lines 17 – 23; Page 17, lines 17 – 20.

2. How does this work relate to the LES hurricane studies by George Bryan (or the LES work of the first author)? My recommendation is to relate this work to previous TC studies that employ an LES approach.

In numerical simulations, the high order terms caused by the nonlinearity of turbulent flow need to be parameterized in order to close the governing equations. In the state-of-the-art numerical models, a SGS parametric model is coded within the model dynamic core (or solver) to account for the SGS mixing. For convection permitting simulations with a horizontal grid-spacing greater than 1 km, large turbulent eddies with scales greater than Kolmogorov inertial subrange are not resolved. These energy-containing eddies generated directly by the instabilities of the mean flow are fundamentally anisotropic. A common method to account for the directional dependent turbulent transport induced by anisotropic eddies is to retain the SGS model built within the model dynamic solver to treat the horizontal turbulent mixing, but to have a separate physics module, often called the planetary boundary layer (PBL) scheme outside the dynamic solver to handle vertical turbulent mixing. The PBL scheme for treating vertical SGS mixing is a one-dimensional (1D) scheme. This method is used by HWRF and many other mesoscale models.

As model grid spacing reduces down to the inertial subrange, large energy-containing eddies are explicitly resolved, and thus, the only eddy processes that need to be parameterized are those with scales smaller than the inertial subrange. These small eddies are commonly

considered to be isotropic. Because of this, there no need to have a separate module to treat vertical turbulent mixing like convection permitting simulations. Rather, the horizontal and vertical SGS mixing induced by isotropic eddies can be handled by the same SGS model built within the model dynamic solver. This type of simulation is the so-called LES. The key is that it requires a 3D SGS model so that both the vertical and horizontal mixing induced by isotropic eddies can be appropriately parameterized. In this sense, the approach of our LES study is similar to that of Bryan et al. (2003), Green and Zhang (2015), and Zhu (2008) in terms of both model grid resolution and the way of treating SGS mixing.

Since eddies with scales smaller than inertial subrange contain much less energy and are less flow-dependent than large energy-containing eddies, the LES methodology is commonly thought to be insensitive to formulaic details and arbitrary parameters of the SGS model, and thus, the turbulent flow generated by LESs are often used as a proxy for reality and a basis for understanding turbulent flow and guiding theories when direct observations are difficult to obtain. In the past, LESs were mainly used to elucidate problems associated with the turbulent processes within the PBL. Here we use this approach to better understand the turbulent processes in the eyewall.

While using LES to simulate TC is promising, evaluation of the fidelity of the simulated TC vortex and the associated fine-scale structures resolved by LES is a challenge. In the absence of decisive observational measurements, the principal method of evaluating LES has been through sensitivity studies of individual LES models with different SGS mixing schemes or inter-comparisons among different LES models. The logic is that the robustness of the simulations testifies to its fidelity. Such sensitivity tests and inter-comparison studies in the past have shed favorable light on the LES approach in general in many meteorological applications, but they also raised questions about the ability of LES to realistically reproduce some unique features in the atmosphere. While there are individual LES studies of TCs, the sensitivity of LES to SGS parameterization has never been examined when the LES approach is used to simulate TCs. Such sensitivity tests are needed since intense turbulence in the eyewall can exist well beyond the PBL. Therefore, our LES work is motivated to gain insight into the global behavior of Giga-LES in TC modeling. We have tested three 3D SGS models commonly used in LESs: (a) 3D Smagorinsky SGS model (Smagorinsky, 1963), (b) 3D 1.5-order TKE SGS model (Deardorff, 1980), and (c) 3D nonlinear backscatter and anisotropy (NBA) SGS model (Kosović, 1997). This work has been completed and submitted to *Journal of Advances in Modeling Earth Systems*. Here we used some of the results from this study. This has been clarified in the revised manuscript. Please see Page 7, lines 9 – 18; Page 9, line 10 – Page 10, line 11.

3. Show aggregate statistics of how much improvement the turbulence parameterization yielded. Even though the authors present more than just a case study, there is no mention of the results from all their simulations. If these aggregate results were included, there would be less suspicion about "cherry picking".

We have been collaborating with the Environmental Modeling Center (EMC), NOAA, on this work. EMC tested the scheme in HWRF full cycle simulations using the HWRF

operational version at that time. The results show that the modified HWRF significantly reduces the bias of maximum wind speed (Fig. 1). The total number of case simulations for different lead time is 1079. The results have been added in the revised manuscript. Please see Page 18, lines 13 – 17 and Figure 16.

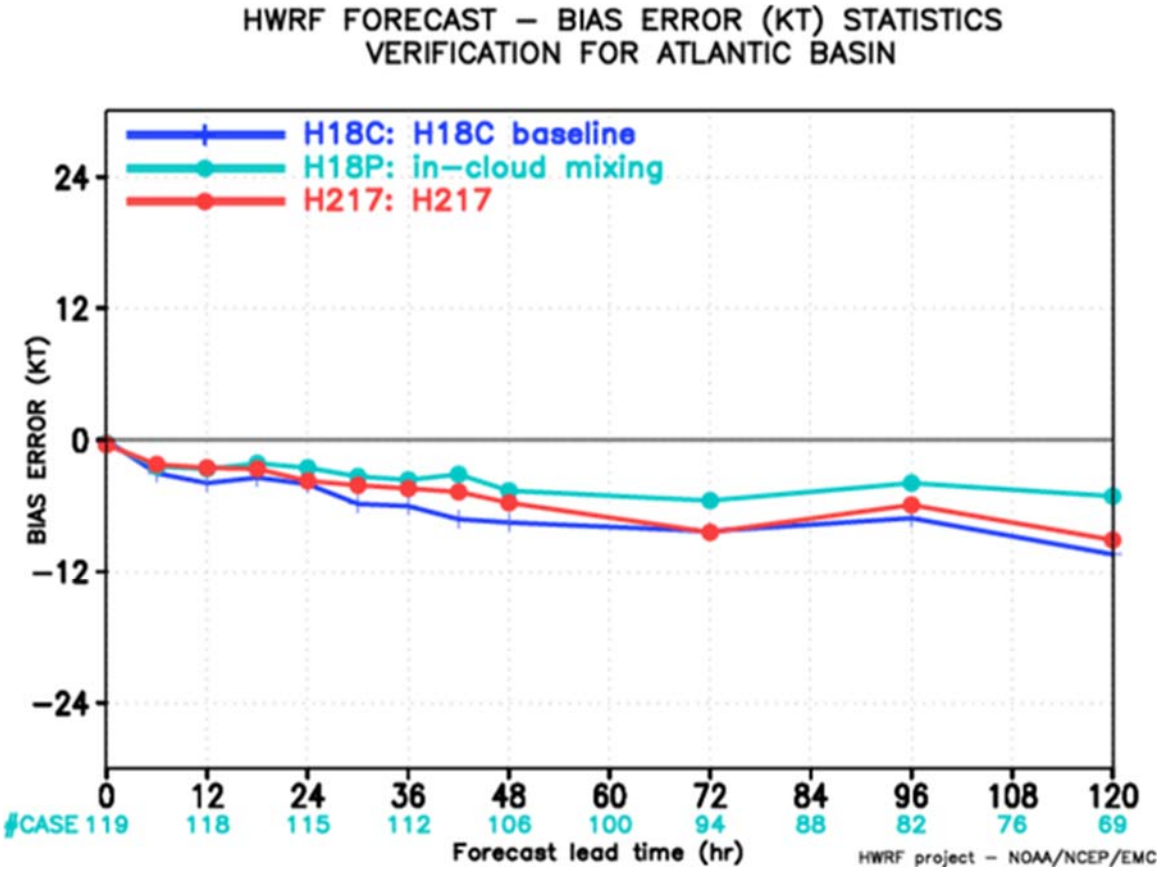

Figure. 1: Maximum wind speed bias error (kt) as a function of forecast lead time (hr) averaged over all tested storms and cycles. Average bias errors are shown for the 2018 HWRF model baseline (H18C, blue), 2018 HWRF model including in-cloud turbulent mixing (H18P, cyan), and 2017 operational HWRF model (H217, red). The storms tested included Hermine (2016), Harvey (2017), Irma (2017), Maria (2017), and Ophelia (2017). The total number of cases for various forecast lead times is indicated by the cyan labels at the bottom (Courtesy to Dr. Sergio Abarca at EMC NOAA).

4. There is no discussion of how large the eddy exchange coefficient of momentum, Km, should be (see also comment XX below). Can't you compute Km from your prior LES work and compare it to the values you get from the parameterization?

It remains a mystery as to what the real value of vertical eddy exchange coefficients in the eyewall should be because of the difficulties to obtain vertical turbulent fluxes in the eyewall observationally. There are also difficulties to calculate vertical turbulent fluxes from the LES output. One of them is how to appropriately define the mean of a variable. For fast responding in-situ observations, the mean is commonly calculated as the average over a time

period, and then, using the eddy correlation method to calculate the covariance of two variables. For classic LES applications in non-TC conditions, the domain-mean is often used when calculating vertical turbulent fluxes, which is appropriate as the ambient condition of the PBL is assumed to be horizontally homogeneous. However, such a method cannot be extended to LES of a TC as the fields of a storm vortex are not horizontally homogeneous. If a mean would include both violent eyewall and peaceful eye, the estimated covariance would be exaggerated. Furthermore, if the eddy correlation method is applied to the entire LES domain, then, one would only obtain one vertical profile of eddy exchange coefficient. It would be incorrect to apply this vertical profile to both eyewall and eye as the turbulent mixing in these two regions is completely different. One way to solve this problem is to define a sub-domain centered at each model grid, and then, use the LES output in the sub-domain for vertical flux calculation at each grid using eddy correlation method via,

$$F_{\varphi} = \overline{w'\varphi'} = \overline{(w - \overline{w})(\varphi - \overline{\varphi})} \quad (1)$$

where φ is a generic scalar, F_{φ} is the vertical flux of φ at each grid, w is the vertical velocity, overbar and prime indicate the average over the sub-domain and the deviation away from the average, respectively. In the first-order closure, the vertical momentum flux components may be represented as,

$$\overline{w'u'} = -k_m \frac{\partial \overline{u}}{\partial z}, \qquad \overline{w'v'} = -k_m \frac{\partial \overline{v}}{\partial z}, \quad (2)$$

where k_m is the eddy exchange coefficient of momentum, $\frac{\partial \overline{u}}{\partial z}$ and $\frac{\partial \overline{v}}{\partial z}$ are the vertical gradient of mean wind components over the sub-domain. In the eyewall, the non-local mixing induced by the convective eddies (or cells) generates a large amount of up-gradient vertical fluxes, thus, to account for the up-gradient vertical transport in the first-order closure, the momentum eddy exchange coefficient is calculated as,

$$K_m = \tau \Big/ \sqrt{(\frac{\partial \overline{u}}{\partial z})^2 + (\frac{\partial \overline{v}}{\partial z})^2} \quad (3)$$

where $\tau = (\overline{w'u'}^{\,2} + \overline{w'v'}^2)^{\frac{1}{2}}$ is the total vertical momentum fluxes.

Another important thing that needs to be considered is how large the sub-domain should be because the size of a sub-domain determines the contributions to the vertical fluxes from different scales of resolved eddies by LES. The horizontal grid resolution of HWRF-v3.8a is 2 km, meaning that eddies with scales greater than 2 km are resolved by HWRF. What need to be parameterized by HWRF PBL scheme are the vertical transport induced by eddies smaller than 2 km. Thus, in this study a 2 x 2 km^2 box is used as the sub-domain for vertical flux calculation at each grid point. Figure 2a below shows the azimuthal-mean radius-height distribution of the total vertical momentum fluxes, τ, induced by the resolved eddies with scales smaller than 2 km from the LES run that uses the 3D NBA SGS model. The vertical profiles of eddy exchange coefficients of momentum from the three LESs that use different SGS models averaged over the radii of 30 - 60 km (where the eyewall is located) are shown in Fig. 2b. Note that the results shown in the figure have been averaged over 3 – 8 simulation hours and the SGS eddy exchange coefficients are the direct output from the SGS models. It clearly shows that the strong vertical momentum fluxes induced by the resolved eddies keep

increasing with height and reach the peak above the PBL (defined in the conventional way) in the low troposphere, and then, extend all the way up to the upper troposphere in the eyewall. There is no discontinuity across the PBL that separates the turbulent transport generated by the surface turbulent processes and cloud turbulent processes aloft in the eyewall. The resolved eddy exchange coefficients in the eyewall appear to be large and dominate the SGS coefficients. This is mainly caused by the limitation of using down-gradient parameterization of the first-order closure to represent non-local mixing in the eyewall where the combined effects of the large up-gradient vertical transport and small vertical gradient of mean variables lead to the large eddy exchange coefficient.

Figure 2 and the related discussions have been included in the revised manuscript. Please see Page 10, line 12 – Page 11, line 21.

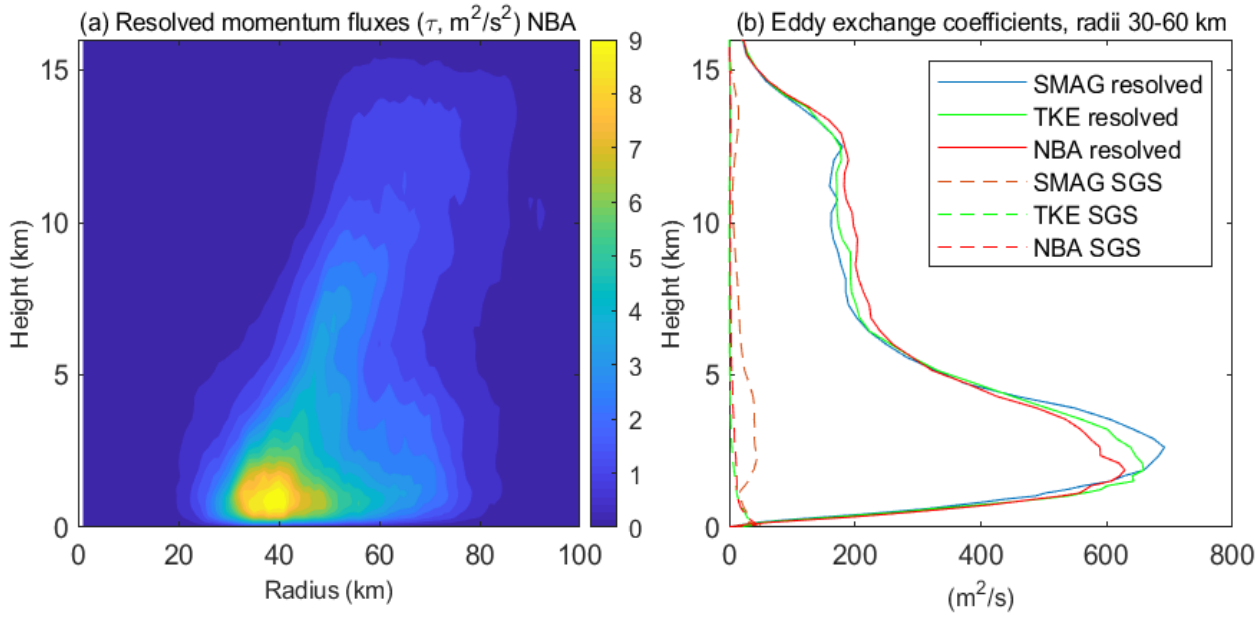

Figure 2: (a): Azimuthal-mean radius-height distribution of the vertical momentum fluxes, $\boldsymbol{\tau = (\overline{w'u'}^{\,2} + \overline{w'v'}^{2})^{\frac{1}{2}}}$, induced by the resolved eddies with scales smaller than 2 km from the WRF-LES that uses the 3D NBA SGS model. (b): Vertical profiles of the parameterized (dashed) and resolved (solid) vertical eddy exchange coefficients of momentum averaged over 30 – 60 km radii (where the eyewall is located) from the three LESs that use different 3D SGS models. Note that the results are averaged over 3 – 8 simulation hours and the SGS eddy exchange coefficients are the direct output from the 3D SGS models used in the simulations.

Specific Comments:

1. The title is misleading. Given this title, I'd expect a more quantitative study on the turbulent processes and their roles, but the actual manuscript is more about describing and applying the turbulence parameterization.

Turbulent processes associated with TC eyewall and rainbands are complicated problems as they are beyond the conventional scope of the PBL. To our knowledge, the importance of eyewall turbulent mixing above the PBL to TC evolution has not been addressed before. In numerical simulations, the asymmetric eddy forcing to TC evolution consists of both resolved and SGS components. In this study, we showed that in the convection permitting simulations at grid resolution of 2 km, the resolved eddy forcing and the TC inner-core structure (and thus the TC intensity) are sensitive to the parameterization of the turbulent mixing in eyewall clouds above the PBL. Indeed, our manuscript describes the in-cloud turbulent mixing parameterization and its application in HWRF, but the main purpose of this paper is to demonstrate and explore the sensitivity of TC intensification to the change in eddy forcing resulting from the SGS turbulent mixing parameterization. As we stated in the summery of the manuscript, our treatment of in-cloud turbulent mixing itself is crude, and thus, the scheme may not be ready for use in operational TC forecasts in its current form. Nonetheless, our results show that numerical simulations of TC intensification are sensitive to the parameterization of SGS turbulent mixing induced by the cloud processes above the PBL in the eyewall and rainbands.

In fact, the PBL scheme used in HWRF is not the only scheme that has problems to represent in-cloud turbulent processes in deep convective clouds. Using WRF-ARW, we simulated a deep convective system with various PBL schemes available in WRF. These include the YSU (Hong et al. 2006), GFS (Hong and Pan 1996), ACM2 (Pleim 2007), MYJ (Janjic 1994), QNSE (Sukoriansky et al. 2005), MYNN-2.5/MYNN-30 (Nakanishi and Niino 2006, 2009), BouLac (Bougeault and Lacarrere 1989), UW (Bretherton and Sungsu 2009), and GB (Grenier and Bretherton 2001) schemes. None of them can appropriately generate the intense turbulent mixing in the deep convective clouds above the boundary layer. For TC simulations, we think that this problem is particularly important and should be addressed in future research. We agree that parts of our paper describes the method to treat in-cloud turbulent mixing and its application in HWRF, but because of this we are able to generate the appropriate eddy forcing above the PBL in the eyewall and rainbands, so that we can look into how eddy forcing in the eyewall and rainbands facilitates the axisymmetric dynamics underlying RI of TCs. We think that the title does reflects this part of our research. We admit that we could do more quantitative analyses on the turbulent processes and their roles in the TC intensification. But as we showed in the paper, the inclusion of an in-cloud turbulent mixing parameterization in the model induces changes not only in the resolved eddy forcing but also TC inner-core structure. On top of that, all these changes are entangled together, thus, we need to find an appropriate method to separate these changes. This will be the focus of our future research.

2. Page 6: “But cumulus schemes are not designed to account for the eddy forcing to the momentum, heat, and moisture budgets but rather serve as a means to remove the convective instability generated by the large-scale flow and alter the thermodynamic structure of the environment based on the parameterized convective fluxes and precipitation (Arakawa and Schubert 1974; Wu and Arakawa 2014).”
—> This is not true for the CLUBB scheme
(https://agupubs.onlinelibrary.wiley.com/doi/full/10.1002/2015GL063672).

We agree that our statement is not accurate. It is true that the original cumulus schemes developed by Arakawa and Schubert (1974) was to remove the convective instability generated by the large-scale flow and alter the thermodynamic structure of the environment based on the parameterized convective fluxes and precipitation. The turbulent mixing was not considered in this regard. However, some later developed more advanced cumulus schemes do consider the effects of turbulent mixing in schemes. The sentence has been rewritten in the revised manuscript. Please see Page 6, lines 1 – 8.

3. Page 12: "In contrast, "TL-HWRF" produces a well-defined closed ring around the storm center that is clearly shown in both dynamic (vertical velocity, Fig. 8b) and thermodynamic (hydrometeor mixing ratio, Fig. 8d) fields." —> Actually, none of the panels in Fig. 8 show a closed ring (although the inner core is much more defined in the TL-HWRF runs). Furthermore, the comparison between observations and model (Figs. 7 and 8) is subjective, hand waving and does not add anything of substance.

We agree with the comments. The convective ring in "TL-HWRF" is not closed, but like the reviewer said, the eyewall structure in "TL-HWRF" is much more well defined than that in the default HWRF. Note that the figures do not means to provide a quantitative comparison between simulations and observations as an apple-to-apple comparison is not possible here because of the apparent difference in satellite images and simulations. However, they do provide a qualitative comparison of how different the TC inner-core structure is in the two HWRF simulations with and without an in-cloud turbulent mixing parameterization when comparing to observations. The inner-core structure difference between the two simulations is apparent and it shows how sensitive the TC inner-core structure to the parameterization of eyewall/rainband turbulent mixing above the PBL. This has been clarified in the revised manuscript and related sentences have been rewritten. Please see Page 14, lines 29 – 31; Page 15, lines 12 – 17.

4. Page 13: "Comparing Fig. 11b with Fig. 10b, it is easy to see that the model resolved eyewall eddy forcing above the PBL in the "TL-HWRF" experiment has a magnitude about 5 times larger than the corresponding SGS eddy forcing, suggesting that the resolved eddy processes provide a major forcing that drives the primary circulation of the TC vortex in this case." —> At first look this contradicts the overall statement that SGS turbulence is important. The authors should comment on this apparent contradiction.

This seemingly paradoxical result can be understood as follows. In a real TC, the eddy forcing consists of a continuous spectrum. But in numerical simulations, the eddy forcing, such as the one in Eq. 2, $\frac{D\widetilde{\bar{M}}}{Dt} = r(F_{\lambda} + F_{sgs\_\lambda})$, is split into the model-resolved and SGS components because of the discretized model grids. Although they appear as two separate terms in the governing equations and are determined separately in numerical simulations, the two split parts of eddy forcing are not independent but interact with each other. This means that we cannot simply judge the importance of resolved and SGS eddy forcings to TC intensification solely based on their individual magnitude, rather, we need to look at how the changes in the SGS parameterization induces the change in the resolved fields and vice versa. Such a mutual dependence is understandable since large energy-containing turbulent eddies, such as kilometer and sub-kilometer convective elements and roll vortices, are not resolved

but parameterized at the current grid spacing of convection permitting simulations. As we showed in the paper, the inclusion of an in-cloud turbulent mixing parameterization substantially changes the structure of the simulated TC vortex, and thus, the changes in the resolved eddy forcing, as well as the axisymmetric TC dynamics. This has been clarified in the revised manuscript. Please see Page 4, lines 14 – 25; Page 20, lines 1 – 2.

5. Page 14: "other 4 major hurricanes" —> four other major hurricanes

Corrected in the revised manuscript.

6. Page 14: As another example, Figure 13 compares the satellite observed vortex inner-core structure of Harvey (2017) with the simulated ones by the two HWRFs during the early and middle stages of Harvey's RI. The asymmetric rainband structure, the closed ring feature around the storm center, and the size of the convective ring shown in satellite observations are reasonably reproduced by TLHWRF." —>Subjective and hand wavy. For a better comparison, the panels should at least be plotted on the same lat/lon domain.

As we replied previously, the limitation of satellite images prevents us performing a quantitative comparison between simulations and observations. Figure 13 is meant to provide a qualitative view of how the inclusion of an in-cloud turbulent mixing parameterization alters the TC inner-core structure when comparing to the observed one. We take the suggestion; this figure has been replotted on the same lat/lon domain in the revised manuscript. Please see the updated Figure 14 in the revised manuscript.

7. Page 14: "one may concern about" —> one may be concerned about

Corrected in the revised manuscript.

8. Fig. 3: Why is there no sign of surface friction?

This is because the figure only shows the resolved vertical fluxes. It does not include the SGS fluxes.

9. Fig. 4e,f: I'm curious, why is there no indication of a melting layer in the reflectivity plots?

In the first version of the Ferrier-Aligo scheme implemented in 2014 version of HWRF, the scheme did include this bright band effect of melting layer. But in the later versions of HWRF, Ferrier and Aligo removed it because they felt that it was resulting in too broad of the convective region when looking at warm season MCSs. This is the reason why there is no indication of a melting layer in the reflectivity plot. But this will not affect our estimation of the depth of "TL" using radar reflectivity.

10. Fig. 5: Why are the Km values 2 and 5 km so much larger than at the surface? (this observation is based off the colorbar range, which goes from 0-80 in Fig. 5a, but from 0-300 or more in Figs. 5b, c).

As we showed previously, the calculated eddy exchange coefficients from LESs are also large above the PBL in the low-mid troposphere. This large eddy exchange coefficients likely result from the combined effects of large up-gradient vertical fluxes and small vertical gradient of mean variables in the eyewall.

Role of eyewall and rainband eddy forcing in tropical cyclone intensification

Ping. Zhu[1], Bryce Tyner[1], Jun A. Zhang[3,4], Eric Aligo[2], Sundararaman Gopalakrishnan[3], Frank D. Marks[3], Avichal Mehra[2], Vijay Tallapragada[2],

[1]Department of Earth and Environment, Extreme Event Institute, Florida International University, Miami, FL 33199, US
[2]Environmental Modeling Center, NCEP, NOAA, College Park, MD 20740, US
[3]Hurricane Research Division, AOML, NOAA, Miami, FL 33149, US
[4]Cooperative Institute for Marine and Atmospheric Studies, University of Miami, Miami, FL 33149, US

Correspondence to: Ping Zhu (zhup@fiu.edu)

Abstract. While turbulence is commonly regarded as a flow feature pertaining to the planetary boundary layer (PBL), intense turbulent mixing generated by cloud processes also exists above the PBL in the eyewall and rainbands of a tropical cyclone (TC). The in-cloud turbulence above the PBL is intimately involved in the development of convective elements in the eyewall and rainbands and consists of a part of asymmetric eddy forcing for the evolution of the primary and secondary circulations of a TC. In this study, we show that the Hurricane Weather Research & forecasting (HWRF) model, one of the operational models used for TC prediction, is unable to generate appropriate sub-grid-scale (SGS) eddy forcing above the PBL due to lack of consideration of intense turbulent mixing generated by the eyewall and rainband clouds. Incorporating an in-cloud turbulent mixing parameterization in the vertical turbulent mixing scheme notably improves HWRF's skills on predicting rapid changes in intensity for several past major hurricanes. While the analyses show that the SGS eddy forcing above the PBL is only about one-fifth of the model-resolved eddy forcing, the simulated TC vortex inner-core structure, secondary overturning circulation, and the model-resolved eddy forcing exhibit a substantial dependence on the parameterized SGS eddy processes. The results highlight the importance of eyewall/rainband SGS eddy forcing to numerical prediction of TC intensification, including rapid intensification at the current resolution of operational models.

1. Introduction

Producing timely and accurate intensity forecasts of tropical cyclones (TCs) continues to be one of the most difficult challenges in numerical weather prediction. The difficulty stems from the fact that TC intensification is not only modulated by environmental conditions, such as large-scale wind shear and underlying sea surface temperature (SST), but also largely depends on TC internal dynamics that involve complicated interactions of physical processes spanning over a spectrum of scales (Marks and Shay 1998). Since numerical models use discretized grids to simulate the continuous atmosphere, the processes with scales smaller than model grid spacing, known as sub-grid scale (SGS) processes, cannot be resolved by

models. Because of the high nonlinearity of the atmospheric system, the SGS processes result in new high-order terms in the grid-box-mean governing equations of the atmosphere. These new high-order terms cause the otherwise closed system no longer to be closed. To close the system, additional equations that govern high-order terms need to be derived. This is the notorious closure problem of any turbulent fluid system. In practice, the high-order terms are determined parametrically in terms of model-resolved grid-box mean variables, known as turbulent mixing parameterization.

TC intensification associated with internal dynamics including SGS processes may be better approached in a cylindrical coordinate with its origin set at the center of a TC vortex. The governing equation for the azimuthal-mean model-resolved tangential velocity of a TC may be written as:

$$\frac{\partial \bar{\tilde{v}}}{\partial t} + \bar{\tilde{u}}\frac{\partial \bar{\tilde{v}}}{\partial r} + \bar{\tilde{w}}\frac{\partial \bar{\tilde{v}}}{\partial z} = -\bar{\tilde{u}}\left(f + \frac{\bar{\tilde{v}}}{r}\right) + F_\lambda + F_{sgs\_\lambda}, \qquad F_\lambda = -\overline{\tilde{u}'\frac{\partial \tilde{v}'}{\partial r}} - \overline{\tilde{v}'\frac{\partial \tilde{v}'}{r\partial \lambda}} - \overline{\tilde{w}'\frac{\partial \tilde{v}'}{\partial z}} - \frac{\overline{\tilde{u}'\tilde{v}'}}{r}, \tag{1}$$

where r, λ, and z represent the radial, azimuthal, and vertical coordinate axes; $\tilde{u}$, $\tilde{v}$, and $\tilde{w}$ are the model-resolved radial, tangential, and vertical wind components, respectively; f is Coriolis parameter. Overbar and prime indicate the azimuthal-mean and the perturbation away from the azimuthal-mean; F_λ is the azimuthal-mean tangential eddy correlation term resulting from the model-resolved asymmetric eddy processes; and F_{sgs_λ} is the azimuthal-mean tangential SGS tendency resulting from the parameterized SGS eddy processes (or turbulence). In the region where friction is appreciable, eddy forcing $F_\lambda + F_{sgs\_\lambda}$ is negative definite (Montgomery and Smith 2014), meaning that it tends to slow down the motion. Defining the azimuthal-mean model-resolved absolute angular momentum per unit mass as $\bar{\tilde{M}} = r\bar{\tilde{v}} + \frac{1}{2}fr^2$, it is easy to show that the azimuthal-mean tangential wind budget equation, Eq. (1), becomes:

$$\frac{D\bar{\tilde{M}}}{Dt} = \frac{\partial \bar{\tilde{M}}}{\partial t} + \bar{\tilde{u}}\frac{\partial \bar{\tilde{M}}}{\partial r} + \bar{\tilde{w}}\frac{\partial \bar{\tilde{M}}}{\partial z} = r(F_\lambda + F_{sgs\_\lambda}), \tag{2}$$

where $\frac{D\bar{\tilde{M}}}{Dt} = \frac{\partial \bar{\tilde{M}}}{\partial t} + \bar{\tilde{u}}\frac{\partial \bar{\tilde{M}}}{\partial r} + \bar{\tilde{w}}\frac{\partial \bar{\tilde{M}}}{\partial z}$ is the material derivative following air particles along the model-resolved axisymmetric flow and $r(F_\lambda + F_{sgs\_\lambda})$ is the torque per unit mass acting on air parcels resulting from the model-resolved and SGS eddy forcing. For $F_\lambda + F_{sgs\_\lambda} = 0$, $\bar{\tilde{M}}$ is materially conserved. As air parcels move radially inward (decrease of r), they must spin up in order to conserve their absolute angular momentum. Conversely, air parcels must spin down as they move radially outward. This provides an essential mechanism for the spin-up process of a vortex free of forcing in an inviscid flow. For $F_\lambda + F_{sgs\_\lambda} \neq 0$, the asymmetric eddy processes provide an important forcing for the evolution of the primary circulation of a TC vortex as indicated by Eq. (1) or Eq. (2).

The asymmetric eddies that produce tangential eddy forcing for driving the mean vortex circulation cover a spectrum of scales from mesovortices, mesoscale convective plumes, down to small scale turbulence. The advanced three-dimensional

(3D) rotating convective updraft paradigm (Montgomery and Smith 2014) recognized the importance of asymmetries, such as hot towers, to TC intensification. Persing et al. (2013) compared the TC intensification rate in a 3D full-physics model with that in an axisymmetric model. Their results show that the 3D eddy processes associated with vortical plumes can assist the intensification process by contributing to the azimuthally averaged heating rate, to the radial contraction of the maximum tangential velocity, and to the vertical extension of tangential winds through the depth of the troposphere. Since mesoscale convective plumes can be explicitly resolved by high resolution regional models, the 3D full-physics simulations provide a means to elucidate the role of the model-resolved eddy forcing in TC intensification.

Small-scale turbulence including large energy-containing eddies (e.g., sub-kilometer convective elements and roll vortices) cannot be resolved by 3D full-physics regional models. The parameterized turbulent mixing results in the SGS eddy forcing (e.g., F_{sgs_λ}) for the evolution of a TC vortex in numerical simulations. Since turbulence is a basic flow feature pertaining to the planetary boundary layer (PBL), SGS eddy forcing is commonly considered to be important only in the PBL. The importance of PBL turbulence to TC evolution has been recognized for a long time. Both the Conditional Instability of the Second Kind (CISK) and cooperative-intensification mechanism (Ooyama 1982), the two early theories for TC intensification, recognized the role of the PBL in converging moisture to sustain deep convection of a TC. Charney and Eliassen (1964) stated, "Friction performs a dual role; it acts to dissipate kinetic energy, but because of the frictional convergence in the moist surface boundary layer, it acts also to supply latent heat energy to the system". Later it was Emanuel's evaporation-wind feedback mechanism (Emanuel 2003) that first articulated the critical role of air-sea interaction in generating a positive feedback between the near-surface wind speed and the rate of evaporation from the underlying ocean during the intensification process. However, in all these theories plus the 3D rotating convective updraft paradigm (Montgomery and Smith 2014), the PBL was treated as a shallow turbulent layer adjacent to Earth's surface with a depth typically less than 1 km. By doing so, they implicitly adopted the basic assumptions of the classic PBL theory: (1) turbulent mixing is responsible for the vertical transport of momentum, heat, and moisture; (2) vertical turbulent transport becomes negligible above the PBL; and (3) the mean vertical velocity $\overline{w}$ in the PBL is negligible compared with the vertical velocity fluctuations w' (Stull 1988).

However, turbulence and the resultant turbulent transport and turbulent kinetic energy (TKE) cannot always be neglected above the PBL. Intense turbulent mixing within the deep convective clouds has been widely observed by aircraft, Doppler radar/lidar, and other advanced remote sensing instruments (e.g., LeMone and Zipser 1980; Marks et al. 2008; Hogan et al. 2009; Giangrande et al. 2013). In particular, using the TKE derived from the airborne radar data collected in Hurricane Rita (2005), Lorsolo et al. (2010) showed that large TKE exists above the PBL in the eyewall and rainbands. Figure 1 shows the composite of TKE derived using Lorsolo et al. (2010)'s method based on the airborne radar observations from 116 radial legs of P3 flights in the 2003-2010 hurricanes seasons. It clearly demonstrates that the intense turbulence exists above the PBL in the conventional definition all the way up to over 10 km in the eyewall.

Realizing the deep convective nature of TCs, Smith et al. (2008) and Smith and Montgomery (2010) warned that the conventional PBL theory may become invalid in the TC inner-core region as the low-level radial inflow ascends swiftly within the eyewall. In fact, the problem of applying conventional PBL theory to a deep convective regime had been recognized early in the 1970s and 1980s. Deardorff (1972) noted, "*The definition of PBL has not included the region of turbulence within towering cumuli but only the average height of surface induced turbulent fluxes outside of such clouds*". Moss and Rosenthal (1975) added, "*The method (of defining the PBL) contains several elements that may or may not be applicable under hurricane conditions*". Shapiro (1983) wrote, "*As the radius of maximum tangential wind is approached, the boundary layer itself becomes ill defined, as air is pulled up into the active convection*". Stull (1988) also acknowledged that "*the conventional definition of PBL is not applicable to the intertropical convergence zone (ITCZ), where the air ascends into deep convective clouds*".

The problem here, however, is not all about how to redefine PBL to encompass all the scenarios including the deep convective regime. This is because the concept of PBL always applies as to the layer adjacent to the surface that is directly affected by the surface processes. From the perspective of TC intensification, the real questions that need to be answered are: (1) Is the intense turbulent mixing above the PBL in the eyewall and rainbands generated by cloud processes important to TC intensification? And (2) how does the parameterized in-cloud eddy processes in the eyewall and rainbands affect model resolved eddy forcing and TC inner-core structure? The answer to the first question is apparent as in-cloud turbulence results in a component of direct eddy forcing for the mean circulation of a vortex according to Eq. (1) or Eq. (2). The complication is that the sign of eddy forcing, $F_\lambda + F_{sgs\_\lambda}$, above the PBL is indefinite depending on the details of eddy processes. Persing et al. (2013) showed that the resolved 3D momentum fluxes above the PBL exhibit counter-gradient characteristics during a key spin-up period, and more generally are not solely diffusive. Thus, for $F_\lambda + F_{sgs\_\lambda}>0$, it provides a mechanism for spinning up a vortex. The second question is important since in numerical simulations the asymmetric eddies with a continuous spectrum are artificially split into the model-resolved and parameterized components because of the discretized model grids. The two split parts of eddy forcing are not independent but interact with each other depending on the model resolution. To date, little work has been done to examine the sensitivity of model-resolved eddy forcing and TC structure to the parameterized SGS eddy processes above the PBL generated by the eyewall/rainband clouds. This issue will be investigated in this study.

In addition to the direct tangential eddy forcing $F_\lambda + F_{sgs\_\lambda}$ to the primary circulation of a TC vortex, the secondary overturning circulation induced by friction and diabatic heating also plays an important role in TC intensification. The azimuthal-mean governing equations for model-resolved radial and vertical velocities of the overturning circulation may be written as:

$$\frac{D\bar{\tilde{u}}}{Dt} - C = -\frac{1}{\bar{\tilde{\rho}}}\frac{\partial \bar{\tilde{p}}}{\partial r} + F_r + F_{sgs\_r}, \quad C = \frac{\bar{\tilde{v}}^2}{r} + f\bar{\tilde{v}}, \quad F_r = -\overline{\tilde{u}'\frac{\partial \tilde{u}'}{\partial r}} - \overline{\tilde{v}'\frac{\partial \tilde{u}'}{r\partial \lambda}} - \overline{\tilde{w}'\frac{\partial \tilde{u}'}{\partial z}} - \frac{\overline{\tilde{v}'^2}}{r}, \tag{3}$$

$$\frac{D\bar{\tilde{w}}}{Dt} = -\frac{1}{\bar{\tilde{\rho}}}\frac{\partial \bar{\tilde{p}}}{\partial z} - g + F_w + F_{sgs\_w}, \qquad F_w = -\overline{\tilde{u}'\frac{\partial \tilde{w}'}{\partial r}} - \overline{\tilde{v}'\frac{\partial \tilde{w}'}{r\partial \lambda}} - \overline{\tilde{w}'\frac{\partial \tilde{w}'}{\partial z}}, \tag{4}$$

where $F_r + F_{sgs\_r}$ and $F_w + F_{sgs\_w}$ are the model-resolved and SGS eddy forcing terms in the radial and vertical direction; $\bar{\tilde{p}}$ and $\bar{\tilde{\rho}}$ are the azimuthal-mean model-resolved pressure and air density, respectively; and g is the gravitational acceleration. In the classic TC studies (e.g., Ooyama 1969 and Emanuel 2003), TC vortices were assumed to follow the gradient wind balance and hydrostatic balance where the accelerations of radial and vertical velocities ($\frac{D\bar{\tilde{u}}}{Dt}, \frac{D\bar{\tilde{w}}}{Dt}$) and the radial and vertical eddy forcing ($F_r + F_{sgs\_r}, F_w + F_{sgs\_w}$) in Eq. (3) and Eq. (4) are neglected. Shapiro and Willoughby (1982); Smith et al. (2005), and Bui et al. (2009) showed that in such a balanced framework the secondary overturning circulation of a TC vortex can be analytically described by an elliptical partial differential equation known as Sawyer-Eliassen equation (SEE). Using this diagnostic tool, Shapiro and Willoughby (1982) examined the acceleration of tangential wind in response to local sources of heating and momentum. Later, Smith et al. (2009) showed that the convergence of absolute angular momentum within the PBL associated with the development of super-gradient wind speeds can provide a spin-up mechanism for the mean tangential circulation of a vortex. Therefore, intensification theories built upon gradient wind balance and hydrostatic balance may lack the ability to explain the rapid intensity changes driven by the internal dynamics when radial or vertical eddy forcing becomes important. Numerical models built upon primitive equations presumably have the ability to capture the eddy forcing associated with convection and PBL turbulence. Advances in computer technology nowadays have reduced model horizontal grid spacing of operational models down to 1-2 km. While higher resolution models allow dynamic eddy forcing (F_λ, F_r, F_w) and thermodynamic eddy forcing for heat and moisture (F_θ, F_q) to be better resolved, it remains to be poorly understood as to what governs the sign, magnitude, and radius-height distribution of eddy forcings above the PBL. Leaving aside the question if high resolution numerical models can generate robust model-resolved eddy forcing, a source of uncertainty in intensity forecast arises from the parametric determination of SGS eddy processes.

In numerical models, the SGS forcings ($F_{sgs\_\lambda}, F_{sgs\_r}, F_{sgs\_w}, F_{sgs\_\theta}$, and F_{sgs_q}) are determined by the turbulent mixing scheme. Current effort mainly focuses on the improvement of parameterization of turbulent mixing within the PBL. The importance of eyewall/rainband SGS eddy forcing above the PBL to TC intensification has been largely overlooked in the past for a few reasons. First, the critical role of radial inflow, PBL processes, and surface latent heating in maintaining and intensifying a TC vortex has overshadowed the importance of the SGS forcing aloft associated with eyewall/rainband convection. Second, unlike turbulence in the PBL, which has a solid theory built upon observations, turbulence aloft in deep convection is difficult to access. Lack of observations largely limits our understanding of the in-cloud turbulent mixing processes and the resultant SGS eddy forcing to the momentum and heat budgets of a TC. Third, for deep convection, the

focus is on the cumulus parameterization. Cumulus schemes (e.g., Arakawa and Schubert 1974; Betts and Miller 1993) were originally designed to remove the convective instability generated by the large-scale flow and alter the thermodynamic structure of the environment based on the parameterized convective fluxes and precipitation. It is commonly assumed and widely accepted that the coherent up-/down-drafts take the central role in establishing the equilibrium between the generation of moist convective instability by the environmental processes and the stabilization of environment by cumulus convection (Arakawa and Schubert 1974; Wu and Arakawa 2014; Zhu 2015). The effect of small scale turbulence is negligible in this perspective although some later developed more advanced cumulus schemes do consider the effects of turbulent mixing in schemes (e.g., Guo et al. 2015). Finally, almost all turbulent mixing schemes used today for TC prediction were originally developed to represent turbulent processes within the PBL in fair-weather conditions in which the turbulent PBL is cleanly separated from the free atmosphere above by a capping inversion. Often in these schemes, a simple method based on the bulk Richardson number is adopted to account for the free atmosphere turbulence if there is any (e.g., Hong and Pan, 1996). These schemes lack the ability to represent the in-cloud turbulence in the eyewall and rainbands generated by the cloud processes. Thus, the contribution of in-cloud turbulence above the PBL to eddy forcing in TC intensification, and the sensitivity of resolved eddy forcing and vortex inner-core structure to the parameterization of in-cloud turbulence are largely unknown.

TC intensification is a complicated process that is affected by a number of environmental factors, such as wind shear and SST. Emanuel et al. (2004) examined the sensitivity of storm intensity simulated by a coupled axisymmetric model known as the Coupled Hurricane Intensity Prediction System (CHIPS) to vortex initialization and various environmental factors. Their results showed that the simulated storm intensity is most sensitive to wind shear. Recently, Vigh et al. (2018) confirmed Emanuel et al. (2004)'s results and showed that very rapid intensification (VRI, ~30 kt in 12 h) and extreme rapid intensification (ERI, ~40 kt in 12 h) can be well captured by CHIPS with the setting of zero wind shear. While environmental conditions appear to be critical to TC intensification, they will not be discussed in this study, rather, we focused on how does eddy forcing resulting from both resolved and parameterized asymmetric eddy process modulate TC intensification under certain environment conditions. In particular, using numerical simulations by the Hurricane Weather Research and Forecast (HWRF) modeling system, one of the operational models used for TC prediction at the Environmental Modeling Center (EMC), NOAA, we investigate the role of eyewall/rainband eddy forcing in governing TC intensity change. We demonstrate the sensitivity of intensification process to parameterization of eyewall/rainband in-cloud turbulent mixing above the PBL in numerical simulations of TCs. This paper is organized as follows. In section 2, we show problems associated with the turbulent mixing scheme used in the operational HWRF in representing eyewall/rainband in-cloud turbulence and discuss methods of how to incorporate the parameterization of in-cloud turbulence in the PBL scheme used in HWRF. The simulation results by the HWRF with the operational setting and the modified PBL scheme that includes an in-cloud turbulent mixing parameterization are presented in section3 followed by a summary in section 4.

2. HWRF PBL scheme and in-cloud turbulent mixing parameterization

The numerical model used in this study is the operational HWRF version 3.8a. It consists of triple-nested domains on an E-grid. The grid-spacing of the three domains is 0.135^0, 0.045^0, and 0.015^0 degree, corresponding approximately to 18 km, 6 km, and 2 km, respectively. There are 61 levels in the vertical. The details of HWRFv3.8a release can be accessed at https://dtcenter.org/HurrWRF/users/docs/index.php. Since this study focuses on the role of internal eyewall/rainband eddy forcing in TC intensification, to avoid the complication from the interactive underlying ocean, all simulations presented in this paper were performed by the uncoupled atmospheric model of HWRF. The initial and boundary conditions for the real-case TC simulations were supplied by the Global Forecast System (GFS) data.

As discussed earlier, in numerical models the SGS eddy forcing is determined by the turbulent mixing scheme. Since large energy-containing turbulent eddies are not resolved by 2-km resolution grids, to appropriately parameterize the anisotropic SGS eddy processes, like other state-of-the-art regional models, the operational HWRF treats horizontal and vertical turbulent mixing separately. The horizontal SGS mixing is handled by a revised two-dimensional (2D) Smagorinsky diffusion model (Zhang et al. 2018) that is built within the model dynamic core. The vertical SGS mixing, on the other hand, is handled by a separate physics module known as the PBL scheme. It is a 1D vertical turbulent mixing scheme, which was formulated based on the one originally proposed by Hong and Pan (1996). Bryan and Rotunno (2009) and Bryan (2012) investigated the sensitivity of TC evolution to horizontal eddy diffusivity by adjusting the mixing length. Recently, Zhang et al. (2018) evaluated the impact of horizontal diffusion parameterization on TC prediction by HWRF. In this study, we only focus on the vertical turbulent mixing parameterization. Horizontal diffusion was not touched.

The HWRF PBL scheme is a typical K-closure (or first-order-closure) turbulent mixing scheme. Although there have been modifications to the scheme throughout the years, the basic formulae used to determine eddy exchange coefficients are kept the same as those originally proposed by Hong and Pan (1996). In this scheme, the eddy exchange coefficients are determined separately based on the diagnosed PBL height. Within the PBL, the momentum eddy viscosity is calculated as:

$$K_m = \kappa \frac{u_*}{\phi_m} \alpha z (1 - \frac{z}{h})^2, \quad (5)$$

where κ is the von Karman constant, u_* is the friction velocity, z is the height above the ground surface, ϕ_m is the surface layer stability function obtained by Businger et al. (1971), and h is the diagnosed PBL height calculated iteratively based on the bulk Richardson number over the PBL depth and the buoyancy of surface-driven thermals. Although there are many sophisticated methods to parameterize SGS turbulent mixing, such as TKE closure, high-order closure, nonlocal mixing, and schemes formulated using variables conserved for moist reversible adiabatic processes, the K-closure scheme is arguably the best choice for operational models at the current stage as it requires the least computational resource. However, Eq. (5) was originally formulated to account for PBL turbulent mixing in non-TC conditions (Troen and Mahrt 1986; Holtslag et al. 1990; Holtslag and Boville 1993). Observations from multiple TCs by Zhang et al. (2011) showed that Eq. (5) substantially

overestimates the eddy viscosity in the PBL. In light of this finding, Gopalakrishnan et al. (2013) introduced a coefficient α ($0< \alpha <1$) in Eq. (5) to reduce eddy viscosity in TC simulations. This tuning of eddy viscosity via α now has been adopted in the operational HWRF. Above the diagnosed PBL height, the momentum eddy viscosity is calculated as:

$$K_m = l^2 f_m(Ri_g)\sqrt{\left|\frac{\partial \tilde{u}}{\partial z}\right|^2 + \left|\frac{\partial \tilde{v}}{\partial z}\right|^2}, \quad (6)$$

where l is the mixing length, $f_m(Ri_g)$ is the stability function of gradient Richardson number, $Ri_g = \frac{g}{\theta_0}\frac{\partial \widetilde{\theta_v}}{\partial x} / \left(\left|\frac{\partial \tilde{u}}{\partial z}\right|^2 + \left|\frac{\partial \tilde{v}}{\partial z}\right|^2\right)$, and $\sqrt{\left|\frac{\partial \tilde{u}}{\partial z}\right|^2 + \left|\frac{\partial \tilde{v}}{\partial z}\right|^2}$ is the vertical wind shear. This is a method that was originally proposed to account for the free-atmosphere diffusion. Once K_m is determined, the eddy viscosity for heat and moisture is calculated by $K_{t,q} = K_m P_r^{-1}$, where P_r is the Prandtl number.

For fair-weather conditions, the parameterization formulated by Eq. (5) and Eq. (6) provides a practical way to appropriately parameterize the SGS turbulent mixing within and above the PBL since the turbulent layer resulting from the surface processes is often cleanly separated from the free atmosphere by a capping inversion. The mid-point of the inversion zone (or entrainment zone) is naturally defined as the PBL height (Stull 1988). In a TC environment, however, turbulence is no longer solely generated by the shear production and buoyancy production associated with the surface processes; it can also be generated by cloud processes aloft due to cloud radiative cooling, evaporative cooling, and inhomogeneous diabatic heating and cooling in the clouds. Thus, although the concept of PBL is still applicable, it becomes ambiguous from the turbulent mixing perspective. In many TC studies, the PBL is defined either as the turbulent layer that is directly affected by the surface processes or as the inflow layer of the secondary circulation. But in either case, the so-defined PBL height is by no means a physical interface that separates the turbulence generated by surface processes and by cloud processes. This is particularly true in the eyewall and rainbands of a TC, where intense turbulence can extend from the surface all the way up to the upper troposphere, as was illustrated in Fig. 1. Thus, from the nature of turbulent mixing, an artificial separation of turbulence using a diagnosed "PBL" height is not a physically sound method to parameterize the internally connected SGS turbulent mixing in the eyewall or any deep convective areas in a TC. Moreover, an artificial separation of the PBL from the free atmosphere above may create an unrealistic discontinuity in the vertical profile of eddy viscosity in this method. Following Eq. (5), as height z approaches the diagnosed "PBL" height h, eddy viscosity K_m becomes zero to result in zero turbulent mixing at a certain model grid level if the diagnosed PBL height falls exactly at this level. Above the diagnosed PBL, the turbulent mixing jumps to whatever value estimated by Eq. (6). This singular point in the vertical profile of eddy exchange coefficient could cause problems in representing turbulent mixing in the eyewall and rainbands.

We carefully examined the eddy exchange coefficients in multiple TC simulations by the operational HWRF and found that the default PBL scheme is unable to generate intense turbulent mixing in the eyewall and rainbands. As an example, Figure 2 shows the horizontal distribution of the HWRF simulated eddy exchange coefficients for momentum (k_m) at different

altitudes and the corresponding azimuthal mean of k_m on the radius-height plane of Hurricane Jimena (2015) at an arbitrary time before the storm reached its maximum intensity. Within the PBL, the magnitude and horizontal spatial distribution reflects well the strong turbulent mixing in the eyewall and rainbands, but above the PBL, the HWRF generated eddy exchange coefficients are virtually zero. This result suggests that the PBL scheme used in the operational HWRF fails to capture the intense turbulent mixing above the PBL in the deep convective eyewall and rainbands. This is not a surprise since Eq. (6) was originally developed to parameterize clear-sky free-atmosphere diffusion and is incapable of representing the intense turbulent mixing generated by cloud processes. We hypothesize that the lack of appropriate SGS eddy forcing associated with deep convection above the PBL in the eyewall and rainbands is one of the culprits for the intensity forecast failure in many cases of HWRF forecasts.

To better understand the characteristics of intense turbulent mixing in eyewall clouds, we performed a series of large eddy simulations (LESs) of Hurricane Isabel (2003) in a hindcasting mode using WRF model with the Advanced Research WRF (ARW) dynamic core. The detailed procedure of configuring a WRF-LES for TC simulations can be found in Zhu (2008a and 2008b) and Zhu et al. (2015). The approach of our LES study is similar to that of Bryan et al. (2003) and Green and Zhang (2015) in that the model horizontal grid resolution falls in the Kolmogorov inertial subrange and a 3D SGS model built within the model dynamic solver is used to treat the horizontal and vertical mixing induced by the presumably isotropic SGS eddies. Since eddies with scales smaller than inertial subrange contain much less energy and are less flow-dependent than large energy-containing eddies, the LES methodology is commonly thought to be insensitive to formulaic details and arbitrary parameters of the SGS model, and thus, the turbulent flow generated by LESs are often used as a proxy for reality and a basis for understanding turbulent flow and guiding theories when direct observations are difficult to obtain. In the past, LESs were mainly used to elucidate problems associated with the turbulent processes within the PBL. Here we use this approach to better understand the turbulent processes in the eyewall.

In this LES study, the innermost domain of the WRF-LES covered the entire eyewall of Isabel (2003) with a horizontal grid-spacing of 100 m. 75 levels were configured in the vertical. The simulation was initialized and forced by the NCEP FNL analyses and run for 8 hours (from 00:00 to 8:00 UTC 12 September 2003). The details and results of this Giga WRF-LES is reported in Li et al. (2019). Figure 3 shows the instantons surface (10-m) wind speeds of Isabel (2003) at the 8th simulation hour from one of the LESs that uses the 3D nonlinear backscatter and anisotropy (NBA) SGS model (Kosović, 1997). Eyewall disturbances with scales of a few kilometers or smaller are clearly shown in the wind fields. These kilometer-scale or sub-kilometer-scale eddies have been also reported in previous LES studies of TCs. For example, Rotunno et al. (2009) found that these 'vigorous small-scale eddies' are the dominant features in the eyewall in their LES run at the resolution of 62 m. Green and Zhang (2015) showed such disturbances existing in all of their LES runs with the 3D NAB SGS model including the simulation at 333-m resolution.

While using LES to simulate TC is promising, evaluation of the fidelity of the simulated TC vortex and the associated fine-scale structures resolved by LES is a challenge. In the absence of decisive observational measurements, the principal method of evaluating LES has been through sensitivity studies of individual LESs with different SGS models or inter-comparisons among different LESs. The logic is that the robustness of the simulations testifies to its fidelity. Such sensitivity tests and inter-comparison studies in the past have shed favorable light on the LES approach in general in many meteorological applications (e.g., Stevens et al. 2005; Moeng et al. 1996), but they also raised questions about the ability of LES to realistically reproduce some unique features in the atmosphere. While there are individual LES studies of TCs, the sensitivity of LES to SGS parameterization has never been examined when the LES approach is used to simulate TCs. Such sensitivity tests are needed since intense turbulence in the eyewall can exist well beyond the PBL. In this study, we have tested three 3D SGS models commonly used in LESs: (a) 3D Smagorinsky SGS model (Smagorinsky, 1963), (b) 3D 1.5-order TKE SGS model (Deardorff, 1980), and (c) 3D NBA SGS model (Kosović, 1997).

It remains a mystery as to what the real value of vertical eddy exchange coefficients in the eyewall should be because of the difficulties to obtain vertical turbulent fluxes in the eyewall observationally. There are also difficulties to calculate vertical turbulent fluxes from the LES output. One of them is how to appropriately define the mean of a variable. For fast responding in-situ observations, the mean is commonly calculated as the average over a time period, and then, using the eddy correlation method to calculate the covariance of two variables. For classic LES applications in non-TC conditions, the domain-mean is often used when calculating vertical turbulent fluxes, which is appropriate as the ambient condition of the PBL is assumed to be horizontally homogeneous. However, such a method cannot be extended to LES of a TC as the fields of a storm vortex are not horizontally homogeneous. If a mean would include both violent eyewall and peaceful eye, the estimated covariance would be exaggerated. Furthermore, if the eddy correlation method is applied to the entire LES domain, then, one would only obtain one vertical profile of eddy exchange coefficient. It would be incorrect to apply this vertical profile to both eyewall and eye as the turbulent mixing in these two regions is completely different. One way to solve this problem is to define a sub-domain centered at each model grid, and then, use the LES output in the sub-domain for vertical flux calculation at each grid using eddy correlation method via,

$$F_\varphi = \overline{w'\varphi'} = \overline{(w-\bar{w})(\varphi-\bar{\varphi})} \tag{7}$$

where φ is a generic scalar, F_φ is the vertical flux of φ at each grid, w is the vertical velocity, overbar and prime indicate the average over the sub-domain and the deviation away from the average, respectively. In the first-order closure, the vertical momentum flux components may be represented as,

$$\overline{w'u'} = -k_m \frac{\partial \bar{u}}{\partial z}, \qquad \overline{w'v'} = -k_m \frac{\partial \bar{v}}{\partial z}, \tag{8}$$

where k_m is the eddy exchange coefficient of momentum, $\frac{\partial \bar{u}}{\partial z}$ and $\frac{\partial \bar{v}}{\partial z}$ are the vertical gradient of mean wind components over the sub-domain. In the eyewall, the non-local mixing induced by the convective eddies (or cells) generates a large amount of

up-gradient vertical fluxes, thus, to account for the up-gradient vertical transport in the first-order closure, the momentum eddy exchange coefficient is calculated as,

$$K_m = \tau / \sqrt{(\frac{\partial \bar{u}}{\partial z})^2 + (\frac{\partial \bar{v}}{\partial z})^2} \quad (9)$$

where $\tau = (\overline{w'u'}^2 + \overline{w'v'}^2)^{\frac{1}{2}}$ is the total vertical momentum fluxes.

Another important thing that needs to be considered is how large the sub-domain should be because the size of a sub-domain determines the contributions to the vertical fluxes from different scales of resolved eddies by LES. The horizontal grid resolution of HWRF-v3.8a is 2 km, meaning that eddies with scales greater than 2 km are resolved by HWRF. What need to be parameterized by HWRF PBL scheme are the vertical transport induced by eddies smaller than 2 km. Thus, in this study a 2 x 2 km^2 box is used as the sub-domain for vertical flux calculation at each grid point. Figure 4a shows the azimuthal-mean radius-height distribution of the total vertical momentum fluxes, τ, induced by the resolved eddies with scales smaller than 2 km from the LES run that uses the 3D NBA SGS model. The vertical profiles of eddy exchange coefficients of momentum from the three LESs that use different SGS models averaged over the radii of 30 - 60 km (where the eyewall is located) are shown in Fig. 4b. Note that the results shown in the figure have been averaged over 3 – 8 simulation hours and the SGS eddy exchange coefficients are the direct output from the SGS models. It clearly shows that the strong vertical momentum fluxes induced by the resolved eddies keep increasing with height and reach the peak above the PBL (defined in the conventional way) in the low troposphere, and then, extend all the way up to the upper troposphere in the eyewall. There is no discontinuity across the PBL that separates the turbulent transport generated by the surface turbulent processes and cloud turbulent processes aloft in the eyewall. The resolved eddy exchange coefficients in the eyewall appear to be large and dominate the SGS coefficients. This is mainly caused by the limitation of using down-gradient parameterization of the first-order closure to represent non-local mixing in the eyewall where the combined effects of the large up-gradient vertical transport and small vertical gradient of mean variables lead to the large eddy exchange coefficient.

The discussion above and the results shown in Figs. 2, 3 and 4 suggest that to appropriately parameterize the turbulent mixing in the eyewall and rainbands, one may have to abandon the idea of using the diagnosed "PBL" height to artificially separate the internally connected turbulence generated by the PBL and cloud processes. From the nature of turbulent mixing, it is more logical to treat the turbulence in the eyewall and rainbands generated by the different processes as a whole, i.e., treat the entire turbulent layer (TL) as an integrated layer. Physically, it makes sense as turbulent mixing generated by different processes in a deep convective environment cannot be artificially separated. It is important to point out that such a change from "PBL" to "TL" will not affect the turbulent mixing parameterization outside the deep convective area since the "TL" is virtually the same as the "PBL" in that case. The remaining question is how to appropriately define and determine a "TL" in the eyewall and rainbands.

One way to improve the representation of turbulent mixing in the eyewall and rainbands is to develop a physically robust scheme using more sophisticated approaches, such as, TKE, high-order, or nonlocal closure, to replace Eqs. (5) and (6) to calculate vertical eddy exchange coefficient. However, a sophisticated method may not necessarily generate the desired results without significant tuning effort and thorough evaluation against observations, since an operational model consists of many physics modules that interact with each other and with the model dynamic core. How to integrate an individual scheme in a model to work in concert with other modules is an important but difficult scientific and technical problem. Moreover, the low vertical resolution above the PBL due to the stretching vertical grids commonly used in models makes it even more difficult to parameterize in-cloud turbulence above the PBL. To avoid possible degrading of HWRF's forecasting performance, a practical way is to keep the current framework of PBL scheme and refine it by incorporating an in-cloud turbulent mixing parameterization with the existing PBL scheme in a unified matter. Technically, this is relatively easy to do and scientifically it makes sense, since the "TL" should be the same as the "PBL" outside deep convective regions, and thus, nothing needs to be changed for the current PBL scheme used in HWRF. The only change that needs to be made is to overwrite the default diagnosed PBL height in the eyewall and rainbands with a newly determined "TL" height.

Since this study focuses on the turbulence generated by the cloud processes, a simple way to determine "TL" is to link "TL" directly to model-predicted cloud properties. A natural choice of such cloud properties is the cloud radar reflectivity, a product normally available from the microphysics module of a model. In the operational HWRF version 3.8a, the Ferrier-Aligo microphysical scheme (Aligo et al. 2018) calculates radar reflectivity at each time step. Figure 5 shows an example of the horizontal spatial distribution of HWRF simulated cloud radar reflectivity at different altitudes for Hurricane Jimena (2015) at an instant time along with an individual vertical profile of radar reflectivity in the eyewall and azimuthal-mean radius-height distribution of radar reflectivity. The vertical profile clearly shows that the simulated radar reflectivity in the eyewall remains nearly constant with height below the freezing level, and then, decreases sharply around 6 – 7 km in altitude. This unique feature allows us to determine "TL" from the radar reflectivity under the assumption that "TL" is virtually the cloud layer with prevalence of turbulence. After many tests, we choose 28 dBZ as a critical value to define "TL" in HWRF simulations. If no such a layer with radar reflectivity consistently greater than 28 dBZ is found or such defined "TL" is lower than the default "PBL", then, the default "PBL" is assumed to be the "TL". Thus, the change from "PBL" to "TL" will not affect the treatment of turbulent mixing elsewhere except for the diagnosed eyewall and rainbands with large reflectivity. Once "TL" is determined, the eddy exchange coefficients below and above the top of the diagnosed "TL" will be calculated following Eqs. (5) and (6), respectively. To retain the HWRF predicted turbulent structure and transport within the PBL, the eddy exchange coefficients below the PBL height are, then, overwritten by the eddy exchange coefficients determined by the default diagnosed "PBL" with a smoothing applied at the top of the "PBL" so that the eddy exchange coefficients in the eyewall and rainband change continuously from the PBL to the cloud layer. Thus, nothing is changed for the HWRF PBL scheme except that the new scheme includes an in-cloud turbulent mixing parameterization in the eyewall and rainbands determined from the "TL".

Note that such defined "TL" does not include the turbulence generated in the anvil clouds in the upper troposphere where the eyewall upward flow turns outward, becoming outflow. Outside a convection regime, the anvil clouds are detached from the PBL in model vertical columns, thus, "TL" concept does not apply. According to Emanuel (2012)'s "self-stratification" intensification hypothesis, the turbulence in the outflow is important because it acts to set the thermal stratification of the outflow. The resultant gradients of outflow temperature provide a control of an intensifying vortex. In their analyses (Emanuel and Rotunno 2011; Emanuel 2012), the instability for generating small-scale mixing in the outflow was estimated by the gradient Richardson number. However, since numerical models use stretching grids in the vertical, it is very difficult to parameterize the SGS turbulent mixing in the outflow regions using bulk Richardson number at a very low vertical resolution. Moreover, since the main focus of this study is on the turbulent mixing above the PBL generated by cloud processes within the convective eyewall and rainbands, we want to isolate this problem from the complication of the outflow turbulence. For these reasons, the effect of outflow turbulence on the intensification process will not be discussed in this study.

Figure 6 shows the horizontal distribution of the simulated eddy exchange coefficients of momentum, k_m, at different altitudes of Hurricane Jimena (2015) by the HWRF with the inclusion of an in-cloud turbulent mixing parameterization along with the azimuthal-mean radius-height distribution of k_m. Compared with Fig.2, the modification from "PBL" to "TL" allows HWRF to successfully capture the in-cloud turbulent mixing. The horizontal spatial distribution of k_m above the PBL well reflects the eyewall and rainband structure of the TC vortex, which is in stark contrast to the default operational HWRF that generates virtually no turbulent mixing above the PBL (Fig. 2). However, the peak of the parameterized k_m appears to be smaller than that from the LESs (Fig. 4b). Note that this difference may result partially from the uncertainty in determination of vertical fluxes using LES output as we pointed out previously and partially from the crude method to treat in-cloud turbulence. As we stated previously, our method itself does not consider the specific mechanisms in generating in-cloud turbulence, and thus, the scheme in its current form may not be directly used in operational forecasts. Nonetheless, this simple modification allows us to look into and examine the role of eyewall and rainband SGS eddy forcing above the PBL in TC intensification. One advantage of the change from "PBL" to "TL" is to allow for a possible internal interaction between microphysics and turbulence. In real TCs, cloud microphysical processes directly interact with in-cloud turbulence to generate the diabatic heating that drives the overturning circulation. The negligible turbulent mixing above the PBL in the operational HWRF virtually removes the microphysics-turbulence interaction in eyewall/rainband clouds. While simple, the inclusion of an in-cloud turbulent mixing parameterization by overwriting the "PBL" height with the "TL" provides an avenue that allows microphysics to directly interact with turbulence in simulations. In the next section, we show that such a modification improves HWRF's skills in predicting TC intensity change, in particular, RI.

3. Results

To evaluate the modified HWRF PBL scheme with the inclusion of an in-cloud turbulent mixing parameterization and investigate the role of eyewall/rainband eddy forcing in modulating TC intensity change, we simulated 16 storms in the Atlantic basin and eastern tropical Pacific in the past four seasons (2014-2017) with different intensities ranging from tropical storms to major hurricanes. For each storm, we simulated 4 cycles with the model initialized at different time. These simulations allow us to provide an initial evaluation of the in-cloud turbulent mixing parameterization and address scientific issues associated with TC intensity change in different TC conditions. In this paper, we mainly focus on RI. Here, we present one of the four simulations of Hurricane Jimena (2015), which was initialized at 12:00 UTC 27 August, 2015. Using this simulation, we investigate how eyewall and rainband eddy forcing modulates the RI of Jimena (2015).

Figure 7 compares the storm track and intensity from the two simulations of Jimena (2015) by HWRF using the default PBL scheme and the PBL scheme that includes an in-cloud turbulent mixing parameterization along with the best track data. These two simulations are named as "DEF-HWRF" and "TL-HWRF" respectively hereafter. While DEF-HWRF does an excellent job in reproducing the observed track, it under-predicts the observed storm intensity by a large margin. The integrated turbulent mixing parameterization in the eyewall and rainbands ("TL-HWRF") shows little impact on the simulated storm track but improves the intensity forecast substantially. It allows HWRF to successfully capture the observed RI of Jimena, suggesting the importance of eyewall/rainband turbulent mixing above the PBL in modulating TC intensification. To see if the resultant improvement in intensity simulation by "TL-HWRF" is mainly caused by the SGS eddy momentum transport or by eddy heat/moisture transport, two additional experiments were executed. In the first experiment, we only modified the eddy exchange coefficient for momentum k_m while keeping the eddy exchange coefficient for heat and moisture $k_{t,q}$ the same as the default. We reversed such a change in the second experiment. As shown in Fig.7, both the modified turbulence closures for momentum alone and for heat/moisture alone show non-negligible impacts on TC intensification. This result is not unexpected. While the tangential eddy forcing for momentum directly involves in the acceleration or deceleration of the primary circulation of a TC, the thermodynamic eddy forcing is sufficiently strong to modulate the secondary overturning circulation that interacts with the primary circulation during TC evolution. Note that in HWRF the eddy exchange coefficients for heat and moisture are treated as the same, thus, we did not further separate them in our study. In the following sections, we explore and discuss the underlying reasons for such an improvement in intensity forecast.

Figure 8 shows the Naval Research laboratory 37 GHz color image from the Advanced Microwave Scanning Radiometer 2 (AMSR2) at 20 UTC 28 August 2015, a time close to the initiation of Jimena's RI. A well-defined inner-core structure including a quasi-closed ring feature around the storm center (somewhat broken in the northwest quadrant) is clearly visible in the satellite image. From a large amount of 37 GHz microwave color products, Kieper and Jiang (2012) showed that the

first appearance of a cyan color ring around the storm center is highly correlated to subsequent RI, provided that environmental conditions are favorable. This result is consistent with the later analyses of Tropical Rainfall Measuring Mission (TRMM) 29 Precipitation Radar (PR) data (Jiang and Ramirez 2013; and Tao and Jiang 2015), which showed that nearly 90% of RI storms in different ocean basins formed a precipitation ring around the storm center prior to RI. The relationship between the ring feature and the subsequent RI obtained from these observational studies is consistent with the theoretical finding of Nolan et al. (2007), who demonstrated that the intensification processes of a balanced, baroclinic TC-like vortex is mainly driven by the TC symmetric response to the azimuthally-averaged diabatic heating, rather than to the heating directly associated with individual asymmetries distributed around the TC vortex. To see if Jimena's RI possesses the similar RI signature found in these observational and theoretical studies, we carefully examined the inner-core structure of the simulated Jimena (2015) prior and during the early stage of RI. Figure 9 shows the horizontal distribution of simulated vertical velocity and hydrometeor mixing ratio at 5 km altitude from the two HWRF simulations with and without an in-cloud turbulent mixing parameterization. The vortex inner-core structure in "DEF-HWRF" is poorly organized and the simulated eyewall appears to be much larger in size than the satellite observed eyewall (Figs. 9a and 9c). It suggests that HWRF with operational model physics is unable to generate the right vortex inner-core structure needed for the subsequent RI. In contrast, "TL-HWRF" produces a well-defined quasi-closed ring around the storm center that is clearly shown in both dynamic (Fig. 9b) and thermodynamic (Fig. 9d) fields. The size of the simulated quasi-closed ring in "TL-HWRF" is similar to that shown in the satellite image. In addition, the simulated asymmetric rainband structure with the strongest convection occurring in the southeast quadrant is consistent with the satellite observation. The similar vortex inner-core structure shown in both satellite observations and "TL-HWRF" simulation implies that the RI of Jimena (2015) is likely governed by the axisymmetric dynamics similar to what was found by Vigh et al. (2018) who showed that some of the VRI and ERI storms, such as Hurricane Patricia (2015), Typhoon Meranti (2016), and Hurricane Maria (2017), can be well captured by the axisymmetric CHIPS with zero-wind shear. The fact that the observed TC inner-core structure including the quasi-closed ring feature is reproduced by "TL-HWRF" but not by the default HWRF suggests that the SGS physics involving with the in-cloud turbulent mixing above the PBL facilitates the realization of the axisymmetric dynamics underlying the RI of TCs in 3D full-physics simulations.

Figure 10 shows the simulated azimuthal-mean radius-height structure of vertical velocity, hydrometeor mixing ratio, radial inflow/outflow, and radial flow convergence averaged over the RI period from 06 UTC 28 to 06 UTC 29 August, 2015. Compared with the "DEF-HWRF", "TL-HWRF" generated much stronger updrafts (thick gray contours) in the eyewall, stronger radial inflow (red contours) within the PBL, and outflow (white contours) above, which are consistent with the strong storm intensity simulated by this experiment (Fig. 7). Furthermore, in the "TL-HWRF" experiment, the radial flow convergence (black contours) matches well with the eyewall updrafts. This feature facilitates an efficient transport of moisture into the eyewall to result in a large amount of condensate (color shading) in the eyewall. The resultant latent heating fosters the rapid converging spin-up processes as air parcels move radially inward and ascend swiftly within the

eyewall. This result suggests the importance of microphysics-turbulence interaction in TC intensification. In contrast, the peaks of persistent radial flow convergence in "DEF-HWRF" do not occur in the eyewall, but rather extend radially outward along the interface of radial inflow and outflow. Such a structure is apparently unfavourable to the rapid development of the vortex, since it cannot generate the efficient converging spin-up processes. Therefore, the simulated storm intensity difference by the two HWRFs may be largely attributed to the differences in the strength and structure of the secondary overturning circulation in this case. However, we note the depth of the radial inflow layer is similar in both HWRF simulations. It suggests that the inclusion of an in-cloud turbulent mixing parameterization aloft in the simulation does not alter the basic structure of the PBL in the TC vortex inner-core region.

To better understand the intensification processes in the two HWRF simulations, we examined the tangential eddy forcing $(F_\lambda + F_{sgs\_\lambda})$ for the primary circulation of the TC vortex. The model-resolved tangential eddy forcing F_λ is calculated by Eq. (1) using the wind fields in the standard HWRF output. As we noted previously, in this study we only focused on the vertical turbulent mixing, therefore, the SGS tangential eddy forcing F_{sgs_λ} diagnosed here is only the one calculated from the tendencies directly generated by the vertical turbulent mixing scheme (or PBL scheme). The SGS eddy forcing resulting from horizontal diffusion is not included. Figure 11 compares the SGS tangential eddy forcing averaged over the RI period from 06 UTC 28 to 06 UTC 29 August, 2015 between the two HWRF simulations, where the upper and bottom panels show the azimuthal-mean radial-height structure of SGS tangential eddy forcing and its horizontal plane view at 3 km altitude, respectively. There are a couple of interesting features shown in the figure. First, the radial-height structure of SGS tangential eddy forcing generated by "DEF-HWRF" (Fig. 11a) is very similar to that from a 3D full-physics TC simulation shown in Persing et al. (2013, their Figs. 10f &11f). The SGS eddy forcing above 2 km in the eyewall region is virtually zero because in-cloud turbulent mixing is not included in these simulations. In contrast, the in-cloud turbulent mixing parameterization in "TL-HWRF" allows HWRF to successfully generate the SGS tangential eddy forcing associated with the eyewall and rainband convection above the PBL (Fig. 11b). Such a SGS eddy forcing in the eyewall region from the layer just above the PBL to the upper troposphere has not been shown and discussed in previous numerical studies. Second, in addition to the expected strong negative SGS tangential eddy forcing within the PBL, the in-cloud turbulent mixing parameterization generates an interesting vertical structure of SGS tangential eddy forcing above the PBL in the eyewall region. Although it is much weaker than that in the PBL, the SGS tangential eddy forcing in the eyewall does show positive values at the heights just above the inflow layer as well as above the mid troposphere, suggesting that the eyewall SGS tangential eddy forcing above the PBL is indeed involved in the vortex spin-up processes during the RI. What remains unclear is the fidelity of the parameterized SGS eddy forcing above the PBL and its sensitivity to specific turbulent mixing parameterization. This constitutes one of the uncertainties in storm intensity simulation.

The model-resolved tangential eddy forcing averaged over the RI period from 06 UTC 28 to 06 UTC 29 August, 2015 is shown in Fig. 12. The basic radial-height structures of the resolved eddy forcing generated by the two simulations are similar

to a certain extent, and share similar features to those from Persing et al. (2013)'s 3D full-physics TC simulation (cf. their Figs. 10g &11g). But the resolved eddy forcing in "TL-HWRF" is much stronger than that in "DEF-HWRF". A robust feature shown in both simulations is the positive eddy forcing right above the inflow layer in the vicinity of the eyewall. From the perspective of absolute angular momentum conservation, this positive tangential eddy forcing is directly linked to the vortex spin-up. But currently we have little knowledge on what determines the sign, magnitude, and vertical structure of eddy forcing. Future research should focus on elucidating these issues regarding how eyewall and rainband eddy processes regulate the TC intensification.

Comparing Fig. 12b with Fig. 11b, it is easy to see that the model-resolved eyewall eddy forcing above the PBL in the "TL-HWRF" experiment has a magnitude about 5 times larger than the corresponding SGS eddy forcing, suggesting that the resolved eddy processes provide a major forcing that drives the primary circulation of the TC vortex in this case. As model resolution keeps increasing, we expect that the resolved eddy forcing will become more dominant. This is certainly a promising result, implying that numerical forecast of TC intensification may be ultimately a resolution problem. The difficulty, however, stems from the strong dependence of model-resolved eddy forcing and TC inner-core structure on the parameterized SGS eddy processes at the current resolution. As we showed in Figs. 9, 10, and 12, the only modification in SGS turbulent mixing parameterization above the PBL in the eyewall and rainbands result in substantial differences in the vortex structure, secondary overturning circulation, and model-resolved eyewall/rainband eddy forcing. Such a dependence of model-resolved TC fields on the parameterization of SGS in-cloud turbulence above the PBL is currently not well understood. It could stem from the fact that the large energy-containing turbulent eddies, such as kilometre and sub-kilometer convective elements or roll vortices (evidenced in the LESs), are not resolved by the current model resolution of 2 km, and could also result from the dynamical-microphysical interaction in TC clouds. The strong dependence of the resolved TC vortex on SGS parameterization poses a great challenge for accurate prediction of TC intensity change.

The results presented previously show that eyewall/rainband eddy forcing plays a key role in Jimena's RI and the inclusion of parameterization of eyewall/rainband in-cloud turbulent mixing above the PBL substantially improves HWRF's skills on generating robust eddy forcing for accurate intensity prediction. Such an improvement is not a special case, but is shown in HWRF simulations of other major TCs as well. Figure 13 shows the HWRF simulated maximum wind speed and storm central pressure of four other major hurricanes compared with the best track data. In all cases, the intensity simulations were improved due to the inclusion of an in-cloud turbulent mixing parameterization, in particular, "TL-HWRF" was able to partially capture the observed RI of Harvey (2017) and Marie (2014), which was largely missed by "DEF-HWRF". Similar to the HWRF simulations of Jimena (2015), our analyses show that the better intensity forecasts of these storms by "TL-HWRF" can be largely attributed to the improved simulation of storm inner-core structure and eyewall/rainband eddy forcing needed for TC vortex spin-up. As another example, Figure 14 compares the satellite observed vortex inner-core structure of Harvey (2017) with the simulated ones by the two HWRFs during the early and middle stages of Harvey's RI.

The asymmetric rainband structure, the size and the structure of the eyewall shown in satellite observations are reasonably reproduced by "TL-HWRF". But "DEF-HWRF" was not able to simulate the observed inner-core structure; in particular, the simulated eyewall is poorly defined and the size is much larger than the observed one. This result once again suggests that at the current model resolution the realization of axisymmetric dynamics underlying RI of TCs is sensitive to the parameterization of in-cloud SGS eddy processes above the PBL in the eyewall and rainbands in 3D full-physics simulations.

Our testing simulations also show that the inclusion of an in-cloud turbulent mixing parameterization in the eyewall and rainbands does not appear to degrade HWRF's performance on those cases that operational HWRF has decent forecasts on or generate false RI for those weak storms. As an example, Figure 15 shows the storm intensity of Hermine (2016) simulated by the two HWRFs compared with the best track data. Hermine (2016) is a weak storm with the peak intensity just reaching Category-1 hurricane strength. The simulation results show that the integrated turbulent mixing parameterization in the eyewall and rainbands only has a marginal impact on the HWRF predicted storm intensity. It did not over-predict storm intensity or generate false RI that one may be concerned about. We have worked with the Environmental Modeling Center (EMC), NOAA, to implement our modified PBL scheme in 2018 operational HWRF and tested it in operational HWRF full cycle simulations. The preliminary results from total 1,079 case simulations for various forecast lead times show that the modified HWRF noticeably reduces the bias error of maximum wind speed (Fig. 16). Currently, we continue working with EMC to improve and refine the parameterization of in-cloud turbulent mixing in the eyewall and rainbands.

4. Summary

Asymmetric eddy processes provide an important forcing for the evolution of the primary and secondary circulations of a TC. Because of the discrete grids used in numerical models, the eddy forcing with a continuous spectrum is split into two parts resulting from the model-resolved and parameterized SGS eddy processes. While higher model resolution allows the model-resolved eddy forcing to be better resolved, the parametric determination of SGS eddy forcing is source of uncertainty in storm intensity prediction.

In numerical simulations, the SGS eddy forcing is determined by the turbulent mixing scheme. Turbulence is commonly regarded as a flow feature of the PBL. In fair-weather conditions the turbulent PBL is often cleanly separated from the free atmosphere above by a capping inversion. Except for occasional clear-sky turbulence, turbulent mixing is negligible above the PBL. The various PBL schemes used today in the state-of-the-art numerical models were designed to best represent the turbulent transport within the PBL. In a TC environment, however, turbulence is no longer solely generated by the shear production and buoyancy production associated with the PBL processes. Intense turbulent mixing can also be generated by cloud processes above the PBL in the eyewall and rainbands due to radiative cooling, evaporative cooling, and inhomogeneous diabatic heating and cooling. While the concept of PBL is still applicable in the eyewall and rainbands as to

the layer that is directly affected by the surface turbulent processes, the treatment of turbulent mixing must go beyond the conventional scope of the PBL. This is particularly true in the TC inner-core region as air parcels ascend swiftly within the eyewall and rainbands where there is no physical interface that separates the turbulence generated by the PBL processes and cloud processes aloft. The conventional PBL theory that treats the PBL as a shallow layer adjacent to Earth's surface becomes insufficient to explain the observed intensity change in some TCs. Such a deficiency of classic PBL theory is reflected in the PBL scheme used in HWRF. The HWRF PBL scheme is a typical first-order K-closure scheme that parameterizes turbulent mixing based on the diagnosed PBL height. Our analyses show that an artificial separation of the PBL from the free atmosphere above cannot appropriately represent the vertical turbulent structure and transport in the eyewall and rainbands, in particular, the simple method of parameterizing turbulent mixing above the PBL based on the bulk Richardson number is unable to account for the intense turbulent mixing aloft generated by eyewall/rainband cloud processes. As a result, the HWRF PBL scheme fails to generate the eyewall/rainband SGS eddy forcing associated with cloud processes above the PBL.

In this study, we developed a method to allow for an integrated turbulent mixing parameterization in the eyewall and rainbands based on the "TL" determined by the simulated radar reflectivity. Such a change from "PBL" to "TL" will not affect the turbulent mixing parameterization outside the eyewall and rainbands since the "TL" is virtually the same as the "PBL" in non-convective regions. This simple adjustment allows HWRF to successfully generate eyewall/rainband SGS eddy forcing above the PBL. Numerical tests on multiple major hurricanes show that the inclusion of an in-cloud turbulent mixing parameterization notably improves HWRF's skills on predicting TC intensity change, in particular, RI in several cases. While the performance of the modified turbulent mixing scheme is promising, our treatment of in-cloud turbulent mixing is very crude, and thus, the scheme may not be ready for use in operational TC forecasts in its current form. Nonetheless, our results show that numerical simulations of TC intensification are sensitive to the parameterization of SGS turbulent mixing induced by the cloud processes above the PBL in the eyewall and rainbands. Future research should focus on developing physically robust scheme to better represent in-cloud turbulent processes in 3D full-physics models and advance our theoretical understanding of how eyewall/rainband eddy forcing above the PBL modulates TC intensification including RI. There are scientific questions that need to be further addressed and clarified, such as, what determines the sign, magnitude, and vertical distribution of eyewall/rainband forcing? And is eddy forcing that leads to TC intensification a stochastic process or deterministic process?

While the improvement of TC intensity forecast due to the inclusion of an in-cloud turbulent mixing parameterization is clearly demonstrated, the underlying reason for such an improvement appears to be complicated. At first glance, the calculated SGS eddy forcing above the PBL is about five times smaller than the model-resolved eddy forcing (Figs. 11b and 12b). This would suggest that the model-resolved eddy forcing is the dominant forcing for the spin-up of the TC vortex at the current model resolution. However, the simulated TC inner-core structure, secondary overturning circulation, and the model-resolved eddy forcing show a strong dependence on the parameterized in-clouds SGS eddy processes above the PBL. The in-

cloud turbulent mixing parameterization appears to facilitate the realization of axisymmetric dynamical mechanism underlying RI of TCs in 3D full-physics simulations. These results suggest that the model-resolved and SGS eddy forcings are not independent, although they appear as two separate terms in the governing equations and are determined separately in numerical simulations. Such a dependence may result from the fact that the dynamical-microphysical interaction and large energy-containing turbulent eddies, such as kilometre and sub-kilometer convective elements and roll vortices, are not resolved but parameterized at a grid spacing of 2 km. Will further increasing of model resolution reduce the dependence of model-resolved fields on parameterized SGS processes? This question cannot be answered until the dynamical-microphysical interaction and large energy-containing eddies can be explicitly resolved. To do so, large-eddy resolution both horizontally and vertically is needed not only in the PBL (like classic LES) but also aloft in the eyewall and rainbands to resolve in-cloud turbulent eddies generated by cloud processes. This is not likely to happen in the near future for operational forecasts even with ever-increasing computational capability. Therefore, as model resolution keeps increasing, research effort should be continuously devoted to improving parametric representation of model physics not only in the PBL but also above the PBL to appropriately account for microphysical processes, in-cloud turbulent processes, and the interaction between microphysical and dynamical processes.

Acknowledgement

This work is supported by NOAA/HFIP under Grants NA14NWS4680030 and NA16NWS4680029, National Science Foundation under Grant AGS-1822238 and AGS-1822128, and BP/The Gulf of Mexico Research Initiative. We are very grateful to Dr. Michael T. Montgomery and an anonymous reviewer for their constructive and insightful comments, which lead to the improvement of the paper. Data used in this study can be accessed at http://vortex.ihrc.fiu.edu/download/HWRF-TUR/.

References

Aligo, E. A., Ferrier, B., and Carley, J. R.: Modified NAM microphysics for forecasts of deep convective storms. Mon. Wea. Rev., doi:10.1175/MWR-D-17- 0277.1, 146, 4115 – 4153, 2018.

Arakawa, A., and Schubert, W. H.: Interaction of a cumulus cloud ensemble with the large-scale environment: Part I. J. Atmos. Sci., 31, 674–701, 1974.

Bryan, G. H.: Effects of surface exchange coefficients and turbulence length scales on the intensity and structure of numerically simulated hurricanes. Mon. Wea. Rev., 140, 1125–1143, https://doi.org/10.1175/MWR-D-11-00231.1, 2012.

Bryan, G. H., and Rotunno, R.: The maximum intensity of tropical cyclones in axisymmetric numerical model simulations. Mon. Wea. Rev., 137, 1770–1789, https://doi.org/10.1175/ 2008MWR2709.1, 2009.

Bryan, G. H., Wyngaard, J. C., and Fritsch, J. M.: Resolution requirements for the simulation of deep moist convection. Mon. Wea. Rev., 131(10), 2394-2416, 2003.

Bui, H. H., Smith, R. K., Montgomery, M. T., and Peng, J.: Balanced and unbalanced aspects of tropical cyclone intensification. Quart. J. Roy. Meteor. Soc., 135, 1715–1731, DOI: 10.1002/qj.502, 2009.

Businger J. A., Wyngaard, J. C., Izumi, I., Bradley, E. F.: Flux-profile relationships in the atmospheric surface layer. J. Atmos. Sci. 28, 181-189, 1971.

Charney, J. G. and Eliassen, A.: On the growth of the hurricane depression. J. Atmos. Sci., 21, 68 - 75, 1964.

Deardorff, J. W.: Stratocumulus-capped mixed layers derived from a three-dimensional model. Bound.-Layer Meteor., 18, 495-527, 1980.

Deardorff, J. W.: Parameterization of the planetary boundary layer for use in general circulation models. Mon. Wea. Rev. 100, 93-106, 1972.

Emanuel, K. A.: Self-stratification of tropical cyclone outflow. Part II: Implications for storm intensification, J. Atmos. Sci., 69, 988– 996, 2012.

Emanuel, K. A. and Rotunno, R.: Self-statification of tropical cyclone outflow. Part I: Implications for storm structure, J. Atmos. Sci., 68, 2236–2249, 2011.

Emanuel, K. A., DesAutels, C., Holloway, C., and Korty, R.: Environmental control of tropical cyclone intensity. J. Atmos. Sci., 61, 843–858, 2004.

Emanuel, K. A.: Tropical cyclone, Annu. Rev. Earth Planet Sci., 31, 75–104, 2003.

Giangrande, S. E., Collis, S., Straka, J., Protat, A., Williams, C., and Krueger, S.: A summary of convective-core vertical velocity properties using ARM UHF wind profilers in Oklahoma. J. of Appl. Meteor. Climate, 52, 2278–2295, 2013.

Gopalakrishnan, S., Marks, F. D., Zhang, J. A., Zhang, X., Bao, J.-W., and Tallapragada, V.: A study of the impact of vertical diffusion on the structure and intensity of tropical cyclones using the high-resolution HWRF system. J. Atmos. Sci. 70, 524-541, 2013.

Green, B. W., and Zhang, F.: Numerical simulations of Hurricane Katrina (2005) in the turbulent gray zone. J. Adv. Modeling Earth Sys., 7(1), 142-161, 2015.

Guo, H., Golaz, J.-C., Donner, L. J., Wyman, B., Zhao, M., and Ginous, P.: CLUBB as a unified cloud parameterization: Opportunities and challenges. Geophys. Res. Lett., 42, 4540-4547, 2015.

Hogan, R. J., Grant, A. L. M., Illingworth, A. J., Pearson, G. N., and O'Connor, E. J.: Vertical velocity variance and skewness in clear and cloud-topped boundary layers as revealed by Doppler lidar. Quart. J. Roy. Meteor. Soc., 135, 635–643, 2009.

Holtslag, A. A. M, and Boville, B. A.: Local versus nonlocal boundarylayer diffusion in a global model. J. Climate, 6, 1825–1842, 1993.

Holtslag, A. A. M, de Bruijn, E. I. F., and Pan, H.-L.: A high-resolution air mass transformation model for short-range weather forecasting. Mon. Wea. Rev., 118, 1561–1575, 1990.

Hong, S.-Y., and Pan, H.-L: Nonlocal boundary layer vertical diffusion in a Medium-Range Forecast model. Mon. Wea. Rev., 124, 2322–2339, 1996.

Jiang, H., and Ramirez, E. M.: Necessary conditions for tropical cyclone rapid intensification as derived from 11 years of TRMM data. J. Climate., 26, 6459-6470, 2013.

Kieper, M. E., and Jiang, H.: Predicting tropical cyclone rapid intensification using the 37GHz ring pattern identified from passive microwave measurements. Geophys. Res. Lett., 39, L13804, dio: 10.1029/2012GL052115, 2012.

Kosović, B.: Subgrid-scale modelling for the large-eddy simulation of high-Reynolds-number boundary layers. J. Fluid Mech., 336, 151-182, 1997.

LeMone, M. A. and Zipser, E. J.: Cumulonimbus vertical velocity events in GATE. Part I: Diameter, intensity and mass flux, J. Atmos. Sci., 37, 2444–2457, 1980.

Li, Y.-B., Zhu, P., Gao, Z.-Q., and Cheung, K.: Sensitivity of large eddy simulations of tropical cyclone to sub-grid scale mixing parameterization. J. Adv. Modeling Earth Sys., submitted, 2019.

Lorsolo, S, Zhang, J. A., Marks, F. D., and Gamache, J.: Estimation and mapping of hurricane turbulent energy using airborne Doppler measurements. Mon. Wea. Rev., 138, 3656-3670, 2010.

Marks, F. D., Black, P. G., Montgomery, M. T., and Burpee, R. W.: Structure of the eye and eyewall of Hurricane Hugo (1989), Mon. Wea. Rev., 136, 1237–1259, 2008.

Marks, F. D. and Shay, L. K.: Landfalling tropical cyclones: Forecast problems and associated research opportunities. Bull. Amer. Meteor. Soc., 79, 305-323, 1998.

Moeng, C.-H., and Coauthors: Simulation of a stratocumulus-topped PBL: Intercomparison among different numerical codes. Bull. Amer. Meteor. Soc., 77, 261–278, 1996.

Montgomery, M. T. and Smith, R. K.: Paradigms for tropical cyclone intensification. Australian Meteor. & Ocean. Journal, 64, 37–66, 2014.

Moss, M. S, and Rosenthal, S. L.: On the estimation of planetary boundary layer variables in mature hurricanes. Mon. Wea. Rev. 103, 980–988, 1975.

Nolan, D. S., Moon, Y., and Stern, D. P.: Tropical cyclone intensification from asymmetric convection: Energetics and efficiency. J. Atmos. Sci., 64, 3377-3405, 2007.

Ooyama K. V.: Conceptual evolution of the theory and modeling of the tropical cyclone. J. Meteor. Soc. Japan, 60, 369–80, 1982.

Ooyama, K. V.: Numerical simulation of the life cycle of tropical cyclones, J. Atmos. Sci., 26, 3-40, 1969.

Persing, J., Montgomery, M. T., McWilliams, J. C., and Smith, R. K.: Asymmetric and axisymmetric dynamics of tropical cyclones. Atmos. Chem. Phys., 13, 12299–12341, 2013.

Rotunno, R., Chen, Y., Wang, W., Davis, C., Dudhia, J., & Holland, G. J.: Large-eddy simulation of an idealized tropical cyclone. Bulletin of the American Meteorological Society, 90(12), 1783-1788, 2009.

Shapiro, L.: The asymmetric boundary-layer flow under a translating hurricane. J. Atmos. Sci,. 40, 1984–1998, 1983.

Shapiro, L. J., and Willoughby, H. E.: The response of balanced hurricanes to local sources of heat and momentum. J. Atmos. Sci., 39, 378–394, doi: 10.1175/1520-0469(1982)039<0378:TROBHT>2.0.CO;2, 1982.

Smagorinsky, J.: General circulation experiments with the primitive equations: I. The basic experiment. Mon. Wea. Rev., 91(3), 99-164, 1963.

Smith, R. K., Montgomery, M. T., and Nguyen, S. V.: Tropical cyclone spin-up revisited, Q. J. R. Meteorol. Soc., 135, 1321–1335, 2009.

Smith, R. K, Montgomery, M. T., and Vogl, S.: A critique of Emanuel's hurricane model and potential intensity theory. Q. J. R. Meteorol. Soc., 134: 551–561, 2008.

Smith, R. K, Montgomery, M. T., and Zhu, H.: Buoyancy in tropical cyclones and other rapidly rotating atmospheric vortices. Dyn. Atmos. & Oceans, 40, 189-208, 2005.

Smith, R. K, and Montgomery, M. T.: Hurricane boundary layer theory. Q. J. R. Meteorol. Soc. 136, 1665–1670, 2010.

Stevens, B., Moeng, C.-H., Ackerman, A. S. Bretherton, C. Chlond, A. De Roode, S. Edwards, J. Golaz, J.-C., Jiang, H., Khairoutdinov, M., Kirkpatrick, M. P., Lewellen, D. C., Lock, A., Muller, F. Stevens, D. E., Whelan, E., Zhu, P.: Evaluation of large-eddy simulations via observations of nocturnal marine stratocumulus. Mon. Wea. Rev., 133, 1443-1462, doi:http://dx.doi.org/10.1175/MWR2930.1, 2005.

Stull, R. B.: An introduction to boundary-layer meteorology. Kluwer: Dordrecht, The Netherlands, 670pp, 1988.

Tao, C., and Jiang, H.: Distributions of shallow to very deep precipitation–convection in rapidly intensifying tropical cyclones. J. Climate, 28, 8791–8824. doi:http://dx.doi.org/10.1175/JCLI-D-14-00448.1, 2015.

Troen, I., and Mahrt, L.: A simple model of the atmospheric boundary layer: Sensitivity to surface evaporation. Bound.-Layer Meteor., 37, 129–148, 1986.

Vigh, J. L., Emanuel, K. A., Biswas, M. K., Hendricks, E. A., and Rozoff, C. M.: Exploring the Upper Bound of Tropical Cyclone Intensification, 33rd Conference on Hurricanes and Tropical Meteorology. Ponte Vedra, FL, 16-20 April, 2018.

Wu, C.-M., and Arakawa, A.: A Unified Representation of Deep Moist Convection in Numerical Modeling of the Atmosphere. Part II. J. Atmos. Sci., 71, 2089-2103, 2014.

Zhang J. A., Marks, F. D., Sippel, J. A., Rogers, R. F., Zhang, X., Gopalakrishnan, S. G., Zhang, Z., and Tallapragada, V.: Evaluating the Impact of Improvement in the Horizontal Diffusion Parameterization on Hurricane Prediction in the Operational Hurricane Weather Research and Forecast (HWRF) Model. Weather & Forecasting, 33, 317 – 329, 2018.

Zhang J. A., Marks, F. D., Montgomery, M. T., and Lorsolo, S.: An estimation of turbulent characteristics in the low-level region of intense Hurricanes Allen (1980) and Hugo (1989). Mon. Wea. Rev., 139, 1447–1462, 2011.

Zhu, P., Wang, Y., Chen, S. S., Curcic, M., Gao, C.: Impact of storm-induced cooling of sea surface temperature on large turbulent eddies and vertical turbulent transport in the atmospheric boundary layer of Hurricane Isaac, J. Geophys. Res. - Oceans, 121, 861-876, doi:10.1002/2015JC011320, 2015.

Zhu, P.: On the mass-flux representation of vertical transport in moist convection, J. Atmos. Sci.. 72, 4445-4468, doi: http://dx.doi.org/10.1175/JAS-D-14-0332.1, 2015.

Zhu, P.: Simulation and parameterization of the turbulent transport in the hurricane boundary layer by large eddies. J. Geophys. Res., 113, D17104, doi:10.1029/2007JD009643, 2008a.

Zhu, P.: A multiple scale modeling system for coastal hurricane wind damage mitigation. Natural Hazards, 47, 577-591. doi:10.1007/s11069-008-9240-8, 2008b.

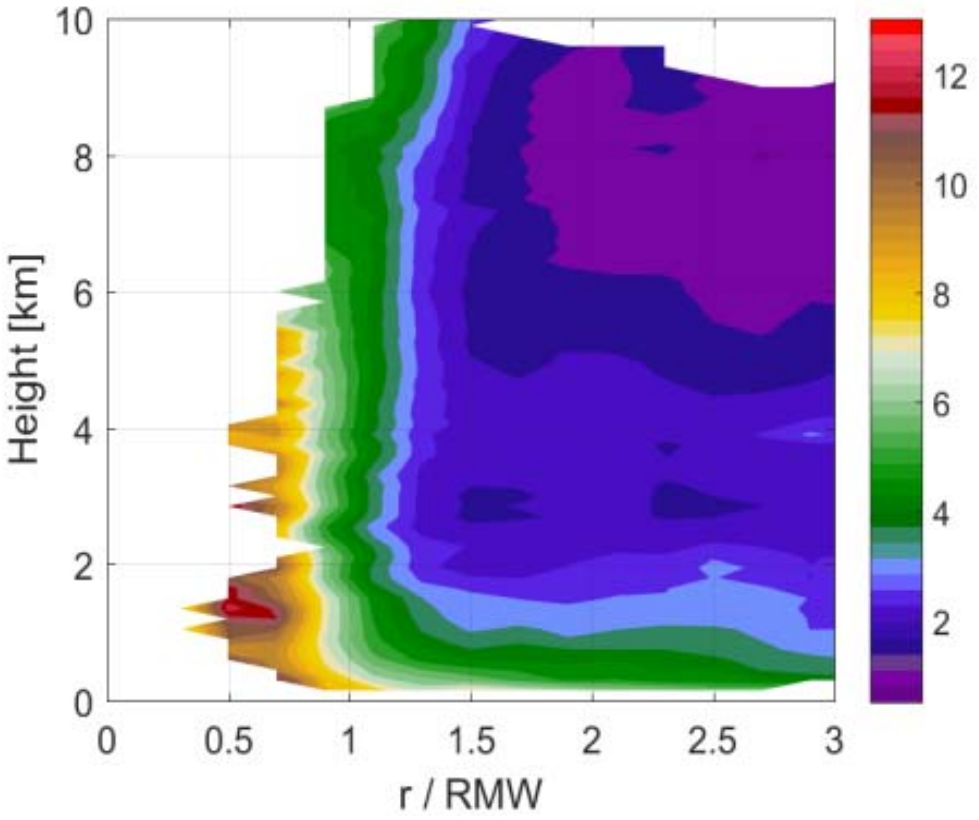

Figure 1: Composite TKE derived from airborne radar data from 116 radial legs of P3 flights in the 2003-2010 hurricane seasons as a function of height and the radius normalized by the radius of maximum wind (RMW).

5

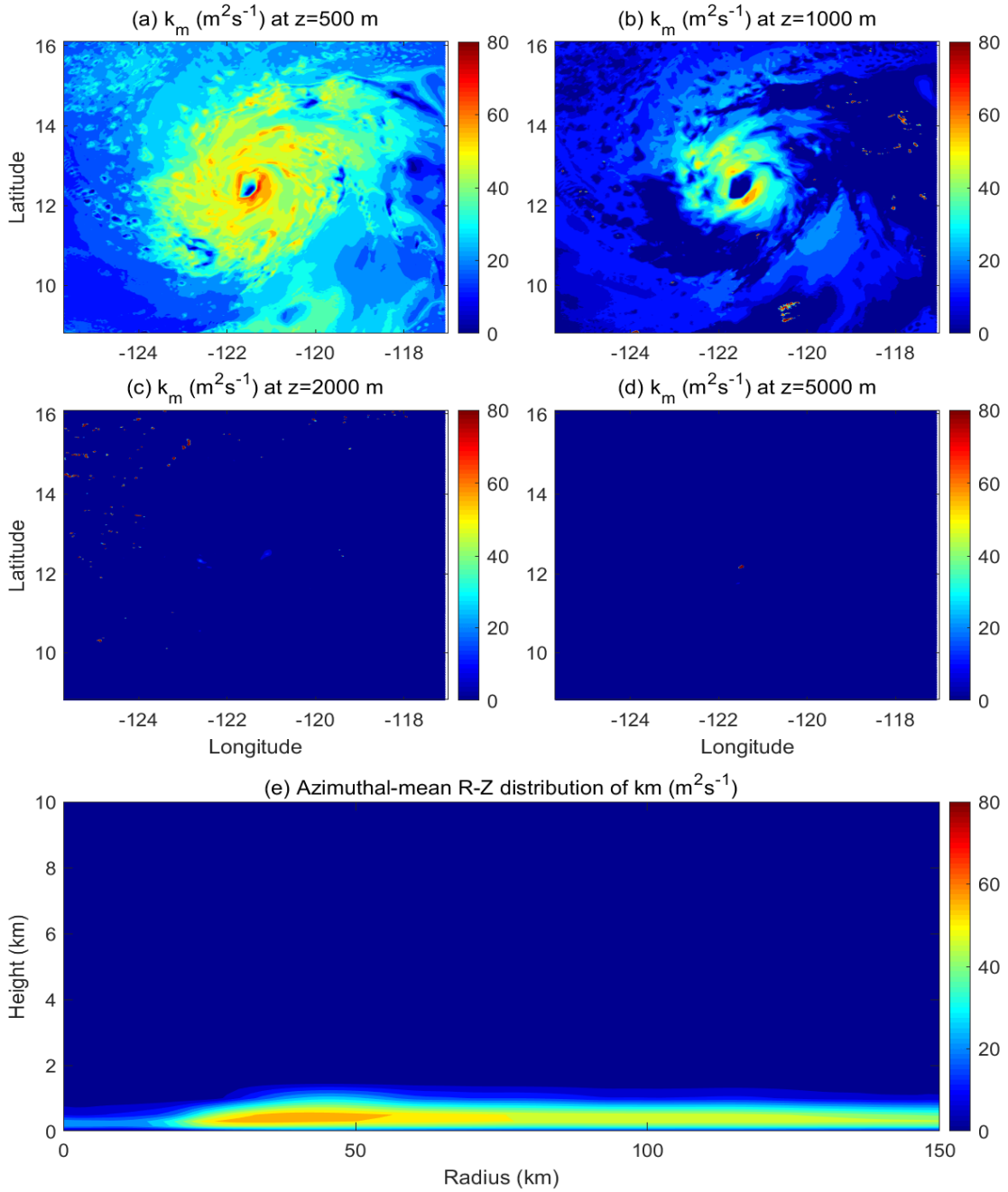

Figure 2: (a) – (d): Horizontal distribution of eddy exchange coefficients of momentum (k_m) at the altitudes of z = 0.5, 1.0, 2.0, and 5.0 km, respectively; (e): Azimuthal-mean radius-height distribution of k_m from a HWRF simulation of Hurricane Jimena (2015) at 12:00 UTC 28 August, 2015.

5

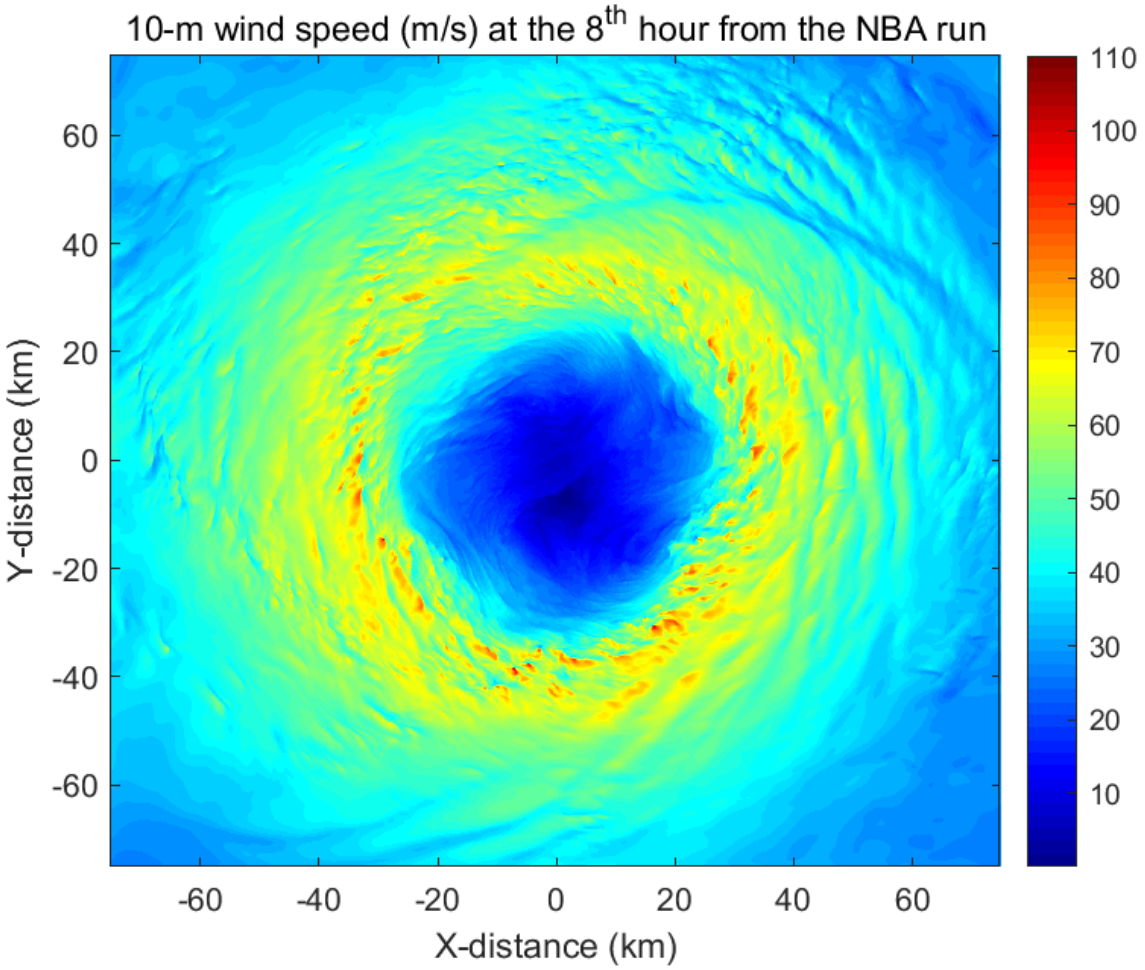

Figure 3: Instantaneous 10-m surface wind speeds of Hurricane Isabel (2003) at the 8th simulation hour by a WRF-LES that uses the 3D NBA SGS model.

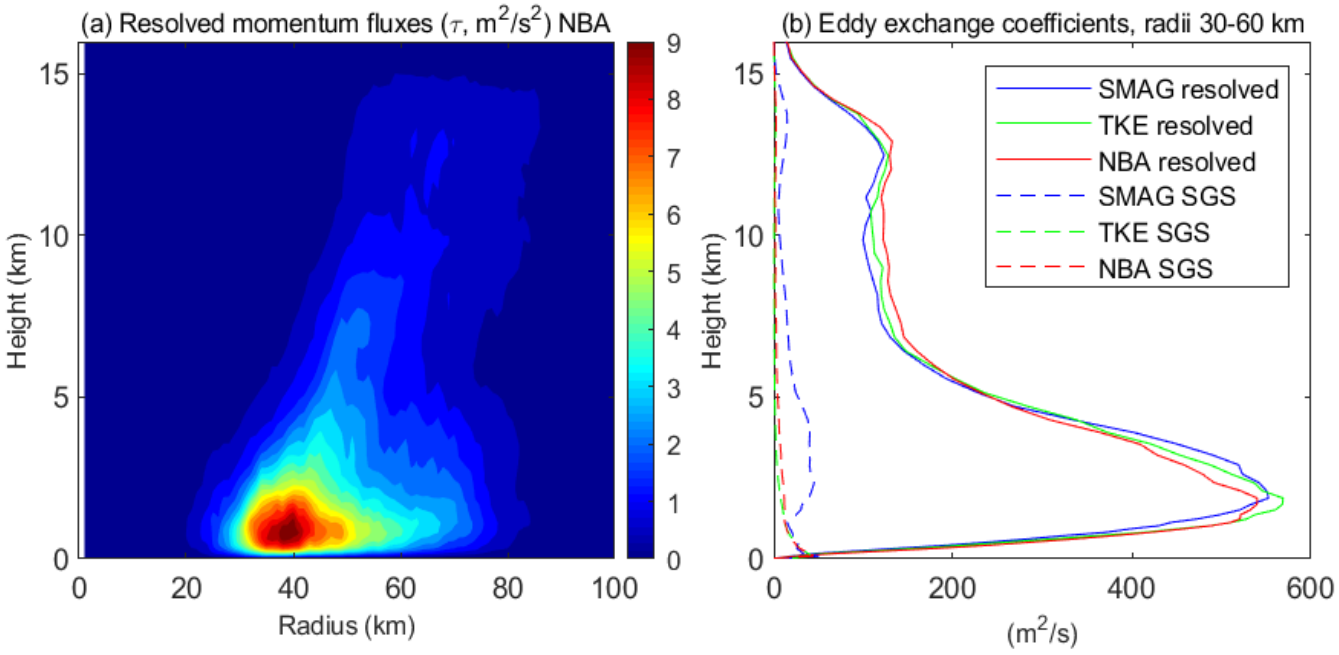

Figure 4: (a): Azimuthal-mean radius-height distribution of the vertical momentum fluxes, $\tau = (\overline{w'u'}^2 + \overline{w'v'}^2)^{\frac{1}{2}}$, induced by the resolved eddies with scales smaller than 2 km from the WRF-LES that uses the 3D NBA SGS model. (b): Vertical profiles of the parameterized (dashed) and resolved (solid) vertical eddy exchange coefficients of momentum averaged over 30 – 60 km radii (where the eyewall is located) from the three LESs that use different 3D SGS models. Note that the results are averaged over 3 – 8 simulation hours and the SGS eddy exchange coefficients are the direct output from the 3D SGS models used in the simulations.

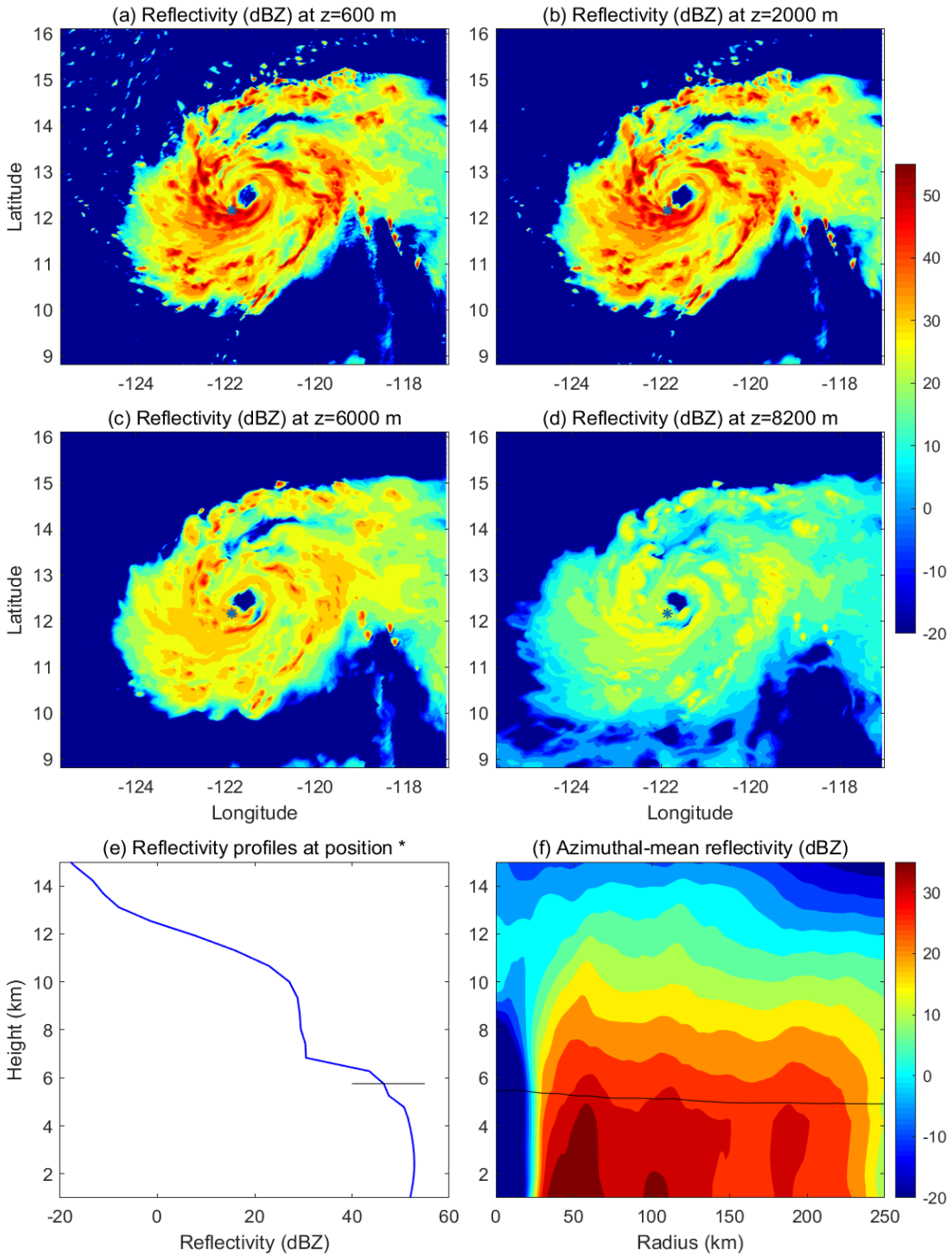

Figure 5: (a)-(d): HWRF simulated radar reflectivity of Hurricane Jimena (2015) at different altitudes (z = 0.6, 2.0, 6.0, and 8.2 km) at 12:00 UTC 28 August, 2015. (e): Vertical profile of radar reflectivity at a location in the eyewall marked by "*" in (a)-(d). (f): Azimuthal-mean radius-height structure of radar reflectivity. Black line in (e) and (f) indicates the freezing line.

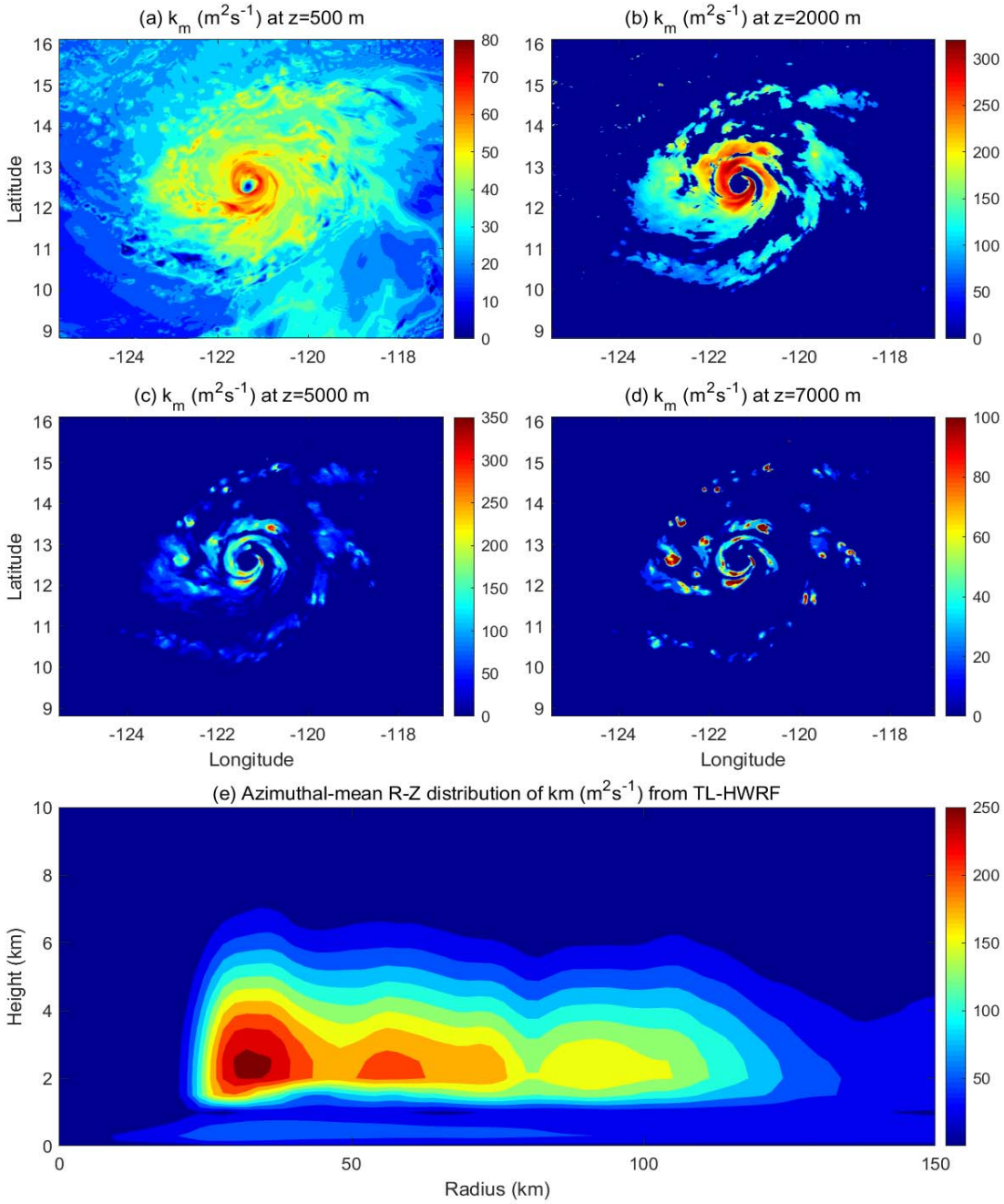

Figure 6: (a) – (d): Horizontal distribution of eddy exchange coefficients of momentum (k_m) at the altitudes of z = 0.5, 2.0, 5.0, and 7.0 km, respectively; (e): Azimuthal-mean radius-height distribution of k_m from the HWRF simulation with the inclusion of an in-cloud turbulent mixing parameterization (TL-HWRF) at 12:00 UTC 28 August, 2015.

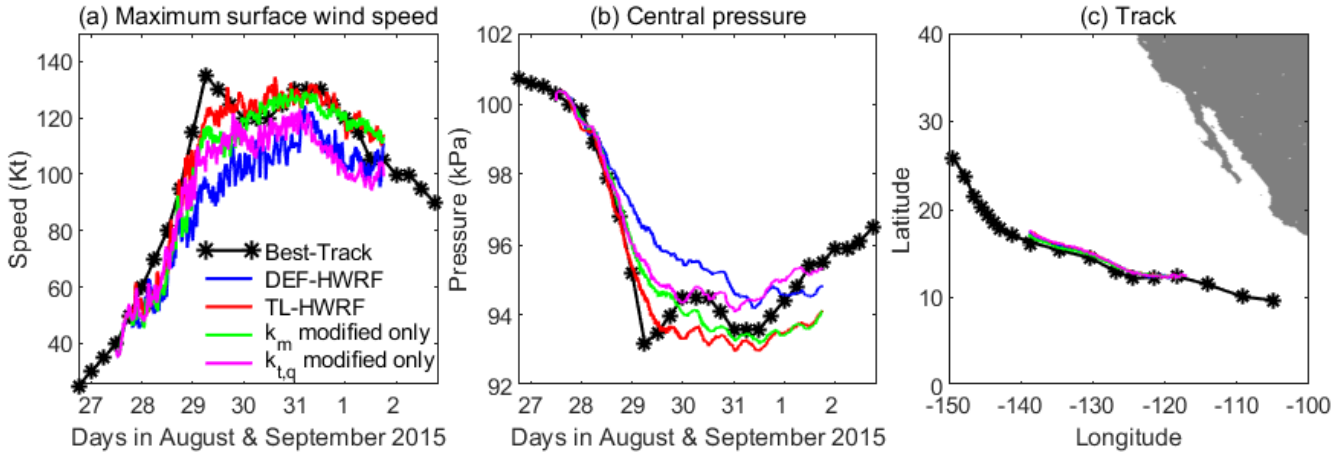

Figure 7: Comparison of HWRF simulated maximum surface wind speed, storm central pressure, and track of Jimena (2015) with the best track data (Black). Blue curve indicates the simulation by the default HWRF ("DEF-HWRF"). Red curve indicates the simulation by the HWRF with inclusion of an in-cloud turbulent mixing parameterization ("TL-HWRF"). Green curve represents the simulation in which only the eddy exchange coefficient for momentum is modified while keeping the eddy exchange coefficient for heat and moisture the same as the default. Magenta curve is opposite to the green curve in which only the eddy exchange coefficient for heat and moisture is modified.

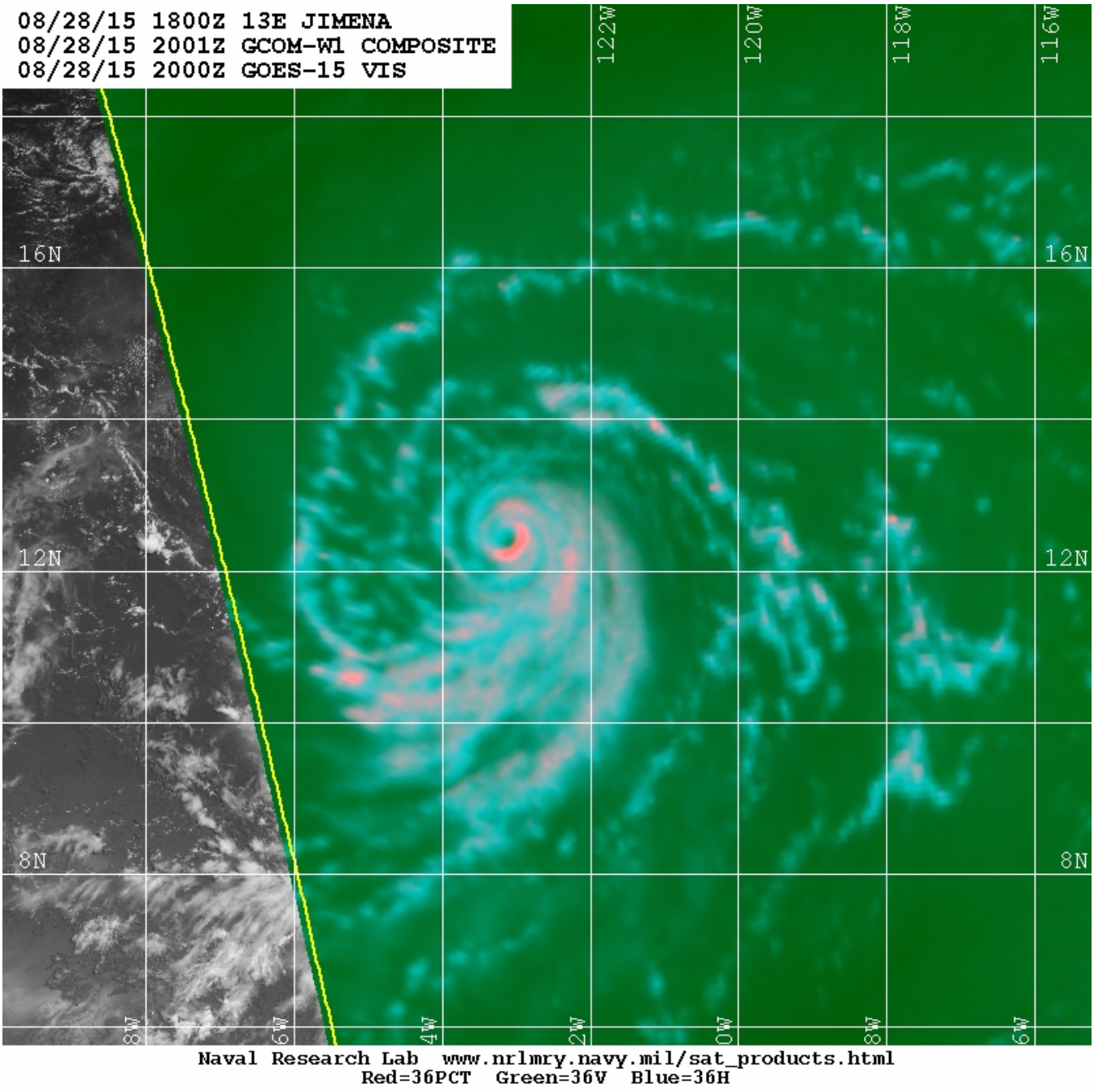

Figure 8: Naval Research Laboratory 37 GHz color image from the Advanced Microwave Scanning Radiometer 2 (AMSR2) at 20:00 UTC 28 August, 2015.

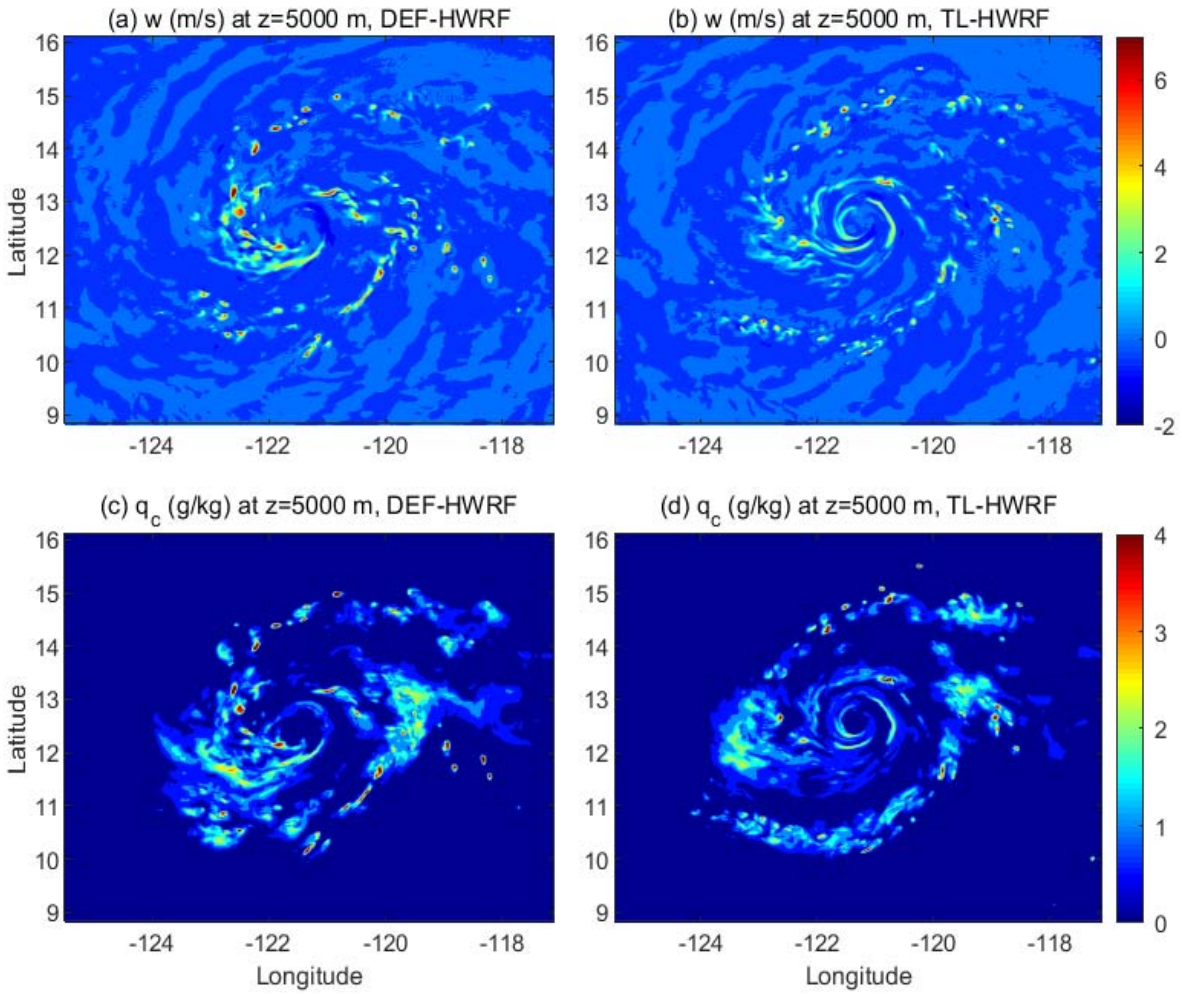

Figure 9: Simulated vertical velocity (ms^{-1}) and hydrometeor mixing ratio (gkg^{-1}) at 5.0 km altitude at 12:00 UTC 28 August, 2015 by the default HWRF (DEF-HWRF) and the HWRF with the inclusion of an in-cloud turbulent mixing parameterization (TL-HWRF).

5

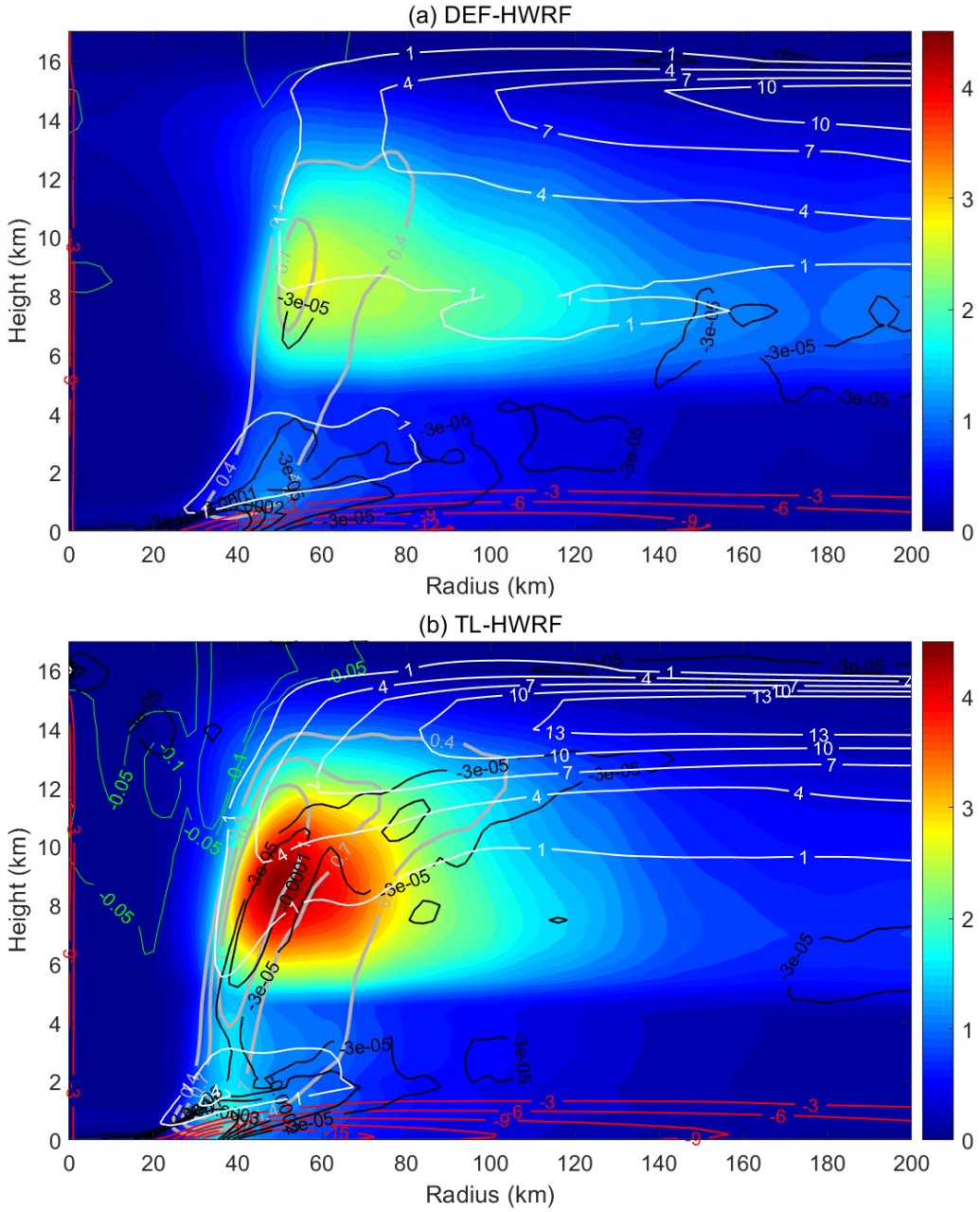

Figure 10: Simulated azimuthal-mean radius-height structure of updrafts (thick grey contours, ms^{-1}), downdrafts (green contours, ms^{-1}), hydrometeor mixing ratio (color shading, gkg^{-1}), radial inflow (red contours, ms^{-1}), outflow (white contours, ms^{-1}), and radial flow convergence (black contours, s^{-1}) averaged over Jimena's RI period from 06:00 UTC 28 to 06:00 UTC 29 August, 2015.

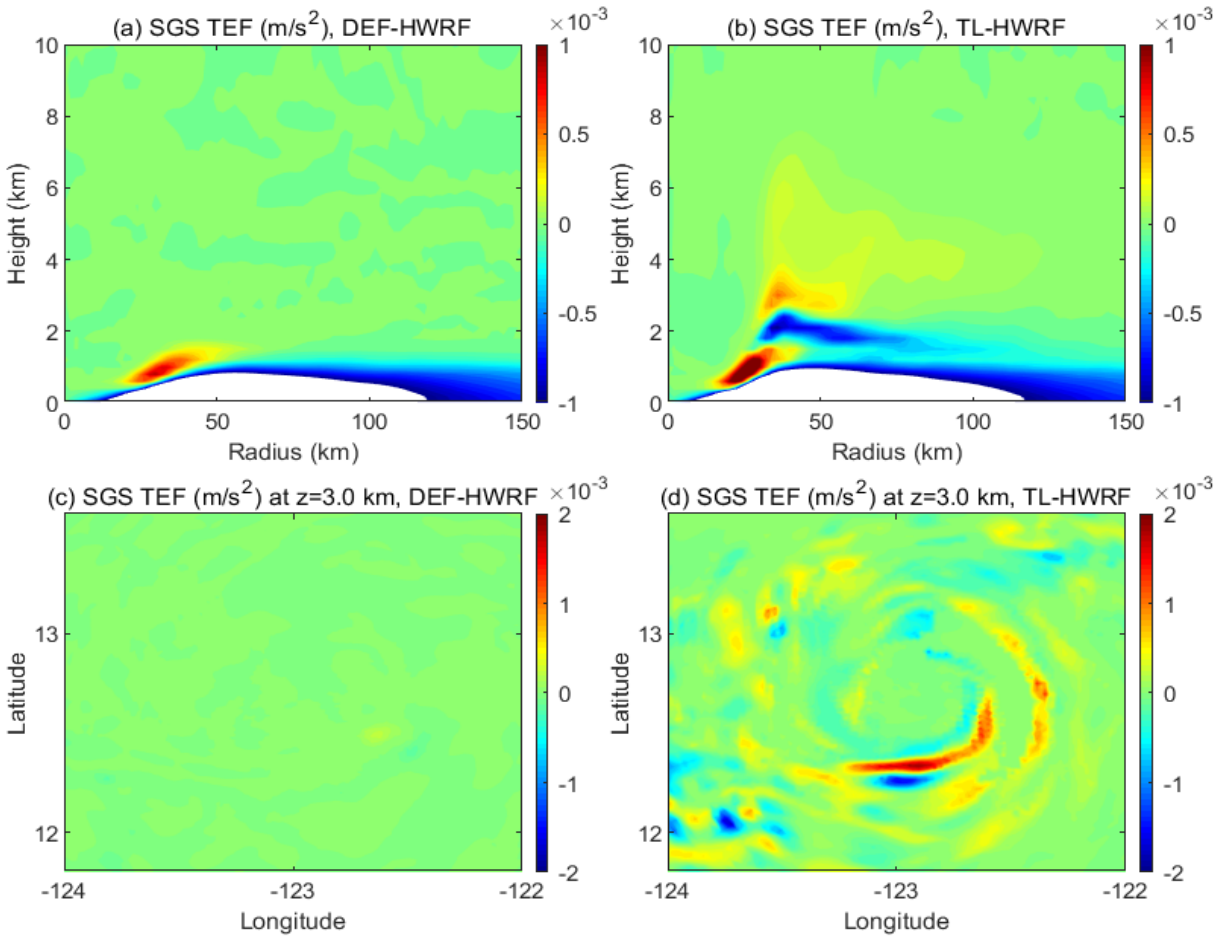

Figure 11: SGS tangential eddy forcing (TEF) averaged over Jimena's RI period from 06:00 UTC 28 to 06: UTC 29 August, 2015 from the two HWRF simulations (DEF-HWRF and TL-HWRF). Top panels: azimuthal-mean radius-height structure of SGS TEF. Note that the SGS TEF smaller than -1.0e-3 (ms^{-2}) is shaded with white color for a clear illustration of SGS TEF above the PBL. Bottom panels: horizontal structure of SGS TEF at 3 km altitude.

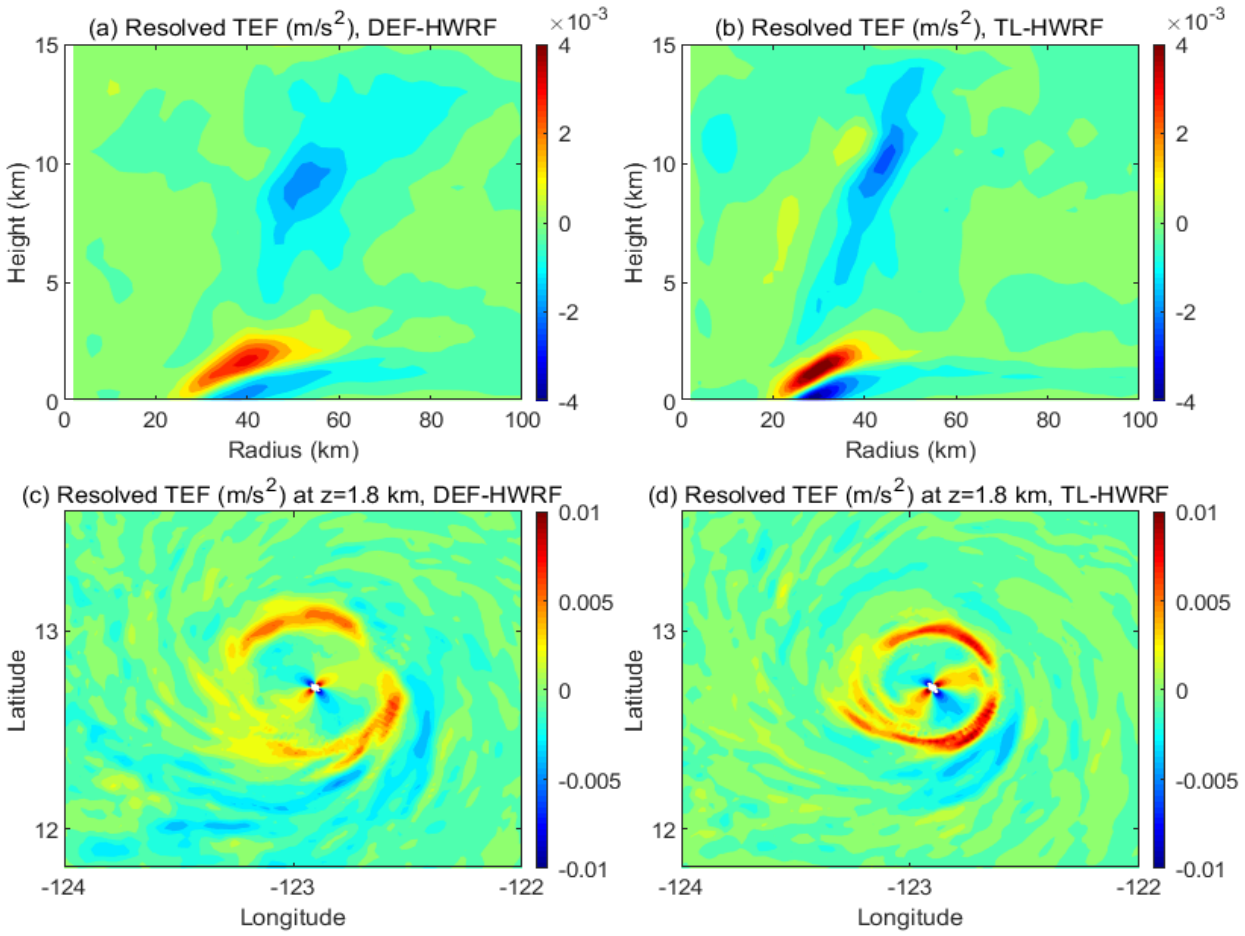

Figure 12: Model-resolved tangential eddy forcing (TEF) averaged over Jimena's RI period from 06:00 UTC 28 to 06:00 UTC 29 August, 2015 from the two HWRF simulations (DEF-HWRF and TL-HWRF). Top panels: azimuthal-mean radius-height structure of resolved TEF. Bottom panels: horizontal structure of resolved TEF at 1.8 km altitude.

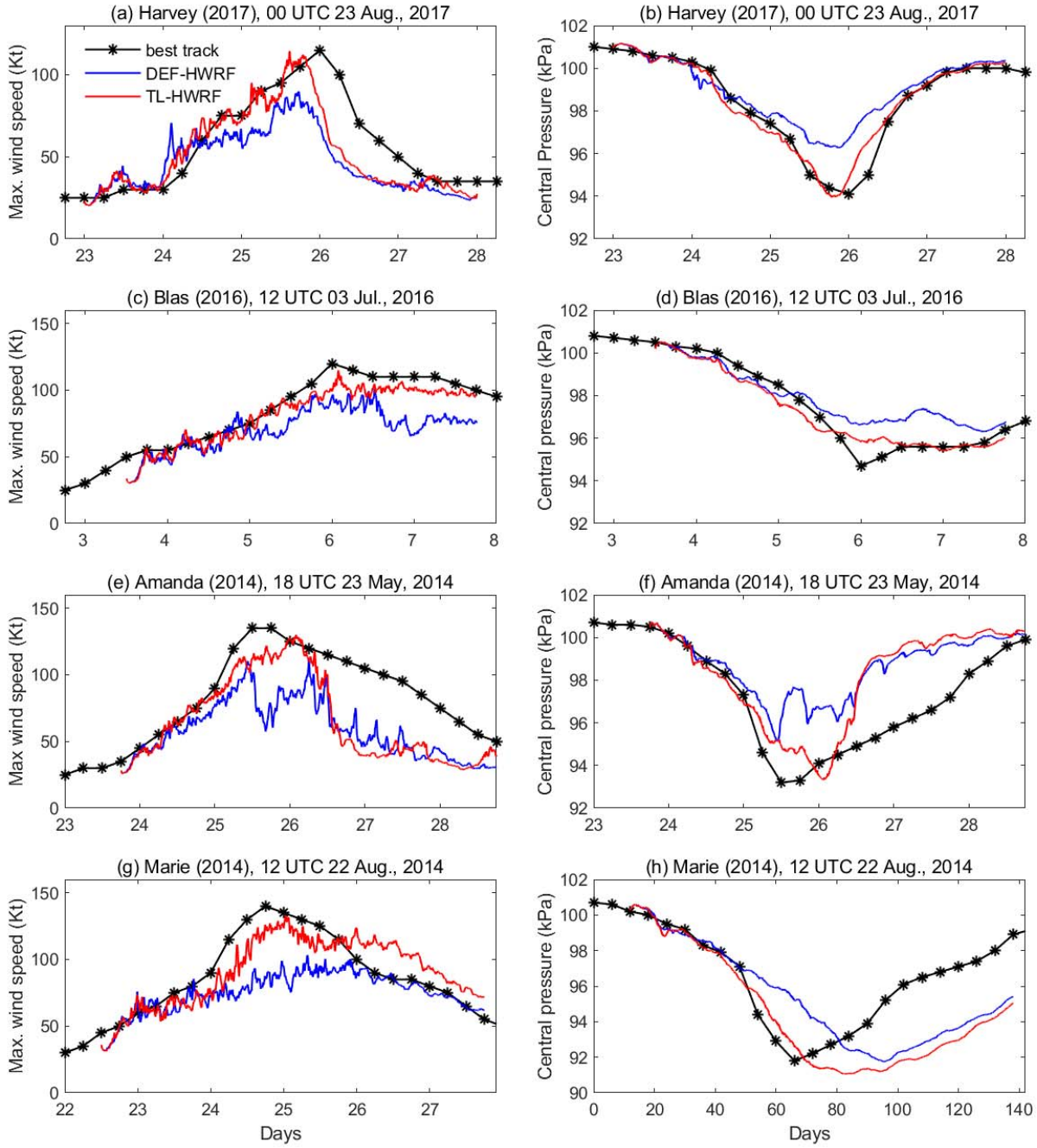

Figure 13: HWRF simulated maximum wind speed and storm central pressure of four other major hurricanes, Harvey (2017), Blas (2016), Amanda (2014), and Marie (2014), compared with the best track data (black curves). Blue curves: DEF-HWRF; Red curves: TL-HWRF.

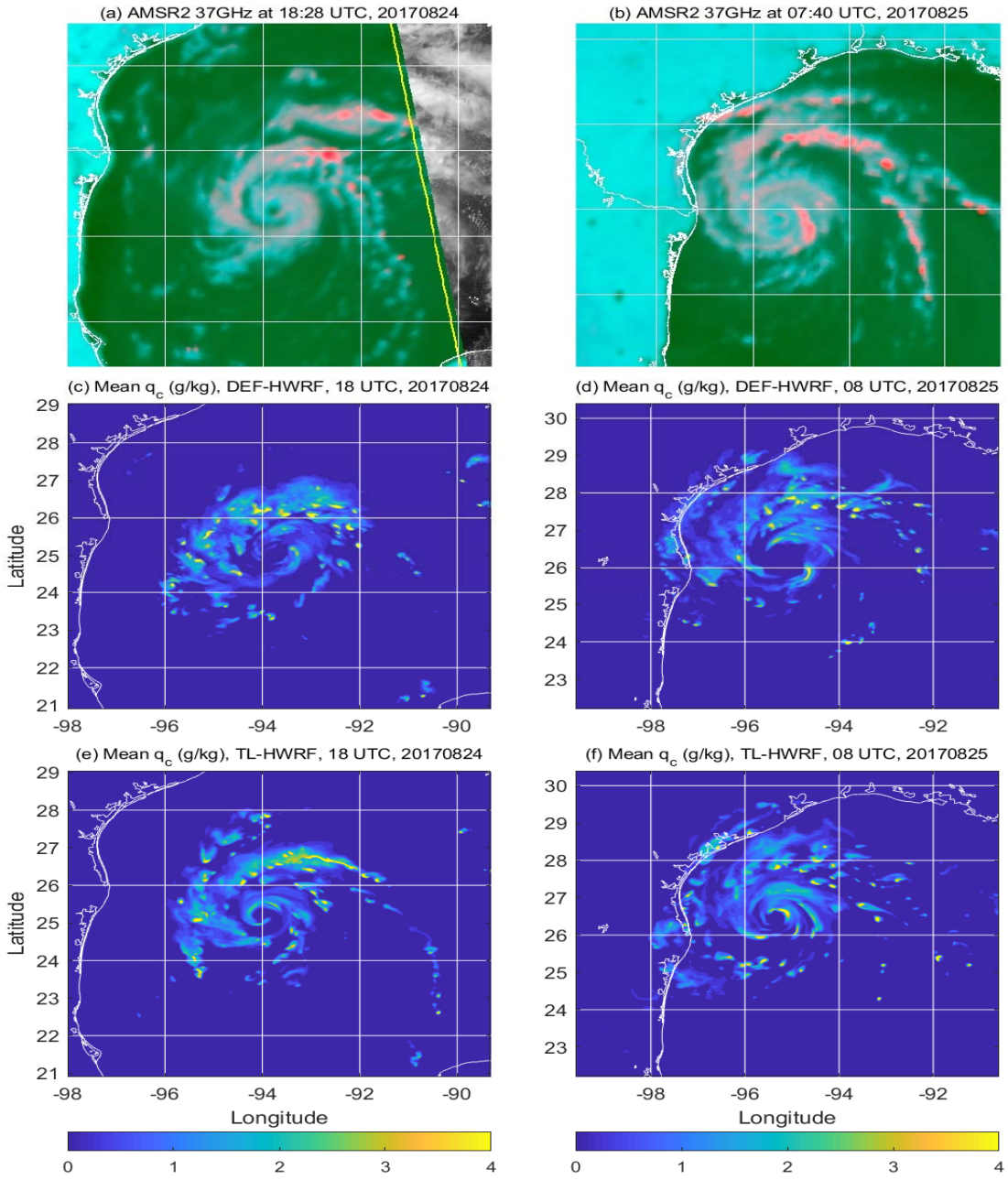

Figure 14: Comparison of vortex inner-core structure during the early stage (left column) and mid stage (right column) of Harvey (2017)'s RI between satellite (AMSR2) observations (top panels) at 18:28 UTC 24 and 07:40 UTC 25 August 2017 and HWRF simulations by DEF-HWRF (middle panels) and TL-HWRF (bottom panels) at 18:00 UTC 24 and 08:00 UTC 25 August 2017. The shown simulated fields are the hydrometeor mixing ratio (gkg^{-1}) at 5.0 km altitude.

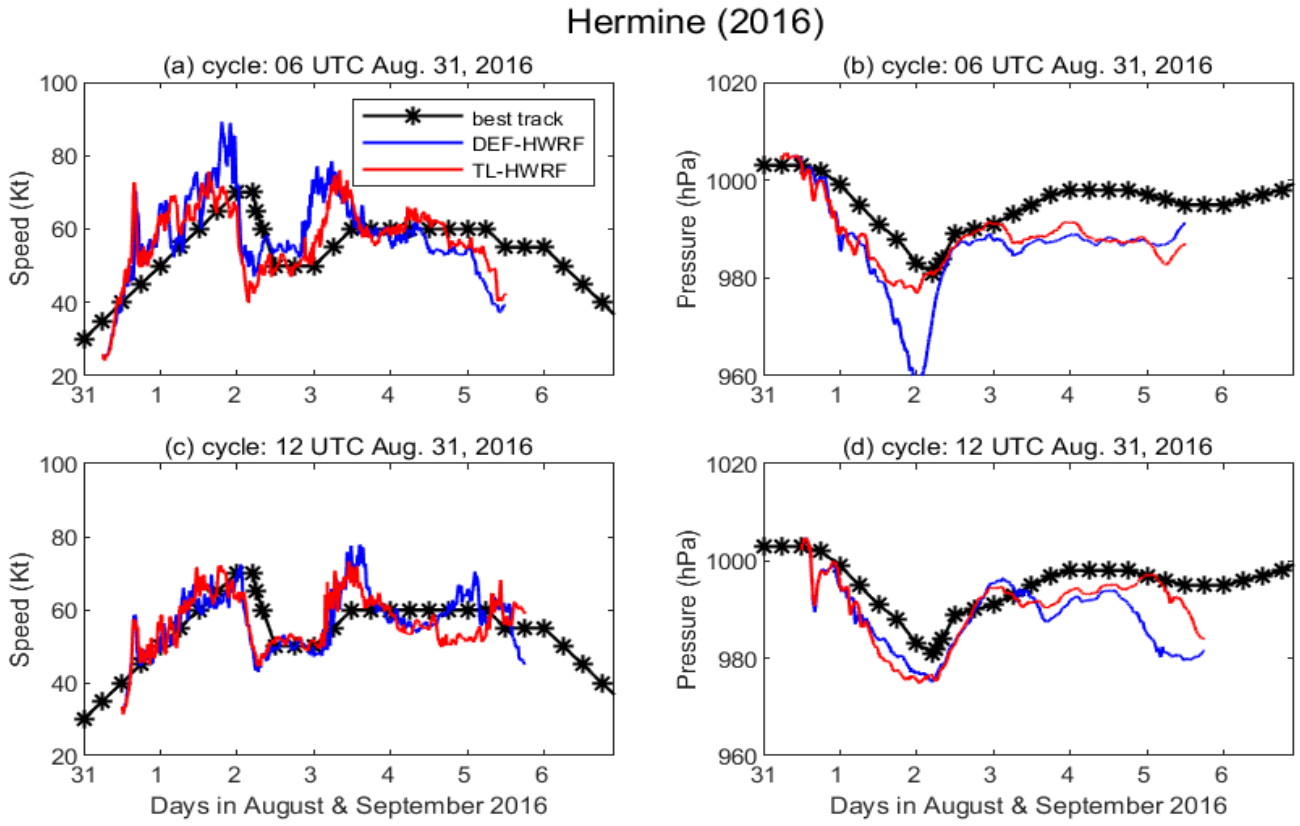

Figure 15: Comparison of HWRF simulated maximum surface wind speed, storm central pressure, and track of Hermine (2016) with the best track data (Black). Blue curves: DEF-HWRF. Red curves: TL-HWRF.

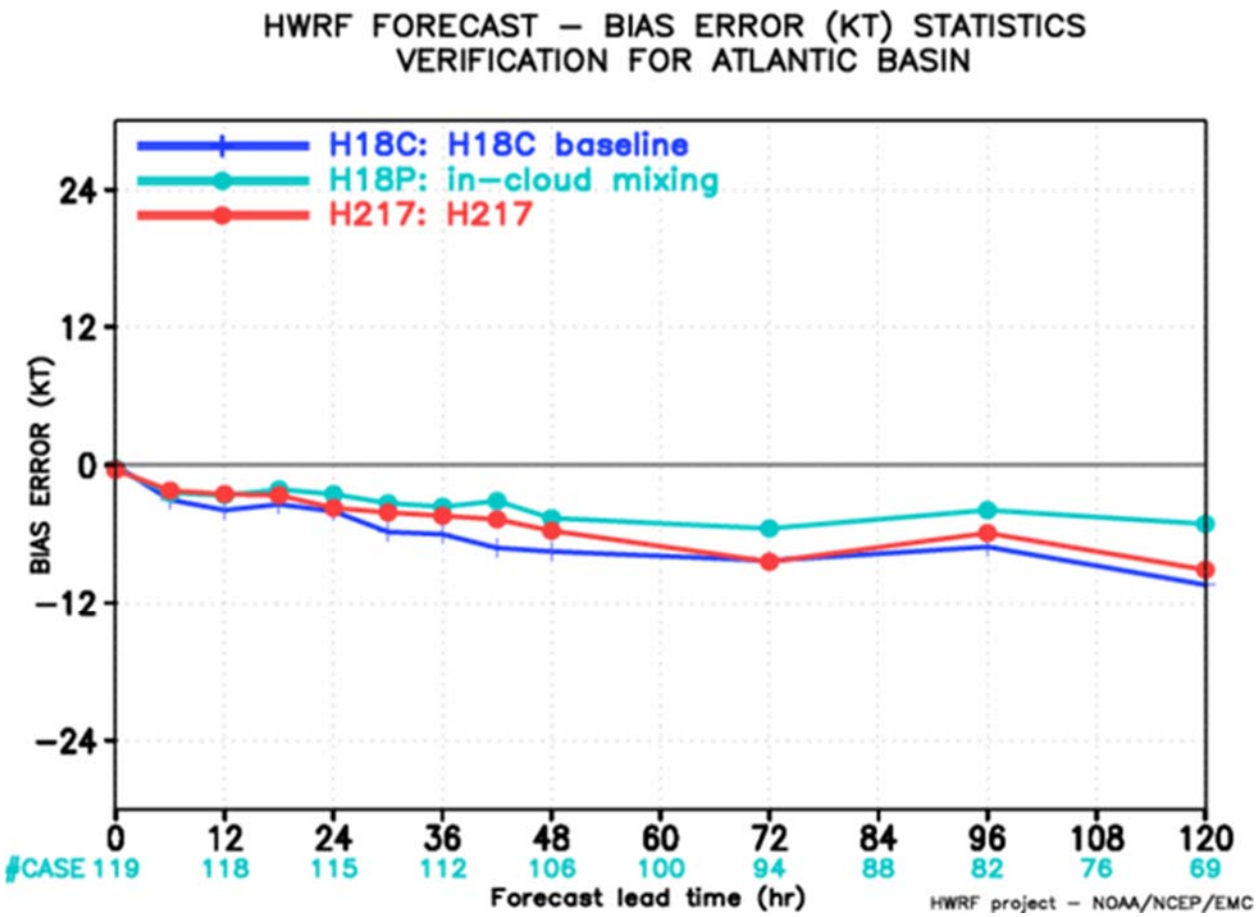

Figure 16: Maximum wind speed bias error (kt) as a function of forecast lead time (hr) averaged over all tested storms and cycles. Average bias errors are shown for the 2018 HWRF model baseline (H18C, blue), 2018 HWRF model with the inclusion an in-cloud turbulent mixing parameterization (H18P, cyan), and 2017 operational HWRF model (H217, red). The storms tested included Hermine (2016), Harvey (2017), Irma (2017), Maria (2017), and Ophelia (2017). The total number of simulation cases for various forecast lead times is indicated by the cyan labels at the bottom (Courtesy to Dr. Sergio Abarca at EMC, NOAA).